UNIVERSITÀ
DI PAVIA

PhD IN BIOMEDICAL SCIENCES

DEPARTMENT OF BIOLOGY AND BIOTECHNOLOGIES "L. SPALLANZANI"

THE SUBPARAVENTRICULAR ZONE OF THE HYPOTHALAMUS:
a circuital, modulatory and systemic study in nocturnal animals.

Ph.D. Tutor: **Professor Gerardo R. Biella**

Ph.D. Co-tutor: Professor Elda Arrigoni

Ph.D. dissertation of
Francesca Raffin

XXXVI° cycle

a.y. 2022-2023

i. LIST OF ABBREVIATIONS

4-AP: 4 aminopyridine

aa: aminoacid

AAV: adeno associated virus

AC: adenylate cyclase

ACSF: artificial cerebral spinal fluid

ACTH: adrenocorticotropic hormone

Arc/ARC: arcuate nucleus

AVP: arginine-vasopressin

BIC: bicuculline

cAMP: cyclic AMP

CCG: clock controlled genes

Cch: carbachol

ChR-2: channel rhodopsin 2

CNS: central nervous system

CRACM: channelrhodopsin assisted circuit mapping

Cre: Cre-recombinase

CRE: cAMP response elements

CREB: cAMP response element binding protein

CRH: corticotropin releasing hormone

Cry: cryptochrome genes (TTFL)

CSF: cerebral spinal fluid

CT: circadian time

DAG: diacylglycerol

DD: dark:dark cycle

DMH: Dorsomedial hypothalamus

DTA: diphteria toxin A

GABA: gamma aminobutyric acid

GAL: galanin

GECI: genetically engineered calcium indicators

GFP: green fluorescent protein. EGFP, enhanced GFP.

GPCR: G protein coupled receptor

KO: knock out

HPA: hypothalamic-pituitary axis

ipRGCs: intrinsically photosensitive retinal ganglion cells

IP3: inositol 3 phosphate

LD: light:dark cycle

LDCV: large dense core vesicle

LH: lateral hypothalamus

MPA: medial preoptic area

MnPO: median preoptic area

MUA: multi unit activity

MEA: multi electrode activity

NMS: neuromedin S

NMU: neuromedin U

PAC 1: pituitary adenylate cyclase-activating polypeptide type 1 receptor

PACAP: pituitary adenylate cyclase-activating polypeptide

PER: period genes (TTFL)

PKC: phopsphokinase C

PKA: phopsphokinase A

POMC: pro- opiomelanocortin

PRC: phase response curve

PVN: paraventricular nucleus of the hypothalamus

RCh: retrochiasmatic area

RG: rabies glycoprotein

RHT: retino-hypothalamic tract

RMP: resting membrane potential

SCN: suprachiasmatic nucleus

SFR: spontaneous firing rate

SPZ: subparaventricular zone. Ventral SPZ (vSPZ); central SPZ (cSPZ), dorsal SPZ (dSPZ)

TTFL: transcriptional-post translational delayed feedback loop

TTX: tetrodotoxin

TVA: avian retroviral receptor

VGAT: vesicular GABA transporter

VIP: vasoactive intestinal polypeptide

VLPO: ventro lateral preoptic area

VMH: ventromedial hypothalamus

VMPO: ventro medial preoptic area

WT: wild-type

ZT: zeitgeiber time

ii. TABLE OF CONTENTS

1. INTRODUCTION

1.1 THE HYPOTHALAMUS: *general anatomy and functions.*

Described for the first time by Galen of Pergamon in the 2nd century, in humans the hypothalamus is a diencephalic structure of about 1cm^3, located posteriorly at the limit of the interpenduncolar fossa, adjacent to the midbrain; superiorly is separated from the thalamus by the hypothalamic sulcus; and moving anteriorly its limits are defined by the optic chiasm, the anterior commissure and the lamina terminalis. While the tuber cinereum, the median eminence, the infundibulum and the accessory pituitary gland residing in the depression of the sphenoid bone, the *sella turcica*, defined the hypothalamus inferiorly.

A sagittal view of the hypothalamus reveals four distinct zones, progressing from the rostral hypothalamus to the caudal hypothalamus are identified,

- the preoptic zone of the hypothalamus, just behind the lamina terminalis with the medio and lateral preoptic nuclei and the sexually dimorphic nuclei;
- the supraoptic zone of the hypothalamus, composed by the suprachiasmatic nuclei, the supraoptic nuclei, the paraventricular nuclei and the anterior hypothalamic nuclei;
- the tuberal zone, which develops above the tuber cinereum, is composed by the arcuate nucleus, the ventro-medial nuclei, the dorso-medial nuclei;
- the mamillary zone, composed by the mamillary nuclei and the posterior hypothalamic nuclei.

Developing as a sheet of grey matter around the wall and the floor of the third ventricle the hypothalamus is also divided in medial and lateral portions by the fornix, a white matter tract connecting the subiculum of the parahippocampal formation with the mamillary bodies. To the medial portion belong the hypothalamic nuclei and the structures reported just above, while the most lateral portion is defined by the extension of the lateral hypothalamic nuclei that develop from the rostral part of the hypothalamic structure to almost the most caudal part of the hypothalamus.

The hypothalamus initiates and modulates a variety of functions within the endocrine system, the autonomic nervous system, and the limbic system. The mamillary bodies represent a key node in the regulation of learning/memory and emotional functions, through their connection with the parahippocampal formation and thalamus, in the known Papez's circuit, and with the amygdala, respectively through three main structures of white matter, the fornical tract, the stria terminalis and the ventral amygdaloid fugal tract, that born in the temporal lobe to terminate into the hypothalamus. The arcuate nucleus acting through the lateral hypothalamus and the ventro-

medial hypothalamus controls the hunger and satiety and rewarding state related to the feeding behavior which is implemented by the mamillary bodies. And with the lateral hypothalamic nuclei it also coordinates the function of drinking, the emotional state of anger and it is directly involved in the activation of the autonomic sympathetic nervous system consolidating a state of arousal.

Most of the endocrine functions of the hypothalamus involve stimulation or inhibition of the cells of the pituitary gland. The pituitary gland is anatomically divided into two parts: the anterior portion, known as the adenohypophysis, and the posterior part, known as the neurohypophysis. The adenohypophysis develops from the oral ectoderm and receives support for its differentiation by growth factors released by the neurohypophysis. The neurohypophysis, the most posterior part of the pituitary gland, originates from the evagination of the third ventricle. The neurohypophysis directly receives the supraoptic hypophysial tract composed by the axons of the magnocellular neurons that, coming from the paraventricular nucleus and the supraoptic nucleus, release in the systemic circulation the hormones oxytocin (for bonding, uterine contraction, empathy) and the arginine-vasopressin (for the antidiuretic effect). The tubero-hypophysial tract is composed mainly of projections from the parvicellular cells of the nucleus arcuate, and some from the paraventricular and the preoptic nuclei, and it releases in the hypothalamic-hypophysial portal system, an intricate network of blood vessels which linked the hypothalamus to the gland, the hormone releasing-hormones and the hormone inhibitory-hormones. This system regulates the production of the growth factor hormones, the thyroid stimulating hormones, the adreno-corticotropin hormone, the follicle stimulating hormone, the luteinizing hormone and the prolactin. Lastly, the hypothalamus controls the epithalamus structures, initiating the secretion of melatonin from the pineal gland. This process is orchestrated by a circuit that originates in the suprachiasmatic nucleus, extends to the paraventricular nucleus, traverses preganglionic cholinergic neurons in the intermediolateral cell column of the spinal cord, continues with the postganglionic noradrenergic neurons in the superior cervical ganglion, interacts with the habenular nuclei and, finally, stimulates the pineal gland. Through these intricate endocrine pathways, the hypothalamus serves as a central hub influencing bone growth, protein synthesis, metabolism, reproductive states and sexual hormones production, stress response, lactation and sleep-wake cycle. Furthermore, this regulatory center directs the rhythmic patterns in which these functions develop throughout the day and across the seasons.

Moreover, the hypothalamus, owing to its anterior and posterior nuclei, serves as a primary center for thermoregulation. It communicates with the parasympathetic autonomic system via the dorsal longitudinal fasciculus and with the sympathetic autonomic system through the hypothalamic-

spinal pathway. These interactions permit the physiologic systemic responses to the environmental temperature changes.

Moreover, the connections of the hypothalamus with the septal area, the fronto-orbital cortex and the olfactory cortex through the medial forebrain bundle, make it a player in the motivation state underling behavior. And the mammilo-tegmental bidirectional network links the hypothalamus to movement generation.

The anatomical description reported here relies on the human hypothalamus (Cattaneo, 1989; Lechan et al., 2016; Hirose et al., 2016; Felten et al., 2017), **[Figure 1.1]**. It is important to note that, hypothalamic structures and functions are highly conserved across mammals. Therefore, this general introduction serves as a base to contextualize the subsequent paragraphs, encompassing the introduction through the discussions. It is noteworthy that most of the results presented and discussed in these sections are derived from studies on nocturnal rodents.

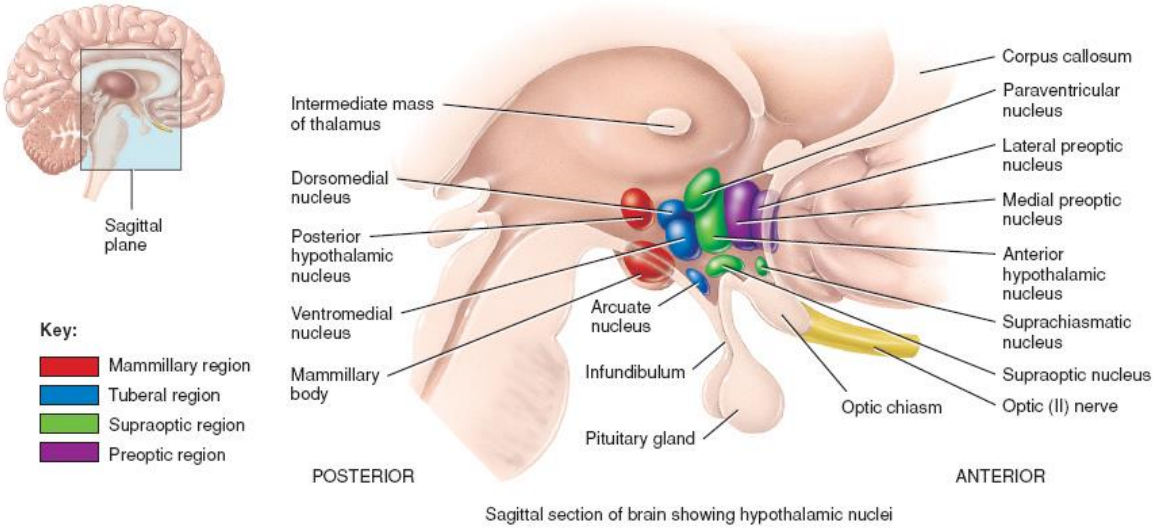

Figure.1.1: human hypothalamus [image from (Rogilmore, 2019)].

The intricate functions of the hypothalamus, spanning from its control over homeostatic systems to behavior modulation, find their roots in the adaptive responses shaped by environmental conditions. Since "nothing in biology makes sense, except in the light of evolution" (Dobzhansky, 1973), as Dobzhansky noted, the wide range of roles of the hypothalamus in mammals encompasses its contribution to the occurrence of various biological phenomena within the organism, which can be described as an adaptive response intricately linked to environmental conditions. The hypothalamus is part of the internal systems responsible for the evolution of feedforward strategies. These strategies enable the anticipation of biological responses in accordance with the regular recurring variations in light, temperature, humidity, ultraviolet radiation, that are connected to the Earth's rotational and revolution motions (Foster

& Kreitzman, 2013). The hypothalamus serves as the center for the development and the regulation of the primarily biological rhythms, which can occur with a period exceeding 24h (infradian rhythms, i.e. migration); shorter than 24h (ultradian rhythm, i.e. excretory activity) and with a period of approximately 24h (circadian rhythms, i.e. sleep/wake cycle). Among these, circadian rhythms shape the daily life of an organism.

The circadian rhythms are so named because they occur with a period (*tau*) of approximately 24 hours. These rhythms are ubiquitous in the nature manifesting in bacteria, algae, fungi, plants and animals. These rhythms are the result of a *well-organized circadian timing system* (Patton and Hastings, 2023). This system comprises *synchronizer inputs*, the zeitgeber (from the German words z*eit*, meaning "time" and *geber* meaning "giver"). Zeitgebers represent environmental oscillations that dictate the timing of biological functions, effectively entraining them to the external environment. These zeitgebers, along with their respective input pathways, play a crucial role in establishing the organism's dependency on its surroundings. Within this circadian timing system, specific *internal structures* decode incoming inputs and adapt to them generating rhythmic outputs through relative output pathways. The synergy among all these elements allows mammals to exhibit different circadian functions including sleep/wake cycle, hormone release (i.e. cortisol or melatonin) and variations in body temperature and cardiovascular parameters (Czeisler and Klerman, 1999; Morf and Schibler, 2013; Pavlova, 2017; Monfredi and Lakatta, 2019). All these functions are vital for an organism, therefore it is not surprising how the impairment of their underlying circadian regulation is followed by the emergence of significant pathologies, such as sleep disorder, cancer, psychiatric and neurodegenerative diseases, cardiovascular, immune, metabolic and endocrine imbalances (Voigt et al., 2013; Logan and McClung, 2019; Leng et al., 2019).

One of the most important aspect of this organized system is the ability of the *internal structures* to work even under *free-running* conditions, such constant light or darkness. This confers a high grade of resistivity and an evolved endogenous nature to the system itself. In mammals, the principal *internal structure* which codifying for the principal external zeitgeber, the light, it dictates the daily rhythms of the organism, is the suprachiasmatic nucleus of the hypothalamus.

1.2 THE HYPOTHALAMIC SUPRACHIASMATIC NUCLEUS (SCN): *the master clock of the mammalian circadian rhythms.*

The suprachiasmatic nucleus (SCN) of the hypothalamus, is located as a bilateral structure at the base of the third ventricle, dorsally to the optic chiasm, at the base of the supraoptic zone in the anterior hypothalamus (Herbert, 1994). The initial evidence establishing hypothalamic

involvement in circadian regulation, comes from the studies of C. Richter in the 1960s. Richter conducted experiments involving lesions in rats and observed that only a lesion in the anterior hypothalamus was able to completely abolish biological circadian rhythmicity (Richter, 1967). Subsequent investigations into the dependency of circadian rhythms on the light-dark cycle led to a tracing study using tritiated amino acids injected into the eyes. This study showed the existence of the retino-hypothalamic tract which projections mainly terminate into the suprachiasmatic nucleus. Subsequent lesion studies focused on the suprachiasmatic nucleus in the 1970s, showed a complete loss in the circadian rhythms for drinking and locomotor activities (Stephan and Zucker, 1972) as well as corticosterone release (Moore and Eichler, 1972). However, it was the studies of M.R. Ralph *et al.* in the 1990 that definitively recognized the SCN as *necessary* and *sufficient* nucleus for the genesis of the circadian rhythms in mammals thanks to the discovery of a mutant hamster named *Tau*. Compared to the 24.1h period in locomotor activity of the wild-type hamster, the *Tau* mutant in homozygosis displays a circadian period of 20.2h whereas in heterozygosis it exhibits a period of 22h. Transplanting the SCN from *Tau* mutant fetuses into wild-type hamster with SCN ablation, and vice versa, both resulted to the host animals recovering their circadian rhythm. The period length in locomotor activity corresponded to that of the donor, regardless of the host's genetic background (Ralph et al., 1990).

This unique role of the SCN as the pacemaker of the circadian rhythms imposes to this nucleus three main characteristics to confirm its position at the top of the hierarchy of the *circadian timing system* (see paragraph "1.3 The circadian timing system"). Firstly, temperature compensation is a functional prerequisite for circadian pacemakers (Pittendrigh, 1960). Most biochemical processes exhibit a linear dependency on temperature, showing a Q10 (the ratio of the rate of a given process at one temperature to the rate at a temperature separate by 10°C) of about "2" or "3" before reaching a critical temperature value at which all biological functions cease entirely. The period length of the circadian pacemaker must remain constant over a wide range of physiological temperatures to be able to maintain the well-being of the animal in its environment. A clock with rapidly and significantly changing *tau,* depending on the temperature, would not reliably predict daily perturbations of the environment. Despite patch-clamp recordings in whole-cell configuration of the SCN neurons display sensitivity to temperature variations, with neurons exhibiting an increase in the firing rate (Burgoon and Boulant, 2001), the SCN demonstrates an ability to compensate for temperature variations within physiological interval. This compensation maintains stable the circadian period, with a Q10 value around "1" (Kuhlman et al., 2018).

The second aspect regards the ability of SCN to be entrained. In light-sensitive organisms, the primary zeitgeber guiding SCN activity is light itself (Munch and Bromundt, 2012). When studied in constant darkness the rhythmic locomotor activity of a mouse exhibits a *free-running* circadian period that does not precisely match the 24h 12h:light/12h:dark (LD) cycle which reflects the activity(rest)/rest(activity) cycle. This discrepancy occurs because the pacemaker is able to maintain the rhythmicity even in *free-running* conditions, but it dictates a *tau* slightly inferior to the 24h, leading to a phase-shift compared to the LD cycle. However, upon entrainment, the internal period *tau* of the SCN becomes synchronized to the external zeitgeber period, resulting in a final phase-alignment of the two rhythms. Precisely, "one oscillator [o] - the SCN of the animal - whose free-running period is tau [τ] can couple to and be entrained by another oscillator [z], sometimes called the zeitgeber – the light - with a different but similar period [T]" (Pittendrigh, 1981; Schmutz et al., 2014). The ability of light to phase-locked the SCN and entrain the biological functions in mammals is mediated by the eyes. In mammals the photic inputs are detected by the eyes, where the photoreceptors, cons and rods, containing their ciliary opsins, convert the photon energy into electrical signals through a process known as phototransduction (Fain and Sampath, 2018). The resulting signal is then relayed to the retinal ganglion cells which project to the central nervous system via the optic nerve. This pathway is crucial to initiate the vision, but it is not exclusive for detecting light. Engineered mice lacking cons and rods still exhibit the pupillary light reflexes, the circadian wheel-running behavior and a normal suppression of melatonin release in response to light. Conversely these behaviors are absent in enucleated mice. Then there must be a third element to catch the light. In the early 20th century D.M. Berson and I. Provencio identified the presence of rhabdomeric melanopsin in intrinsically photosensitive retinal ganglion cells (ipRGCs) (Provencio et al., 2000; Hattar et al., 2002). The ipRGCs constitute only 5% of the retinal ganglion cells population (Graham and Wong, 2016) but they play a fundamental role in the entrainment processes. Ablation of ipRGCs results in a loss of a circadian light responses and entrainment in animals (Berson and Takao, 2022). The presence of the monosynaptic projection via the retino-hypothalamic tract (RHT) between the ipRGCs and the ventral region of the SCN has been demonstrated through retrograde tracing (Canteras et al., 2011; Lokshin et al., 2015). This pathway is so crucial for circadian behaviors that it shows partial redundancy in its functioning. Studies have proved indeed that melanopsin is not essential for the activation of the ipRGCs, since knockout (KO) mice for the *Opn4*, the gene encoding melanopsin, maintain entrainment under the LD cycle and exhibit a circadian pattern of rhythms in constant darkness. Both rods and cones contact the ipRGCs contributing to the plasticity and redundancy of the processes. However, the presence of

melanopsin remains necessary for decoding the intensity of the light input (Rubyet al., 2002; Panda, 2002; Do and Yau, 2010).

The last essential feature is auto-sustainment. A biological pacemaker is intended as a group of cells that retains the ability to generate a rhythmic or cyclic activity in the absence of specific trigger, when isolated from inputs. This property is exemplified by the specialized cardiomyocytes located in the sinoatrial node of the heart which generate cardiac action potentials and heart contraction even when the heart is isolated from the body. Similarly, the SCN possesses this property and this ability to be auto-sustaining in isolated conditions, that is a crucial aspect to behave as pacemaker. Cultures of neonatal dissociated SCN neurons from rats, display circadian firing rhythms with different phases that re-emerge after treatment to block action potentials. This indicates the ability of these neurons to maintain a circadian activity even in the absence of action potentials. However, it also highlights the necessity of a network integration and neurochemical communication for the SCN to work as a pacemaker (Welsh et al., 1995). Notably, the knife cut of hypothalamic "island" containing the SCN in blinded rats, has been crucial to demonstrate with multi-unit activity (MUA) recordings, that the "island" is able to maintain circadian rhythmicity in firing rate. This rhythmic pattern was not observed in the external island brain region, suggesting that the ability of the SCN to fire cyclically is an internal property of the nucleus itself, independent from external inputs (Inouye and Kawamura, 1979). Moreover, a non-invasive study employing the autoradiographic 2-deossi-D-[14C]glucose method has shown that the glucose utilization in the SCN follows a circadian rhythm, with a 60% higher amplitude during the light phase compared to the dark phase (Schwartz et al., 1980). This ability of the internal structure to generate stable rhythms, even in the absence of zeitgeber, derives from the fact that these rhythms are primarily initiated at an endogenous molecular level. The rhythms are initially encoded into the DNA (Dvornyk et al., 2003; Jindrich et al., 2017).

1.2.1 The molecular basis of the biological circadian rhythms*: the mammalian Transcriptional/post-Translational delayed Feedback Loop (TTFL).*

First demonstrated in *Drosophila Melanogaster* (Hardin et al., 1990), the autoregulatory negative feedback circuit loop is a complex molecular process composed of positive and negative components. The positive components include two helix-loop-helix (bHLH) transcription factors, BMAL1 (Brain and Muscle Aryl hydrocarbon receptor nuclear translocator-Like protein 1) and CLOCK (Circadian Locomotor Output Cycles Kaput). During the circadian day CLOCK and BMAL1 dimerize via PER-ARNT-SIM (PAS) domain (Vogt and Shippers, 2015). As heterodimer BMAL1-CLOCK binds the Enhancer Boxes (E/E'-box) DNA (CACGTG)

sequences in the promoters of the clock genes, Period (Per-1-2-3) and Cryptochrome (Cry-1-2), activating their transcription (Antoch et al., 1997). The translated mRNA of Period and Cryptochrome genes and their protein products PER and CRY, accumulate in the cytoplasm where they heterodimerize. During the circadian night the heterodimer PER-CRY acts as the negative component of the loop by translocating in the nucleus and providing negative feedback onto the BMAL1-CLOCK complex, inhibiting their own expression. This process is facilitated by post-translational phosphorylation of PER which stabilize its biochemical interaction with CLOCK (Lee et al., 2001). In the meantime, in the cytoplasm the PER-CRY complex is gradually targeted for ubiquitination and proteasome degradation. This process involves the action of the Casein kinases 1-delta and 1-epsilon which tag the complex for polyubiquitylation (Eide et al., 2002). The degradation of PER-CRY complex leads to the release of the inhibition on CLOCK/BMAL1 complex, allowing the cycle to recommence. The entire cycle encompassing gene expression, protein synthesis, feedback inhibition and degradation takes approximately 24 hours**,** confirming the TTFL as the molecular scaffold of the circadian processes.

This mechanism is more complex than this and with other regulatory cyclic elements it forms an intricate molecular network. These other cyclic elements within the circadian network, belong to the nuclear receptor families (Shearman et al. 2000; Solt et al., 2011) and exert their influence on components of the TTFL. Specifically, REV-ERBs (alfa-beta) (Preitner et al., 2002) and RORs (retinoic acid receptor-related orphan receptors) (Sato et al. 2004; Crumbley et al., 2010) repress and activate Bmal1-Clock transcription respectively. They compete for the REV response elements (RREs) within the Bmal1-Clock promoter. Simultaneously, the expression of REV-ERBs/RORs elements is directed by the BMAL1/CLOCK vie E-box sequences, while the transcription of REV-ERBs is trans-repressed by CRY/PER heterodimer (Solt et al., 2011). The resulting oscillating expression of REV-ERBs/RORs elements feeds back to control the circadian pattern of BMAL1/CLOCK expression adding stability and precision to the network (Cho, 2012). Moreover, the clock genes can also be controlled by other elements acting at D-boxes or cyclic AMP (cAMP) response elements (CREs), providing an entry point for input pathways that can influence and regulate the TTFL allowing the TTFL access to external inputs (Takahashi, 2017). For example, as will be described later, vasoactive intestinal polypeptide in the suprachiasmatic nucleus is capable of inducing the expression of the Per gene exactly via CREs DNA sequence, thereby influencing at molecular level the SCN neuronal activity.

The positive elements of the TTFL and other transcription factors, such as ROR/REV-ERB, also genetically direct the principal output of the TTFL. These elements acting through E-boxes, ROR elements, and others via D-boxes and CREs sequences, can directly operate on the promoters of

the *clock-controlled genes* (CCGs) (Chowdhury et al., 2019). The CCGs represent approximately 10% of all mammalian genes (Bozek et al., 2002; Korenčič et al., 2014) and the expression of some of these genes is shared across different tissues, while most of them are tissue specific. It is within this pool of genes that the complexity of the circadian responses and the subtlety of the process at the single cell level reside (Storch et al., 2002). **[Figure 1.2]**

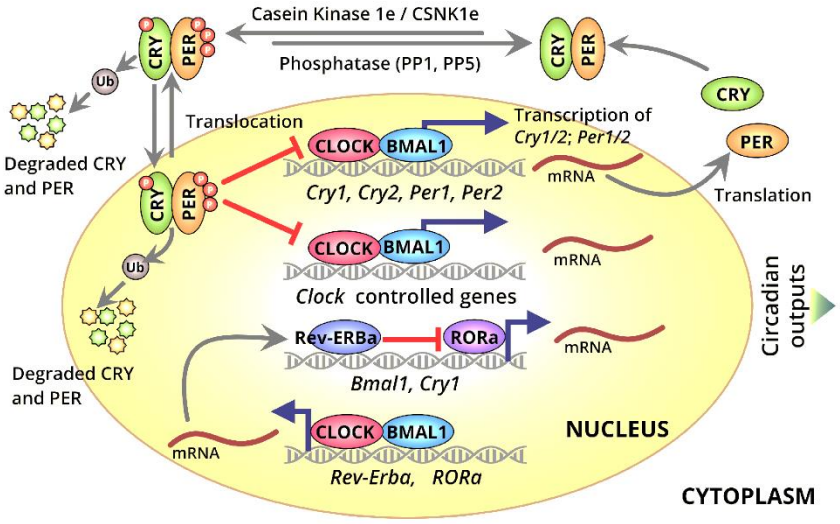

Figure 1.2: the mammalian molecular clock. Schematic representation of the TTFL negative, positive and regulatory components [image from (Chowdhury et al., 2019)].

This molecular base of circadian rhythmicity provides the principal substrate to the SCN to act as a pacemaker and offers compelling evidence about the evolutionary significance of the circadian rhythms. Bioluminescent studies reveal that the components of the TTFL continue to oscillate in SCN neurons even when cultured as dissociated neurons or as organotypic cultures (Green et al., 1982). This continuous regulation of downstream CCGs within the SCN neurons influences the properties and outcome of this nucleus. MUA recordings of electrical SCN activity demonstrate that the Clock-deficient mice lack of rhythmicity in the SCN (Albus et al., 2002). Interestingly Per1:GFP reporter mice highlight a positive correlation between Per1 transcription and the circadian changes in firing rate in SCN neurons. It is well-established that the SCN undergoes changes in firing rate throughout the 24h period (Belle et al., 2009) and ionic currents have been proposed as responsible for these changes (Colwell, 2011). The depolarized resting membrane potential (RMP) of approximately -50/-55mV in the SCN during the daytime seems to be generated by the potential contribution of persistent Na^{2+} current, hyperpolarized-activated cyclic nucleotide gated (HCN) channels and T- and L-type Ca^{2+} currents. Additionally, calcium-activated potassium channels (Kent and Meredith, 2008) or A-type potassium channels, play a crucial role in bringing the RMP over the threshold level, resulting in spontaneous firing rate (SFR) of about 7-10Hz. Instead, the hyperpolarized state during the night, with a SFR of about

1Hz, could be attributed to the increase in K^+ leakage conductance. Regarding both excitatory and inhibitory conductances, there is evidence that the Cav1.2 subunits of the L-type channels are under the genetical control of REV-ERBs (Schmutz, 2014).

Different levels, both transcriptional and post-translational, of action for the TTFL components contribute to the variation in SCN activity. These levels are all crucial, as the electrophysiological status of the SCN during the daytime is one of the most important outcomes. This status translates into different neuronal messages conveyed by neurotransmitters or neuropeptides, that are released in a timely manner (Jin et al., 1999, Ueda et al., 2002, Hogenesch et al., 2003).

Moreover, light itself influences the SCN activity by acting on the TTFL elements. ipRGCs primarily release the neurotransmitter glutamate and the pituitary adenylate cyclase-activating polypeptide (PACAP) (Hannibal, 2002). These neurotransmitters, acting via NMDA receptors and G protein coupled receptors (GPCRs) respectively, determine the influx of Ca^{2+} or the PKA phosphorylation responsible for the regulation of the TTFLs elements. The activation of calcium/calmodulin-dependent protein kinase (CaMK) and mitogen-activated protein kinase (MAPK) pathways, leads to the phosphorylation of the cAMP response element-binding protein (CREB). CREB binding CREs within the promoter of clock genes, entrains the molecular clock to light (Mejer and Schwartz, 2003). Finally, it is known that brief pulses of light can phase-shift the SCN oscillation, primarily during dusk or nighttime, and not during the day when the SCN activity is already saturated at a high level (Hastings and Herzog, 2004). However, how these changes within the SCN are actually translated by downstream targets remain an unresolved question.

1.2.2 The suprachiasmatic nucleus organization: *internal asset and connectivity.*

In rodents, the SCN is composed by ~20.000 neuronal cell oscillators with a diameter ranging between 5-15µm and a neuron to astroglia ratio of about 3:1 (Güldner, 1983). However, in humans, the SCN is comprised of around ~90.000 neurons, a number that does not align with the evolution of the human brain in terms of weight and total count of neurons. This observation suggests that the SCN may have reached its computational stability as a small nucleus, as proposed by Yan *et al*., 2007 (Yan et al., 2007). Despite its size, or perhaps because of it, this small nucleus is able to act as the circadian pacemaker primarily due to the molecular nature of its oscillatory properties. However, what is crucial, in maintaining its robustness, plasticity and serving as the mediator between the external environment and the internal body (Reppert and Weaver, 2002), is its internal organization.

We know that the oscillatory activity of the SCN originates at the molecular level and characterizes each SCN cells. SCN neurons in rats can oscillate even in culture conditions with a different period ranging between 20 to 28 hours and exhibiting different amplitude and phase (Welsh et al., 1995; Honma et al., 1998). Remarkable it is the observation that the denser the cultures, in terms of cell density, the greater the ability of these neurons to couple their oscillations in terms of both phase and period (Aton et al., 2005; Brown and Piggins, 2009). Moreover, the oscillation in the SCN seems to develop from the prenatal stage E15.5 in mice and stabilizes at postnatal P2, a period associated with a peak of synaptogenesis (Carmona-Alcocer et al., 2017). These observations suggest that internal communication is essential to generate a single coherent output.

Developmental immunocytochemistry studies in wild-type mice using bromodeoxyuridine (BrdU) mitotic tracing reveal that the SCN cytogenesis occurs between E12-E14 following a spatiotemporal organizational program with a ventrolateral to dorsomedial and rostral to caudal gradient. Specifically, cells born first occupy the more posterior and ventral region of the nucleus, and subsequently born cells surround the posterior-ventral cells and occupy the more anterior and dorsal region of the nucleus (Kabrita and Davis, 2007). This spatiotemporal ontogeny of the SCN is not only a developmental organization, but also mirrors one of the most classical subdivisions of the SCN into ventral and dorsal subregions. These subregions are characterized by the expression of vasoactive intestinal polypeptide (VIP) together with gastrin releasing peptide (GRP) in the ventral region, and arginine-vasopressin (AVP) in the dorsal region. Basically, all neurons of the SCN are mostly GABAergic, but is possible to discriminate different subregions and neuronal clusters based on peptidergic expression, with VIP and AVP being two of the most important peptides in the SCN. Their disposition and organized projections suggest possible differential functions of the SCN subregions in processing information flow (Leak and Moore, 2001; Moore et al., 2002; Morin et al., 2006). The VIP-positive neurons of the ventral SCN constitute the so called “core”, representing the retino-recipient region of the incoming RHT pathway. On the other hand, the dorsal SCN, defined by the expression of the AVP, is referred as the “shell” and it does not receive significant input from the retina. Instead, it is strongly innervated by the VIP neurons of the core (Leak et al., 1999) and almost all the AVP cells express VPAC2 receptor, which is the principal GPCR receptor for VIP action (Aton et al., 2005; An et al., 2012). However, this classical view of the SCN is not sufficient to describe the complexity of the nucleus.

The SCN is characterized by the expression of a variety of neuropeptides defining different cellular clusters and their expression redefines the nuclei organization. Studies using single-cell

RNA-sequencing reveal heterogeneity **[Figure 1.3]** within the SCN, including differences in the distribution of different receptors, neurotransmitters or neuropeptides along the rostro/caudal and ventral/dorsal axis. The expression of VIP/GRP positive cells appears to localize in the core and their lack of circadianity suggests a specific role as reader of photic input. Conversely, VIP neurons not co-expressing GRP show a strong circadian pattern of activity, contributing to the timekeeping in the SCN. Most of the neurons expressing the VIP and AVP also express neuromedin S (NMS), whose roles as neuromodulator or marker is still under study**.** Prokineticin-2 has been proposed as an important SCN output molecule exhibiting circadian protein expression, localization along the ventro-dorsal axis and a ramified projection schema to most of the SCN targets (Zhang et al., 2009). Other peptides, such as neurotensin (NTS), calretinin (CALR), somatostatin (SS), substance P (SP), angiotensin II (AII), calbindin (CALB), cholecystokinin (CCK), galanin (GAL), are all expressed in the SCN, either co-localizing or not with each other. Very little is however known about the role of these peptides in generating a response as autocrine factors within the SCN, as paracrine factors outside the SNC, or being released at synaptic level, or serving as marker of specific neurons in the SCN with specific functions. The mechanism of their release, the timing, and the stimuli triggering their release, are also not well understood (Bedont et al., 2015; Wen et al., 2020; Todd et al., 2020). The neuropeptidergic diversity in the SCN highlights then how the outcome and internal activity of the SCN can be mediated by different neuronal clusters and messengers.

Another crucial candidate responsible for the SCN oscillation and external communication is gamma-aminobutyric acid (GABA). Although the specific role of GABA is still a subject of debate, studies outline its importance as internal synchronizer (Ono et al., 2018). GABA is produced by nearly all cells in the SCN and blocking GABA transmission with a $GABA_A$ antagonist like bicuculline, results in the loss of communication between the ventral and dorsal SCN subregions (Albus et al., 2005) corroborating the necessity of the internal synaptic connection within the SCN (Gillespie et al., 1997; Mintz et al., 2002). An intriguing aspect about the role of GABA in the SCN regards the dual electrophysiological action dependent on the intracellular chloride concentration. Classically, the physiological intracellular concentration for chloride ions in adult neurons is around 5mM, leading to a hyperpolarizing effect mediated by $GABA_A$ transmission due to the higher external concentration of around 140mM. However, in some or many SCN neurons this concentration seems to be inverted allowing GABA signaling to depolarize cells instead of hyperpolarizing them (Wagner et al., 1995; De Jeu and Pennartz, 2002; Choi et al., 2008; Irwin and Allen, 2009). This opposite concentration seems to be related to higher activity or higher membrane expression of the cotransporter NKCC (Sodium-

Potassium-Chloride cotransporter) (Olde et al., 2018). One study has indicated that this GABA switch characterized the dorsal and ventral subregions depending to the circadian time, with the excitatory effect being restricted to the dorsal SCN during the day, and in the ventral SCN during the night (Alamilla et al., 2014). These suggest a model in which GABA released within the SCN can modulate the neuronal response to circadian input.

More recent studies, still in progress, reveal the contribution of the astrocytes to the dynamics of SCN. Astrocytes are mainly known for their homeostatic role in the brain, and their emergence as a component of the tetrapartite synapses is gaining recognition in neuronal processing. One of their initial influences on the SCN is their buffer effect on glutamate. Pharmacological inhibition of glutamate uptake results in a total dysregulation of the neuronal PER2:LUC oscillation (Brancaccio et al., 2017). [To clarify, the PER2:LUC system is a molecular tool designed to monitor variations in Per gene expression (or other genes of interest) through the measurement of luminescence signals. The luciferase (LUC) reporter gene fused with the Per gene, allows to monitor the daily changes in genetic expression within a specific subset of cells.] Moreover, astrocytes as many other cells outside the SCN possess the TTFL circadian clock (Prolo et al., 2005; Tso et al., 2017). Their activity varies over the time and the genetic deletion of Bmal1 gene within SCN astrocytes lengthens the circadian period of clock gene expression in the SCN and in locomotor behavior. In the 2019 Brancaccio *et al.* demonstrated, for the first time, that in mice the SCN astrocytes can drive behavior. Astrocytes can initiate molecular oscillations in the SCN neurons and circadian locomotor activity when both are impaired in KO mice for Cry1/2 genes. This trigger mechanism involves glutamatergic transmission and starts the typical calcium waves in the SCN with a phase-advance in the dorsal SCN that then propagates to the ventral SCN dictating the physiology of a wild-type animals under not-masking condition (Tso et al., 2017; Barca-Mayo et al., 2017; Brancaccio et al., 2019).

Finally, gap-junction play a crucial role in the pacemaking activity of the SCN, as they couple approximately 30% of the SCN neurons. Is indeed proved that electrical connection in the SCN is reduced in Cx36-KO mice (protein connexin-36 is a key component of the gap-junction molecular asset) (Ramkisoensing et al., 2015) and the inhibition of the Cx43 (protein connexin-43 is the principal component for the gap junctions in the astrocytes) with TAT-Gap19 significantly compromised Per2:LUC oscillations in wild-type SCN and in the Cry1/2 KO SCN when the TTFL is driven by astrocytes (Brancaccio et al., 2019).

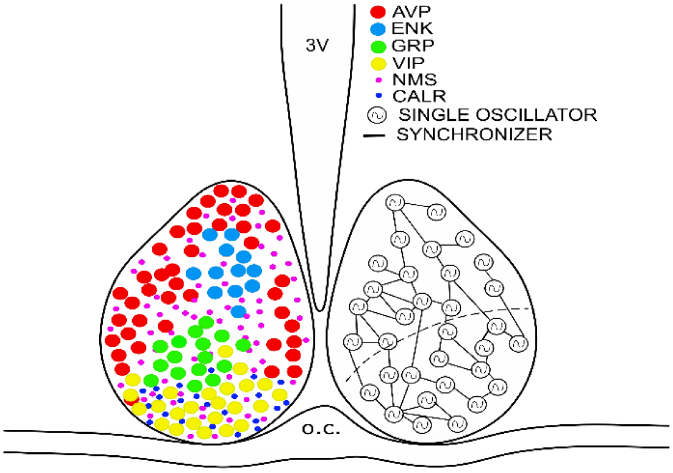

Figure 1.3: *left SCN,* schematic representation of peptides distribution in the SCN. Vasopressin (AVP) defines the dorsal SCN (*red*). Vasoactive intestinal polypeptide (VIP) defines the ventral SCN (*yellow*), along with gastrin releasing factor GRP (*green*). Neuromedin S (NMS) is expressed randomly in about 40% of the cells within the SCN (*pink*). Enkephalin (ENK) (*light blue*) is mostly present in the dorsal region and calretinin (CALR) is found in the core region (*blue*). Other SCN markers such as neurotensin (NT), somatostatin (SS), substance P (SP), angiotensin II (AII) and calbindin (CLAB), are not shown. The drawing is only representative, the size of the dots doesn't have a specific meaning. *Right SCN*, the SCN neurons are single oscillators which they can act in synchrony to generate a coherent output. *3V*, third ventricle; *o.c.*, optic chiasm. [Image adapted from (Ramkisoensing et al., 2015). For more information see reference (Wen et al., 2020; Ono et al., 2021; Yoshikawa et al., 2021; Carmona-Alcocer et al., 2023)].

Certainly, understanding the internal organization of the pacemaker is crucial, but equal importance is placed on the connectivity of the SCN. The neuronal network around the SCN represents a principal pathway through which the SCN can act as mediator between the external environment and the internal body. This network has been dissected by retrograde and anterograde tracing studies in rodents and some of these results are reported below.

THE AFFERENTS: generally, the ventral and dorsal subregions of the SCN are closely connected through ipsilateral as well as contralateral projections, ensuring internal network integration and communication (Moga and Moore, 1997). More specifically, as already introduced in paragraph "1.2 The hypothalamic suprachiasmatic nucleus (SCN): *the master clock of the mammalian circadian rhythms"* one of the most important SCN input is represented by the RHT which brings the fibers of the ipRGCs mostly to the VIP-GRP cells in the SCN core regions transmitting the information regarding the light intensity and determining the entrainment process. The ipRGCs establish connections with other hypothalamic brain regions such the SCN shell, the ventral subparaventricular zone (vSPZ), the lateral hypothalamus (LH), the ventro-lateral preoptic area (VLPO) and the supraoptic nucleus (SON). These connections play a role in various physiological functions including sleep, locomotor activity, body temperature and

neuroendocrine functions. Moreover, projections to the intergeniculate leaflet (IGL) of the thalamus, the pretectal olivary nucleus (OPN), and the superior colliculus suggest a broader involvement in coordinating the pupillary reflex, orienting movements and non-image visual inputs processing (Hattar et al., 2006). The core receives also indirect photic input and non-photic input from the intergeniculate-leaflet of the thalamus via the geniculo-hypothalamic tract (GHT) with a communication probably mediated by the neuropeptide Y (Hasting and Herzog, 2004) which influence the SCN entrainment; and non-photic serotoninergic input coming from the median raphe nucleus (Moga and Moore, 1997). The SCN is also reached by different hypothalamic nuclei as ventromedial hypothalamus (VMH), medial and median preoptic area (MPOA-MnPO), dorsomedial hypothalamus (DMH), nucleus arcuate (ARC) and most of these projections terminate almost only into the SCN shell, with the exception for the tuberomammillary and subparaventricular zone projection which seems interest also the SCN core. Furthermore, the shell receives a strong projection from the core and a dense galanin projections coming from the anterior hypothalamus and the preoptic area. Information comes also from limbic areas, such as the ventral subiculum and infralimbic cortex, carrying information about the emotional, cognitive and stress level states. Both the core and shell regions also receive excitatory input from the paraventricular nucleus of the thalamus (PVT), with a non-essential role in the circadian entrainment (Krout et al., 2002).
Concluding, R.Y. Moore and R.K. Leak (Leak and Moore, 2001) from their anatomical studies and observations describe a topographic organization of the incoming afferent returning a functional distinct role of the two subregions, where the core represent the pathway for the entrainment of the pacemaker to the environmental light/dark cycle, while the shell represents the modulatory part of the pacemaker, and both contact the effector targets.

THE EFFERENTS: The SCN targets directly or indirectly many hypothalamic nuclei regulating essential homeostatic functions and behaviors. Known and thoroughly described are the projections to the paraventricular nucleus of the hypothalamus (PVN), by which regulates the hormonal secretion and the secretory activity of the epiphysis (Klein et al., 1983) with the release of melatonin during the dark phase both in diurnal and nocturnal animals (Gandhi et al., 2015). Results from monosynaptic tracer studies at the level of the MnPO area suggest a direct control of body temperature, while the projection to the organum vasculosum of the lamina terminalis (OVLT), ARC and DMH underlying the influence onto the fluid intake, the feeding behavior and sleep-wake cycle. The strong projection to the subparaventricular zone (SPZ) seems to serve as relay node since the SPZ is directly connected to the same regions of the SCN controlling

thermoregulation, locomotor activity and sleep/wake cycle (Chou et al., 2003; Saper, 2013; Buijs et al., 2017). Moreover, it is worth mentioning that the SPZ also provides connections between the SCN and the thalamus and the amygdala, and these pathways are linked to the circadian regulation of arousal and emotional functions (Vujovic et al., 2015) **[Figure1.4].**

Collectively, these studies delve into the internal organization of the SCN, its peculiar oscillatory properties, and the incoming inputs and output pathways. They reveal the existence of an intricate network within the SCN that justifies and explains how its position on the circadian axis is established.

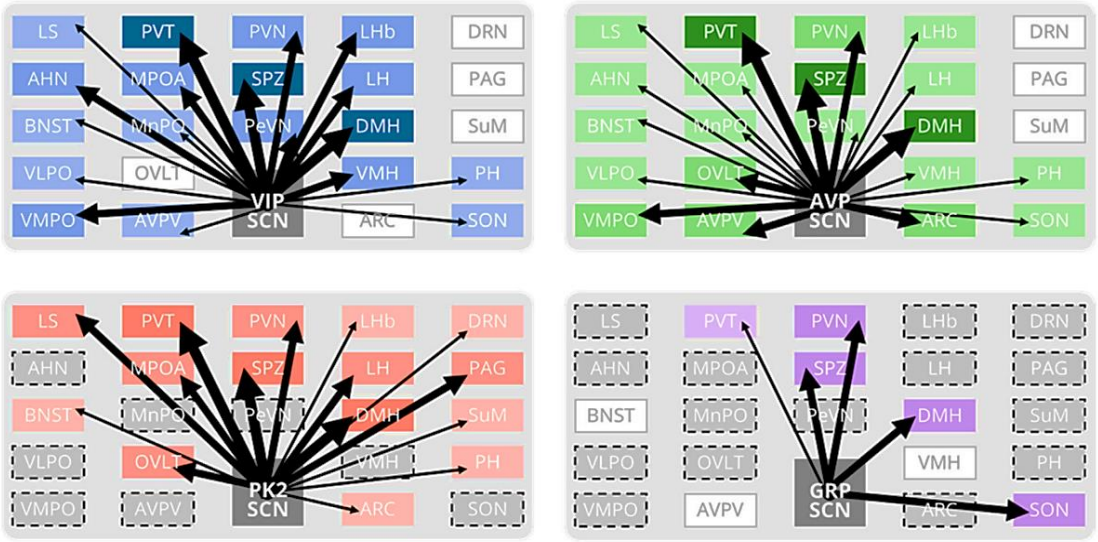

Figure 1.4: schematic representation of the SCN main efferents targeting the principal central substrates of the *circadian timing system* [image from (Starnes and Jones, 2023)].

1.2.3 Neuropeptides: *a closer look to three of the most known neuropeptides of the master circadian clock.*

The nervous system uses a wide spectrum of communication strategies to meet the complexity of its role in a living organism. Among these strategies belongs the involvement of neuropeptides. Neuropeptides can act as neurotransmitters, neuromodulators of synaptic communication, as autocrine or paracrine regulators of the environment or as hormone in a long-range action.

For a molecule to be classified as a neuropeptide it has to be a genetic product of neurons and possess a signal peptide that directs it through the ER-Golgi regulatory pathway for the synthesis. This synthesis ends in crucial post-transduction modifications (i.e. endoproteolytic and exoproteolytic cleavage, amidation of the C-terminal etc.) of the neuropeptide to make it active and protected by degradation, until it is stored in granules and large-core vesicles. These large-dense core vesicles (LDCV), typically 80-120nm in diameter, originate from the trans-Golgi network and traverse neuronal terminals through a dynein/kinesin dependent mechanism along

the cytoskeleton. Evidence suggest that these LDCVs can be secreted following high-frequency neuronal activity and significant changes in intracellular calcium concentration, but the precise mechanism of their release remains unclear. Once released, neuropeptides exert their influence by directly interacting with G protein coupled receptors located on the neuronal plasma membrane of post-synaptic neurons, or diffuse and reach other neighboring neurons in a process named *volume transmission*, or they can regulate glial cells or act on the surface of other cells as hormones (Eiden et al., 2022). The precise quantity of peptide contained within the LDCVs and the extent of its release upon demand remain unclear. Microdialysis studies suggest concentrations ranging from pico- to nanomolar levels, although the technique's limitations may lead to underestimations (Kendrick, 1990).

Neurons, within the same cell types, can express different types of neuropeptides. Interestingly, these molecules can elicit effects opposite to their colocalized neurotransmitters, thereby modulating communication rapidly. As an example, dynorphin's action on the mossy fiber of the hippocampus is recognized for its essential role in retro-feedback, effectively reducing glutamate release by acting on the pre-synaptic terminals (Iremonger and Bains, 2009).

The direct role of neuropeptides can be crucial for the physiology, or they can be essential in defining specific cell groups. In the case of the SCN, as described earlier, a multitude of neuropeptides play a critical role in neuronal activity and processes related to circadian rhythm and behaviors. Neuropeptides associated with the SCN output have proven to be central for humoral communication. SCN transplantation from a donor to a host animal results in a restoration of rhythmic behavior, but not in the restoration of synaptic output/input contact. Interestingly, when the SCN is transplanted within a semipermeable polymeric capsule, which prevents synaptic communication, the transplanted SCN partially restores circadian rhythms. This suggest that in fulfilling its role the SCN relies not exclusively on synaptic communication but also on humoral communication facilitated through the release of neuropeptides. Notably, neuropeptides such as AVP and VIP were detectable in the polymeric graft (Lehman et al., 1987; Silver et al., 1996).

Therefore, when discussing the SCN output, it becomes essential to consider not only GABA, the principal neurotransmitter, but also the ability of peptides to mediate or modulate a response, even though the precise pathway and timing of their release remain unclear.

Neuromedin U and Neuromedin S (NMU/NMS): peptide, receptors and physiology.

Neuromedin U (NMU) was isolated in the porcine spinal cord in 1985 by Minamino *et al*. (Minamino et al. 1985) and the structurally related Neuromedin S (NMS) was isolated from the

rat brain in 2004 by Mori *et al.* (Mori et al. 2004). As reported by L.K. Malendowicz and M. Rucinski (Malendowicz and Rucinski, 2021) NMU and NMS are the products of alternative splicing from the precursors prepro-NMU and prepro-NMS which are localized in the chromosome 5 and chromosome 1 in *Mus musculus*. The final active protein is about 23 amino acids (aa) for NMU and 36 aa for the NMS.

NMU is highly expressed in peripheral tissue (adrenal gland, uterus, gut, and testes) and in the rat brain it is localized in different nuclei of the hypothalamus (suprachiasmatic nucleus, hypothalamic median eminence, nucleus arcuate, in the ventromedial hypothalamus). It is also found in the caudal brainstem (nucleus of solitary tract, area postrema, dorsal motor nucleus of the vague nerve and inferior olive) (Howard et al., 2000; Graham et al., 2003; Graham et al., 2005). The NMS shows a relative low expression in the spleen, testes, lung, thymus, and gut with its main localization restricted to the central nervous system (CNS). Quantitative RT-PCRs of CNS tissue show very low levels of mRNA in the LH, VMH, median eminence, PVN, ARC, SON, dorsal raphe (DR), substantia nigra (SN), locus coeruleus (LC). However, in the suprachiasmatic nucleus of the hypothalamus the expression is extremely high, with a predominant localization in the core of the nucleus (Mori et al., 2004).

While structurally different especially in the N-terminal amino acidic sequence, both peptides share a similar biochemical structure enabling the ligand's agonistic activity onto the GPCRs NMUR1 and NMUR2. In both peptides the amidated (Asn) C-terminal pentapeptide (-Phe-Arg-Pro-Arg-Asn-NH2) is crucial for receptor activation, while the N-terminal is thought to be responsible for receptor affinity. NMU exhibits high affinity for both receptors at nanomolar concentrations, whereas NMS binds to both receptors, showing higher affinity for NMUR2 already at picomolar concentrations (Hsu et al., 2007).

Both NMU and NMS exert their effects by binding the GPCRs NMUR1 and NMUR2. However, while NMUR2 is predominantly expressed in the CNS, NMUR1 is apparently linked to the modulation of peripheral biological processes (i.e. testis, pancreas, gut, lung, kidney, uterus). In the rat brain, studies of NMUR2 expression using *in situ* hybridization localized the receptor primarily in the PVN, on the wall of the third ventricle, in the CA1 region of the hippocampus and the spinal cord, and very low signal is also detected in the cortex, cerebellum and thalamus (Howard et al., 2000; Fujii et al., 2000; Hosoya et al., 2000; Guan et al., 2001). There is also evidence of some expression in the ARC and in clusters of neurons in the DMH as well as surrounding the VMH (Graham et al., 2005).

The signaling pathway activated by NMUR1 and NMUR2 can differ significantly. Both receptors can initiate an intracellular signaling cascade mediated by the Gq/11 or Gi proteins, suggesting

activating or inhibiting response, respectively. Specifically, NMUR2 primarily appears to act through the inhibitory Gα protein (Brighton et al., 2004; Hsu et al., 2007; You et al., 2022). At the CNS level, their impact on the electrophysiological properties of the neurons has been less explored. In PVN brain slices, where NMUR2 is highly expressed, NMU has been associated with an enhancement of the firing activity of a specific neuronal subpopulation. This mechanism involves the production of cGMP and its effect on activating the hyperpolarization-activated inward conductance (Ih) (Qiu et al., 2003). This finding is confirmed by multi-electrode arrays (MEA) recordings, where NMU application led to an increase in the number of spikes in both the PVN and ARC in rat brain slices (Nakahara et al., 2010).

Most of the research on the physiological role of these peptides focuses on NMU, the first isolated peptide. However, there is compelling evidence suggesting a role in the control of autonomic functions at both central and peripheral levels, by both NMU and NMS. NMU administration elicits a sustained increase in blood pressure (Minamino et al., 1985) and NMS directly regulates the L-Type calcium channel currents in cardiomyocytes (Chen et al., 2012). The action of NMU is highly involved in the central regulation of feeding and digestive processes. Peripherally NMU affects smooth muscle contraction in the gut and inhibits insulin secretion (Kaczmark et al., 2006). The intracerebroventricular (i.c.v.) administration of NMU results in the suppression of food intake in rats (Howard et al., 2000), along with an increased in core body temperature within the first hour after the administration and elevated locomotor activity. These effects suggest an anorexinergic and catabolic role for the peptide. A similar and more effective role in energy homeostasis is exerted by NMS, as shown by Nakahara *et al.* (Nakahara et al., 2010), likely through a specific mechanism that could involve the stimulation of pro-opiomelanocortin (POMC) neurons in the ARC. Both peptides are associated with an increase in mRNA expression of POMC in ARC and corticotropin-releasing hormone (CRH) in PVN neurons.

In addition to their roles in energy homeostasis, NMU/NMS signaling is closely associated with the stress response, particularly involving the hypothalamic-pituitary-adrenal axis (HPA). For instance, CRH receptor antagonists have been found to attenuate the grooming behavior induced by i.c.v administration of NMU (Hanada et al., 2001). Moreover, plasma concentration of adrenocorticotropic hormone (ACTH) and corticosterone significantly increase in a dose-dependent manner following direct injection of NMU into the PVN, a major site expressing the NMUR2 receptor and housing the CRH neurons (Wren et al., 2002). Similarly, like NMU, NMS also induces a marked activation of the HPA system, displaying a linear dose-response curve in enhancing ACTH release (Jászberényi et al., 2007).

In addition to their roles in stress response and energy homeostasis, NMU and NMS display functions related to the circadian system. As already mentioned, both peptides are expressed in the SCN neurons, with the NMRs being present, particularly with NMUR2 being more represented. *In situ* hybridization studies have revealed that NMU mRNA in the SCN follows a clear circadian rhythm, peaking between zeitgeber time (ZT) ZT6 and ZT10. This pattern is maintained in constant darkness, suggesting a strong genetic circadian control over NMU expression (Graham et al., 2005). In "*The gut-brain peptide neuromedin U is involved in the mammalian circadian oscillator system*" Nakahara *et al.* show that both NMUR2 and NMUR1 (albeit less expressed) mRNA are expressed in the SCN and subjected to a circadian rhythmicity of expression. Given these findings, it should not be surprising that both NMU and NMS are able to influence the circadianity of biological processes, inducing a significant shift in the phase response curve (PRC) when administered intracerebroventricularly (Nakahara et al., 2004).

Several neuropeptides are implicated in the mechanisms of circadian entrainment, acting as non-photic regulators. In the SCN, such as with NMU, the expression of NMS mRNA fluctuates under light/dark condition, but not under constant darkness. This rhythm aligns with an independence of the peptide to the clock genes, given the absence of the CACGTG E-box, while it remains as a regulator influenced by light conditions. However, being a regulator doesn't necessarily imply essentiality for a function to occur. Although the two peptides exhibit a significant correlation with the circadian system and play a role in circadian regulation, their specific actions are not essential for determining circadianity. Monitoring locomotor activity in both LD and constant darkness (DD) highlights that the KO mice NMS ($Nms^{-/-}$), NMU ($Nmu^{-/-}$), and both peptides ($Nms^{-/-}Nmu^{-/-}$) exhibit normal free running periods and amplitudes comparable to wild-type (WT). Indeed, the overlapping of NMS/NMU expression with VIP and AVP neurons (Lee et al., 2015), underscores how the absence of NMS/NMU can be compensated by two stronger circadian regulators, VIP and AVP. Despite this compensation, the action of SCN neurons expressing NMU and NMS remains highly necessary for SCN synchrony and circadian periodicity establishment, confirming a more adaptive role of these signaling molecules. Indeed, the re-entrainment after an LD shift in NMU knockout mice took longer than in wild-type (Nakahara et al., 2004).

In summary, the precise mechanisms through which NMU and NMS influence circadian rhythms are not fully understood. However, their rhythmic expression patterns, along with evidence of their role in food intake, stress regulation, and phase shifting, strongly suggest their involvement in circadian regulation.

Vasoactive Intestinal Polypeptide (VIP): peptide, receptors and physiology.

Isolated in 1970 from the porcine gut (Said and Mutt, 1970), vasoactive intestinal peptide (VIP) is a 28 amino acid neuropeptide belonging to the secretin superfamily (Moody et al., 2011). Located in the chromosome 10 in *Mus musculus*, the gene encodes for a 170 amino acids precursor peptide (prepro-VIP) from which the active VIP-28 derives. VIP-28 is characterized by a random coil structure at the N-terminal (position 1-6), which represents the biochemical link for receptor binding (Tan et al., 2006).

VIP primarily functions through the VPAC1 and VPAC2 subclasses of G-protein receptors, and sharing 68% sequence homology with PACAP, it exhibits also limited affinity for the pituitary adenylate cyclase-activating polypeptide type 1 (PAC1) receptor (Harmar et al., 2012). These receptors belong to the class B of G-protein coupled receptors (GPCRs), also known as the "secretin-like" family receptors. Sharing the similar structure of the GPCRs family (seven hydrophobic transmembrane helices and the intracellular C-terminal), they possess a specific N-terminal ectodomain (>120 residues named N-ted) containing a hydrophobic signal peptide and the hormone binding domain (Laburthe et al., 2007). Conversely, ligands such as VIP have a specific N-cap sequence at the N-terminal, which is crucial for binding interaction and receptor activation (Neumann et al., 2008).

The intracellular signaling activated by VPACRs involves the stimulation of the adenylate cyclase (AC) and the relative production of cAMP via the $G\alpha_s$ subunit. The cAMP accumulation can lead to the activation of cyclic nucleotide-gated ion channels (CNG) (Biel and Michalakis, 2009) and of protein kinase A (PKA). Through phosphorylation PKA can modulate the activity of ion channels and synaptic release, and acting on CREB it influences gene expression. In addition, other signaling pathways independent of cAMP are associated with VPAC receptor activation. *In vitro* studies have shown that, depending on cellular activity, the intracellular pathway of VAPCRs can involve also the $G\alpha_q$ pathway (Laburthe et al., 2002; Langer, 2012). The activation of phospholipase C (PLC) leads to the formation of the diacylglycerol (DAG) and inositol-3-phopsphate (IP3) that trigger phosphokinase C activation and intracellular calcium release from intracellular calcium stores, respectively. These two mechanisms, in turn, can regulate gene expression through a MAPK pathway. Indeed, the antagonism of ERK1/2, component of the MAPK pathway, significantly reduces the phase-shift effect induced by VIP application in SCN slice expressing PER2::LUC. Moreover, increased phosphorylation of ERK1/2 is detectable after VIP action (Hammett et al., 2019).

VIP has shown to be involved in many physiological processes and is even considered as a candidate therapeutic agent for the treatment of various pathological conditions. It exhibits anti-

inflammatory properties (central and peripherical) in autoimmune disorders (Ganea et al., 2015). It acts as a vasodilator factor with potential application in the treatment of pulmonary hypertension (Petkov et al., 2003) and asthma (Wu et al., 2011). Its role in promoting neuronal trophism and neuroprotection suggest it could be used to limit the progression of neurodegenerative disease, like Alzheimer's disease (Morel et al. 2012; Cunha-Reis and Caulino-Rocha, 2020). VIP is expressed in many tissues of the body, where it regulates a wide range of homeostatic function related to metabolism, respiratory and endocrine systems (Winzell & Ahren, 2007; Human protein atlas, 2020; Carrion et al., 2020).

In the brain, single cell RNA analysis revealed that VIP expression correlates with inhibitory neurons. Moreover, subcellular cytoplasmic analysis of its localization in the endoplasmic reticulum, predicts its secretions and its action as neurotransmitter or neuromodulator (Sjöstedt et al., 2020). In the brain, VIP plays crucial roles in the neuronal growth, learning and plasticity processes, modulating the neuronal activity in regions such as the hippocampus (Cunha-Reis and Caulino-Rocha, 2020). Remarkable is its action on the HPA axis. VIP secreted by the pituitary gland can elicit the release of CRH, and VIP receptors are present along various components of the HPA axis (Nussdorfer, 1998). Above all these biological effects, VIP is recognized to be the peptide that defines the core of the suprachiasmatic nucleus and to be one of the most essential neuromodulators for the stability, mechanism and development of circadian rhythms.

While the VPAC1 receptor is strongly associated with learning and memory processes in the brain, VPAC2, along with its ligand VIP, constitutes an authentic regulatory axis for maintaining the biological balance of circadian rhythms (Usdin et al., 1994; Morell et al., 2012). VIP and its receptor VPAC2 are highly expressed in the suprachiasmatic nucleus. In the SCN, different neuronal population express VPAC2 mainly in the soma and dendrites (An et al., 2012). Notably, approximately 91% of the AVP neurons in the SCN express VPCA2 mRNA (Kalamatianos et al., 2004). While VIP is expressed only in 10% of SCN neurons, restricted to the SCN core, SCN^{VIP} positive neurons form synapses with 50% of neurons in the SCN (Mazuski et al., 2018). This high degree of internal communication between SCN^{VIP} neurons and other neuronal populations suggests a first-line role in SCN neuronal synchronization. Indeed, their strategic position as principal contacted neurons of the RHT, suggests that SCN^{VIP} can work as linker between incoming photic input and SCN outcome, thereby favoring the stability of the phase of the nuclei (Jones et al., 2018). Given these observations, is not surprising that there is a synergistic action of VIP and SCN^{VIP} neurons in serving as a photic codifier and activity synchronizer. In the SCN both VIP and VPAC2 exhibit circadian regulation. VIP is released in a circadian fashion, peaking in the early night under light/dark conditions (Albers et al., 1990;

Shinohara et al., 1993). However, no circadian rhythm is observed under constant conditions (LL or DD) (Shinohara and Inouye, 1995). Interestingly, under constant light conditions, VIP release becomes non-rhythmic, indicating a dependence relation between the LD cycle and peptide signaling. VPAC2 mRNA levels (Shinohara et al., 1999) show rhythmicity under LD cycle, but not in DD. VPAC2R mRNA levels do not change, suggesting that the oscillations of the VPAC2R are more related to post-translational control (An et al., 2012). Moreover, as shown by Jones *et al.* (Jones et al., 2018) VIP neurons in the SCN show a daily rhythm in spontaneous calcium activity *in vivo* as well as daily rhythms of VIP spontaneous or NMDA-evoked release, which align with the time in which the light has the major power on phase-shifting, particularly at dusk. Finally, chemogenetic blocking of the activity of these neurons attenuates light-induced phase shifts. Consistent with this study, the administration of VIP *in vitro* and *in vivo* can phase-shifts the SCN activity rhythm (Piggins et al., 1995; Meyer-Spasche and Piggins, 2004). Indeed, one of the most important effects of VIP is its ability to act genetically at the level of the TTFL in the SCN neurons, inducing the expression of clock genes such as Per1-2. This effect is mediated by the AC/cAMP/PKA/CREB pathway, serving as principal mediator between the photic input and the oscillatory activity mediated by VIP through VPAC2R (Nielsen et al., 2002). Moreover, the observation that the cells of the shell desynchronize when separated from the core (Yamaguchi et al., 2003) is consistent with the ability of the VIP neurons to maintain internal synchrony in the SCN, and in Vipr2-/- KO mice the rhythm of AVP is abolished. Both Vip-/- and Vipr2-/- KO mice show an inability for the SCN to be synchronized *in vitro*, and the amplitude of electrical activity is attenuated. While these genotypes lose many daily rhythms in constant darkness conditions *in vivo*, they are not affected by the LD cycle (Harmar et al., 2002; Aton et al., 2005; Maywood et al., 2006). The application of VPAC2 agonist in Vip-/- SCN neurons restores rhythmicity and synchrony in the SCN (Maywood et al., 2006), while the Vipr2-/- SCN show low and arrhythmic expression of clock genes (Nielsen et al., 2002). Moreover, mice overexpressing VPAC2R in the SCN have a shortened free-running period in constant darkness and show faster re-synchronization to the LD cycle (Shen et al., 2000). These findings collectively underscore the importance of the VIP/VPAC2 axis in maintaining circadian rhythmicity and synchronicity within the SCN.

In conclusion, it is noteworthy that SCN^{VIP} neurons and their relative pathway appear to play a crucial role in regulating locomotor activity and temperature rhythms, rather than directly influencing the sleep/wake cycle. Optogenetic stimulation of SCN^{VIP} neurons in enucleated animals induces a phase-shift in both the molecular clock and locomotor activity (Mazuski et al., 2018). Disrupting the circadian molecular clock by specifically targeting SCN^{VIP} neurons or

selectively eliminating these neurons, leads to changes in the rhythmic patterns of locomotor activity and body temperature when exposed to the LD cycle, ultimately resulting in complete arrhythmicity in constant darkness. Notably, the deletion of SCN^{AVP} neurons does not yield the same outcomes. While, chemogenetic activation and *in vivo* fiber photometry studies suggest that the SCN^{VIP} neuronal subregion may not directly drive sleep or arousal but more likely influences the expression of the sleep-wake rhythm (Todd et al., 2020).

Arginine-Vasopressin (AVP): peptide, receptors and physiology.

Coded by the AVP gene on chromosome 2 of *Mus musculus*, arginine-vasopressin undergoes cleavage steps from the 164 amino acidic sequence that defines the prepro-vasopressin (pre-proAVP) to the final sequence of the active nonapeptide.

The primary source of vasopressin is represented by the magnocellular neurosecretory neurons of the paraventricular nucleus and the supraoptic nucleus of the hypothalamus, which are directly connected with the hypophysis gland. Here, AVP is stored in granules and released into the system especially in response to changes in extracellular osmolality. The principal function known of vasopressin is its antidiuretic effect, exerted along the epithelium of the collecting duct in the kidney, where it stimulates processes of water reabsorption, contributing to an increase in blood pressure and volume, cardiac output and the consequently stability of the serum osmolality in the range of 290-294 mosmol/kg. In addition to its antidiuretic effect, as a hormone, AVP stimulates the production of the adrenocortical hormone by acting on adrenal cortex and medulla cells (Vallotton, 1991) and induces insulin production in β-pancreatic cells (Folny et al., 2003).

There are three AVP receptors: V1a (Avpr1a), V1b (Avpr1b) and V2 (Avpr2). In the periphery, AVP primarily acts through the V2 receptors, for which two different intracellular mechanisms have been described. One involves the activation of adenylate cyclase and the production of cAMP, while the other is associated with a transient intracellular increase in calcium concentration (Champigneulle et al., 1983, Ecelbarger et al., 1996). In primary cultures of the inner medullar collecting duct, the latter mechanism involves the activation of the ryanodine receptors on intracellular membrane compartments (Chou et al., 2000, Hoffert et al., 2012). In rodents the V1a receptor is the most abundantly expressed central AVP receptor and has been detected in various brain regions, including the prefrontal cortex, hippocampus, throughout the hypothalamus, amygdala, lateral septum, ventral tegmental area, substantia nigra, superior colliculus, dorsal raphe and the inferior olive. While the V1b is more known as the vasopressin receptors regulating the HPA axis and stress response and its presence in limbic brain areas

together with the V1a, can explain the central role of behavioral effects induced by the vasopressin (Caldwell et al., 2007, Rae et al., 2021).

Both V1a and V1b act via Gq/11 and Gi/o-mediated signaling pathways, whereas V1b is also coupled to Gs-mediated signaling. And a specific observation done by Thibonnier *et al*. in humans (Thibonnier et al., 1998) highlights how very little differences in the density of the receptors on the cell's surface can have deep consequences in the final effect of the ligand: a low density is coupled to the activation of the $G\alpha_q$ pathway, while a high density is coupled to the recruitment of $G\alpha_s$ pathway.

AVP is also expressed in neurons of the medial amygdala, the bed nucleus of the stria terminalis (BNTS) and their projection to the preoptic and the olfactory areas confers (Sofroniew, 1983) to AVP behavioral aspects regarding social recognition, aggression, bonding and sexual behaviors. However, its presence in the SCN is particularly important, as it widens the spectrum of its action also to the regulation of circadian rhythms.

As circadian neuromodulator the AVP starts its action by being released by RHT cells of the retina. In a study conducted *in vivo* in rats AVP modulates the SCN activity, with its release triggered by light stimulation or electrical stimulation of RHT (Tsuji et al., 2017). Another circadian aspect for AVP involves its expression pattern. In wild-type animals AVP shows a high amplitude level during the early day, and low amplitude level during the late afternoon in the SCN. In contrast, in Clock-mutant mice, the expression curve is flat, indicating a lack of circadianity. Not surprising, the genetic analysis proved that the AVP promoter contains E-box elements, the DNA sequence for the action of CLOCK:BMAL1. Molecular assays confirmed the interaction between these elements and the AVP expression dependence on them (Schwartz et al., 1985). Moreover, the *in situ* hybridization for the V1a receptor in the SCN under DD defines a rhythm for the V1a with a peak in the early subjective night (Jolkkonen et al., 1988).

More interesting are the phenotype resulting from the double KO mice for the V1a/V1b receptors. These mice do not exhibit the profound consequences in the circadian rhythms of clock genes and behavior seen with the removal of one of the components of the VIP-VPAC2 axis. For example, the V1a KO leads only to attenuation in locomotor activity rhythms. However, this milder circadian impaired phenotype shows a remarkable resistance to experimental jet-lag conditions with almost immediate re-entrainment after an 8h advanced shift in light onset. This resistance persists even in DD conditions and is not masked by the LD cycle. And most remarkable *in vivo* stimulation of SCN neurons through antagonist of the AVP receptors, speeds up the jet-lag adaptation of wild-type mice (Yamaguchi et al., 2013). These results indicate that the absence of AVP modulation may indicate weaker network coupling within the SCN, and that

AVP act as a strong brake to environmental changes, contributing to the robustness of the pacemaker. Interestingly, AVP characterizes and defines the boundaries of the dorsal region of the SCN. Specifically, expression of AVP is high in the dorso-medial SCN, a region that has been demonstrated to be the phase-leading and the starting point of circadian calcium oscillations in the SCN. These oscillations develop as a dorso-ventral topological wave with a dorso-ventral coupling via a firing-dependent mechanism (Jin et al., 1999; Yamaguchi et al., 2003; Li et al., 2009; Enoki et al., 2012).

Concluding, the direct release of AVP from the SCN^{AVP} neurons represents a mechanism through which the SCN can regulate the physiology of the entire central nervous system. It is well established that a circadian rhythm in the AVP concentration can be observed in the cerebral spinal fluid (CSF), which is not abolished by the lesion of PVN or SON, but is flattened by lesions of the SCN. Recently histological evidence confirmed that the SCN^{AVP} neurons can indeed reach the epithelium of the third ventricle (Schwartz et al., 1985; Jolkkonen et al., 1988; Taub et al., 2021) providing a pathway for the paracrine effect of AVP.

1.3 THE CIRCADIAN TIMING SYSTEM.

The SCN has been defined as the pacemaker of circadian rhythms and this function begins primarily at a molecular level in orchestrating timing through a coordinated interplay of proteins and ribonucleic acid – a process described as "*protein tic and ribonucleic tac*" (Foster and Kreitzman, 2012). The discovery of this genetic engine behind circadian rhythms, has opened the door to specific manipulations and investigations which has permitted to reveal that the structures that regulate the circadian rhythms form an organized circadian system composed of many clocks throughout the body. The system operates through a TTFL that acts within each cell, allowing each cell to work as a biological circadian oscillator capable of controlling ubiquitous and tissue specific functions. Real-time bioluminescent and fluorescent reporters fused with TTFL components, such as Per1, Per2, Cry1 has permitted to understand the spatio-temporal dynamics of these elements in peripheral organs including liver, heart, pancreas, stomach, skeletal, retina, thyroid, adrenal gland and lungs (Kuhlman et al., 2000; Yoo et al., 2004; Yamamoto et al., 2004). The molecular oscillation in these tissues persists from the *in vivo* conditions to the *in vitro* cell cultures for several cycles, but these oscillators tend to de-synchronized and to dampen over time in the absence of specific input (Balsalbore, 1998). For example, fibroblast cultures exhibit strong oscillations without the contribution of input from surrounding cells for several days; this oscillation are temperature compensated and the rhythm can be restored by a secondary stimulus after damping down the oscillation (Izumo et al., 2003).

However, peripheral oscillators are desynchronized with each other and over time they lose phase and amplitude coherence in absence of specific input or system integrity (Nagoshi et al., 2004) highlighting differences between peripheral clocks and the central clock in the SCN. Thus, the SCN serves as the master clock, providing incoming input to synchronize peripheral clocks into an integrated circadian system. Both the humoral effectors and the synaptic connection are important for the SCN to communicate with other organs allowing for top-down control of circadian rhythms. Indeed, SCN ablated mice show a loss of coherence in the peripheral TTFL, together with the disruption of several circadian rhythms. However, the transplant of an intact SCN in the lesioned animal can restore coherent oscillations in liver and kidneys, probably through humoral communication. Instead, organs like the heart, spleen and adrenal gland may require an intact network to be entrained by the master clock (Guo et al., 2006; Tahara et al., 2012), as demonstrated by tracing studies revealing multisynaptic circuit from the SCN through the PVN, to the heart. A recent work (Paul et al., 2020), for example, has even shown how the chemogenetic activation of the SCN^{VIP} neurons can modulate the heart rate in a time-dependent manner, inhibiting it especially during the early-day.

Transneuronal tracing using virus (i.e. alpha herpes viruses) have found several polysynaptic connections between the SCN and various organs or glands. One of the primary pathways through which the SCN controls circadian rhythms is the SCN–PVN–intermediolateral horn of the spinal cord–superior cervical ganglia–pineal gland circuit. This pathway regulates the circadian secretion of the hormone melatonin, which plays a crucial role in the sleep-wake cycle. In addition, connections passing through the sympathetic nervous system link the SCN with the white adipose tissue and the brown adipose tissue, influencing the lipolysis/lipogenesis cycle and thermogenesis. Generally, polysynaptic circuit passing through the sympathetic and parasympathetic branches of the autonomic nervous system has been described also for organ such as the spleen, pancreas and adrenal gland. This robust, long range and integrate network allows the SCN to exert its control over various physiological functions throughout the body (Bartness et al., 2001).

The SCN serves as the master regulator of the hierarchy Circadian Timing System (CTS), exerting its primary control at central level on a “network of interconnected diencephalic structures” (Moore, 2013) (PVN, DMH, VMH, ARC, SON, VLPO, SPZ, etc). Through both humoral and neural output pathways, the SCN communicates with these interconnected brain regions to coordinate rhythms **[Figure1.5].** Thus, the exploration of the characteristics of the main nuclei targets by the SCN becomes fundamental to understand how the SCN works and then how the biological processes develop.

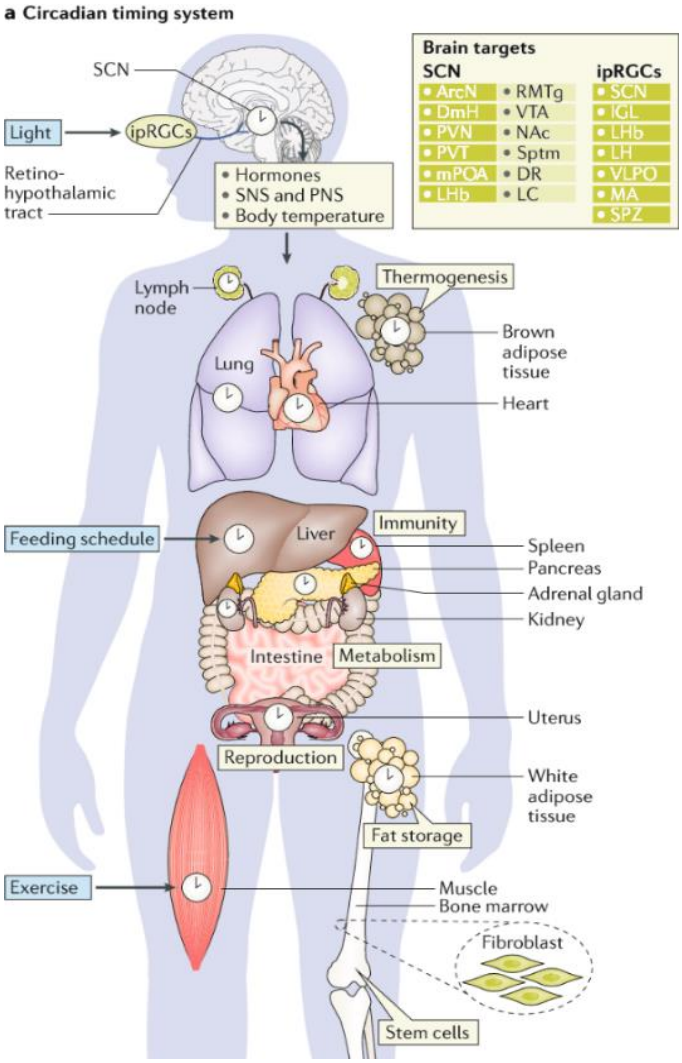

Figure 1.5: the circadian timing system. The light represents the principal zeitgeber for the regulation of the circadian functions, but other vital stimuli can participate in the synchronization of the circadian elements, such as feeding schedule or exercise or more psychological like social interaction. In this complex network of central and peripheral oscillators, the suprachiasmatic nucleus is the pacemaker core and integration center of external and internal stimuli that determine daily homeostatic body physiology, [image from (Logan and McCLung, 2019)].

1.3.1 A first diencephalic node of the SCN output: *the subparaventricular zone (SPZ) internal organization and connectivity.*

The SPZ **[Figure 1.6]** is considered the first node for the majority of SCN synaptic output, and a developmental study has found that rhythms of locomotor activity and hormone release are disconnected from the SCN oscillation until the formation of the efferent connection with the SPZ (Ban et al., 1997). The SPZ is located just dorsally to the SCN, laterally to the third ventricle, and ventrally to the hypothalamic paraventricular nucleus (Paxinos and Franklin, 2001), and its ventro-dorsal division extends along the antero-posterior axis between Bregma –0.34mm and Bregma -0.94mm, with the most ventral part located in the rostral portion and the most dorsal

region located in the caudal area. The signal for the glutamate vesicular transporter in the SPZ is practically absent, while the GABA vesicular transporter and glutamic acid decarboxylase 67 are highly expressed, making the SPZ a GABAergic nucleus (Lei et al., 2007). Regarding the neurochemical asset of the SPZ, information in literature is practically absent. Some evidence suggests the presence of a dopaminergic cluster (Vujovic, 2014) located primarily in the medial SPZ, an observation that correlates with a positive signal for the tyrosine hydroxylase from the *in situ* hybridization data of the Allen Brain Atlas. From the same atlas it is possible to recognize a clear signal for Sst (somatostatin), Avp (AVP), Adcyap1 (PACAP) and a very high signal for Penk (pro-enkephalin), Pnoc (pro-pre-nociceptin) and for the Trh (thyrotropin releasing hormone) genes. As marker is highly expressed Calb2 (calbindin 2) which correlates with the presence of the vitamin D receptors (Vdr), and interesting is a good signal for the Nos-1 (nitric oxide synthase 1) gene. A light signal for Gal (galanin) and Ox (oxytocin) seems also to characterize some neurons of this area (Allen Mouse Brain Atlas, 2004). What is the role of these peptides and proteins, or of the populations that produce them, remain completely an object of study.

If for the SPZ we cannot talk of a specific neuronal population involved in a specific function, the complexity of the nucleus and its implication in circadian function have already been addressed at an anatomical and functional level. Regarding the SPZ input, the evidence in the literature primarily describe the afferents from the SCN and RHT. The SPZ receives a strong input from the SCN as demonstrated by the anatomical SCN tracing studies. Specifically, the SCN^{AVP} and SCN^{VIP} neurons project to the SPZ with a topographical organization which is conserved across mammals (Campos et al., 2014). The SCN^{AVP} neurons mainly innervate the medial SPZ whereas the SCN^{VIP} project to the lateral SPZ with a small zone of partial overlapping in the central region of the SPZ (Vujovic et al., 2015). This organization helps to define the boundaries of the SPZ along the anterior-posterior axis (Abrahamson and Moore, 2001; Todd et al., 2018). Additionally, the double KO mutant for the prokineticin 2 signal show a deep state of torpor induced by food deprivation compared to the WT and the lack of ProkR2 impairs locomotor activity and the thermoregulation cycle. Interestingly, SCN prokineticin 2 positive neurons project to the medial and dorsal SPZ, a region which has been associated with the circadian control of temperature (Zhang et al., 2009).

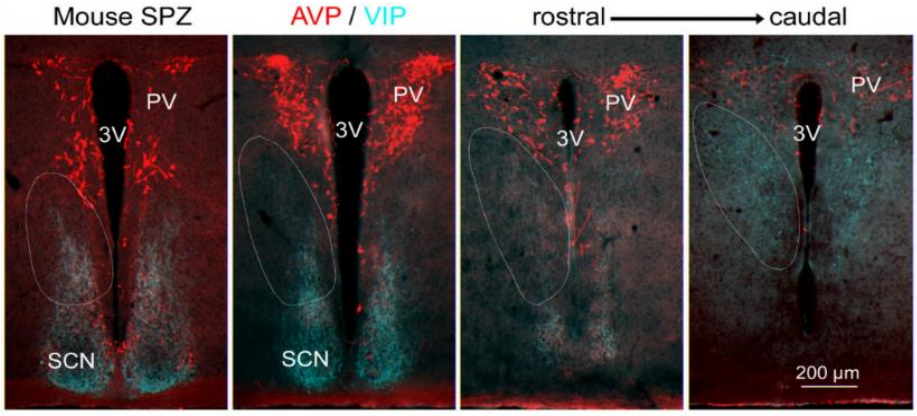

Figure 1.6: image showing the rostro-caudal development of the mouse hypothalamic subparaventricular zone (white ovals) defined by SCN^{VIP} fibers (*turquoise*) and AVP-somata (*red*). [Image from (Todd et al., 2018)].

As previously described the ipRGCs send input to the ventral SPZ (Hattar et al., 2006) and the establishment of this connection is particularly evident in nocturnal animal respect to the diurnal animal. The post-natal formation of this circuit seems to be related to the consolidation of nigh-time vs. day-time wakefulness (Todd et al., 2012). Interestingly, the possible role for the ventral SPZ in mediating the light masking effect, is an effect that actually has been excluded for the diurnal Nile grass rats where the lesion of the SPZ is not able to abolish behavioral acute response to light (Gall et al., 2016). This suggests that other retinorecipient areas, such as the intergeniculate leaflet, are involved in the response to acute light exposure.

The functional significance of the ventral and dorsal SPZ has been elucidated through lesion studies. The lesion of the ventral SPZ drastically reduce the circadian rhythms of sleep/wake cycle and locomotor activity. Conversely, lesions of the dorsal SPZ abolish the circadian oscillations of body temperature. Interestingly, in these studies the SCN remained unaffected, apparently resistant to the cytotoxic effect of ibotenic acid used for SPZ neuronal lesions. This resistance of the SCN, underscores the necessity of the synaptic specific connections between the SCN and SPZ to establish a normal circadian rhythmicity. These regulatory roles of the SPZ in the establishment of circadian behaviors, positions it as a key node in the circadian timing system, working in concert with the SCN to maintain robust circadian rhythms (Lu et al., 2001, Moore and Danchenko, 2002).

Based on the described functional and tracing studies, the SPZ can be subdivided in four quadrants: a ventro-medial and ventro-lateral SPZ (vmSPZ-vlSPZ), and a dorso-medial and dorsolateral SPZ (dmSPZ-dlSPZ) (Vujovic et al., 2015). A systematic analysis of the output tracing data of the SPZ conducted in rats has delineated different major roles for these subregions, highlighting their similarity to the target regions of the SCN and positioning the SPZ as relay nuclei of the circadian pacemaker. The vmSPZ plays as regulator of the sleep/wake cycle through

its projections to the parabrachial nucleus (PB), LC, pre-coeruleus region (pre-LC), DR and the hypothalamic VLPO and DMH. In addition, the projections to the DMH and to the ARC involve the vmSPZ in the regulation of feeding and corticosteroids release. The dlSPZ projects to the ventral tegmental area (VTA) suggesting a role in reward behavior. Furthermore, projections to the VMH have been implicated in a specific circuit for the circadian regulation of aggression behavior (Todd et al., 2018). Instead, dlSPZ projections to the preoptic area (POA) contribute to thermoregulation. Finally, all these subregions show a significant internal communication within the SPZ, supporting the role of the SPZ in the integration of information from different brain regions. This internal connectivity expands the complexity of the SPZ and underscores its importance in coordinating various physiological and behavioral processes regulated by the circadian timing system.

Finally, as many other regions of the CNS the SPZ show a circadian pattern of its neuronal activity. Unlike the activity of the SCN neurons which is in phase with the light cycle in both diurnal and nocturnal animals, the firing of the neurons in the ventral SPZ is independent of the light cues. Instead, as shown by multi-unit-activity recordings, it is in phase with the arousal state and locomotor activity in both diurnal (Sato et al., 1984) and nocturnal (Nakamura et al., 2008) species, indicating a potential role for the SPZ in the evolution of diurnal and nocturnal adapting behaviors (Schwartz et al., 2004; Schwartz et al., 2009). Moreover light stimulation of the SCN inhibits the SPZ activity and locomotor activity *in vivo*, indicating a correlation between these two nuclei (Nakamura et al., 2008). Additionally, the SPZ shows circadian oscillation *in vivo* in clock gene *Cry* with rhythms that are phase advanced compare to those of the SCN (Mei et al., 2018).

Therefore, the available functional and anatomical data support the idea that SPZ may function as an integrator and amplifier, relaying information from the SCN to downstream pathways (Saper et al., 2005). However, due to limited scientific work on SPZ, further research specifically focused on the SPZ is needed to fully understand its role in circadian regulation and behavior.

1.3.2 Circadian rhythm outcome: *the circadian physiology of corticosterone release.*

The diurnal fluctuations of the rhythmic circadian outcomes are the results of the SCN communication with the body in a synergistic way where the timing of the events is synchronized to the light/dark cycle which in turn reflects the sleep-wake cycle pattern. Like a connection between these two cycles, is located the hormonal circadian cycle of glucocorticoids, such as cortisol in human and corticosterone in rodents (Touitou et al., 1990; van Weerden et al., 1992; Raff, 2016).

Corticosterone pathway of release.

As many other rhythms also the corticosterone rhythm is mainly governed by the hypothalamus**.** In the paragraph "1.1 The hypothalamus" has indeed been discussed how the hypothalamus exerts its control on the endocrine system working on top of the pituitary gland. Specifically, the corticotropin releasing hormone, or CRH, is a 41-aminoacidic peptide produced by CRH positive neurons which compose the parvocellular neuronal cluster of the hypothalamic PVN. When stimulated under specific conditions the CRH neurons release the CRH into the hypothalamic-hypophysial portal system at the level of the adenohypophysis and here, by binding to its CRH-R1 GPCR receptors, it stimulates the corticotropes cells to release in the systemic circulation the ACTH. ACTH is then released by the adenohypophysis into the blood stream and then travels to the adrenal gland, where it acts on the cells of the zona fasciculata activating the melanocortin-2-receptor (MC2R). Activation of MC2R by ACTH triggers a signaling cascade leading to the *ex novo* production and release of glucocorticoids, such as corticosterone. This pathway represents the known hypothalamic-hypophysial-adrenal axis.

Corticosterone upon reaching and activating the low affinity intracellular glucocorticoid receptors alpha and beta (GRs) and the high affinity mineralocorticoid receptors (MRs) in the cytoplasm of the cells of almost all the tissues of the body such the adipose tissue, muscle, bones, liver, lungs, nervous system exerts profound effects on physiology and metabolism mostly redistributing energy resources. Corticosterone operates also as time-giver of the circadian timing system for peripheral clocks by influencing their phase and amplitude, but not directly acting onto the SCN which lacks GRs and MRs. Corticosterone then represents an indirect way through which the SCN exerts control over physiological processes mediated through the activation of GRs and MRs, which can directly regulate the expression of clock genes, such as Period. Moreover, corticosterone plays a crucial role in negative feedback regulations of the HPA axis. It inhibits its own release inhibiting the transcription of genes encoding POMC and CRH receptors, thereby reducing the synthesis and release of ACTH. This negative feedback loop, onto PVN and PVN^{CRH} neurons, helps to maintain homeostasis and prevent excessive activation of the HPA axis in response to stressors (Uht et al., 1988), **]Figure 1.7]**.

Corticosterone and circadian aspects.

Generally, corticosterone release can occur in response to two different needs: to maintain the body homeostasis and to response to stressor events. Under physiological condition corticosterone is released in a pulsatile manner, with acute increase of concentration occurring every one to two hours throughout the day establishing an ultradian rhythm, which changes in

amplitude describe a circadian rhythm. As a stressor mediator, corticosterone is released in response to a systemic or psychogenic trigger, either as an acute release in response to an unexpected event (allostasis) or as chronic release (allostatic load) in response to prolonged stressors, which develop along days or months, leading to a decreased GABAergic input and/or higher excitatory input to the CRH neurons (McEwen et al., 2015; Fuller and Arrigoni *in preparation*), resulting in sustained elevations of corticosterone levels over extended periods.

The HPA axis is the main route through which corticosterone is released, but the triggers and the underlying neuronal circuits which regulate these different releasing patterns - acute or chronic, ultradian or circadian - are still object of study. Nonetheless, different studies have delineated certain aspects about the circadian corticosterone release. Both in diurnal and nocturnal animal the plasma level of ACTH and then of corticosterone tends to rise in amplitude (not frequency) after 3 to 5 hours from the beginning of the rest phase of the animal, which coincides with the dark phase for diurnal and the light phase for nocturnal animal. A peak in hormone concentration typically occurs around the time of awakening, ensuring adequate energy availability prior to the daily phase of activity and promoting food-intake behavior (Challet et al., 1995). From the acrophase point, the level of corticosterone then starts to damp down and, gradually declining over several hours, it reaches back the nadir (Allen-Rowlands et al., 1980; Kassi and Chrousos, 2013). This cyclic pattern of hormone secretion repeats over a 24-hour period, aligning with the animal's daily activity-rest cycle.

The corticosterone cycle, as many other circadian rhythms, is governed by the TTFL. The Tau mutated hamster shows *free running* circadian rhythms for the cortisol, melatonin and luteinizing hormones that are synchronized with the activity rhythms, exhibiting a period of around 20h for the homozygous mutants and 22h for heterozygous (Lucas et al., 1999). These rhythms are also maintained in constant dark conditions (Fischman et al., 1988), confirming their endogenous nature. Moreover, bilateral lesions of the SCN abolish the circadianity of plasma corticosterone (Moore and Eichler, 1972), but even if in brain slices the SCN graft can restore rhythmicity in the PVN activity (Tousson et al., 2004), *in vivo* the SCN graft transplants do not restore the neuroendocrine rhythm. This suggests that an intact neuronal circuit is necessary to trigger the corticosterone production in a circadian fashion (Meyer-Bernstein et al., 1999). These neuronal SCN connections could directly or indirectly control the PVN or other related structures and play a crucial role in transmitting circadian signals that regulate corticosterone release. The anatomical juxtaposition of the SCN terminals into the PVN suggests a direct neuronal connection between these two structures. And more interestingly some evidence indicate that this connection could be excitatory. Accordingly, in the SCN has been described a possible pool of glutamatergic

neurons (Hermes et al., 1996; Cui et al., 2001; Perreau-Lenz et al., 2003) that generates monosynaptic excitatory post-synaptic potentials in the parvocellular neurons of the PVN when electrical stimulated. This observation increases the circuital complexity, but needs a better clarification.

In Jones *et al.* (Jones et al., 2021), optogenetic experiments have shown that stimulating SCN^{VIP} terminals in the PVN inhibits the calcium signal in PVN^{CRH} neurons, while inhibiting SCN^{VIP} increases this signal. Results from tracing studies show how the SCN neurons could contact the CRH neurons in the PVN (Vrang et al., 1995; Kalsbeek et al., 2006). But even if these experiments suggest a direct interplay between the SCN and PVN^{CRH} neurons, more conclusive evidence of this connection should be obtained in the future with optogenetic channel-rhodopsin-assisted circuit mapping (CRACM) experiments of a monosynaptic $SCN \rightarrow PVN^{CRH}$ input, in the presence of tetrodotoxin and 4-amino pyridine. Moreover, in the same paper Jones *et al*. also showed how the deregulation of the TTFL components in the PVN^{CRH} neurons influence and abolish the circadian release of hormones. And with the *in vivo* optogenetic activation of the SCN^{VIP} neurons they showed an inhibition of the corticosterone peak, highlighting the importance of the SCN-PVN circuit in regulating hormonal rhythms. The findings from Paul *et al*. (Paul et al., 2020) provide further support for the role of SCN^{VIP} neurons. The *in vitro* optogenetic manipulation of the SCN^{VIP} neurons inhibits the firing activity of the PVN neurons and, additionally, the *in vivo* chemogenetic inhibition of the SCN^{VIP} neurons elicits a time-dependent release of corticosterone, with the highest effect observed when these neurons are at their activity peak. The role of the SCN^{VIP} neurons extend beyond these findings. Studies using VPAC2 null mice demonstrated that in these animals the corticosterone rhythm is compromised, and the expression of circadian genes is disrupted in peripheral tissues (Sheward et al., 2007). Additionally, Cre-driven Caspase-3 induced apoptosis selectively in VIP neurons of adult mice, resulted in deficiencies in locomotory activity and corticosterone secretion (Mazuski et al., 2020).

Another important circadian player in the regulation of corticosterone release is the AVP. AVP acts synergistically with CRH to potentiate the activation of the HPA axis stimulating the corticotropes. AVP through the activation of PKC induces the inhibition of the background TWIK-related potassium current (TREK-1), augmenting the depolarizing effect of the CRH on the excitable corticotropes (Lee et al., 2015; Zemkova et al., 2016). Instead, the study conducted by Kalsbeek *et al.* (Kalsbeek et al., 1996) investigates the role of AVP *in vivo*. In rats the reverse microdyalisis experiments have demonstrated that the administration of AVP in the DMH during the late light phase, inhibits the daily peak of corticosterone before the onset of the active phase. This evidence is supported by the observation that the administration of an antagonist for AVP

signaling in the DMH during the second half of the light phase, causes a dose dependent increase of plasma corticosterone with a strong time dependency. This study explores both the role of DMH in the circadian control for corticosterone release and the role of one of the most important SCN peptides, AVP, and it suggests as the cessation of AVP signaling in the DMH could be a pre-requisite for the onset of the circadian peak of glucocorticoids. Notably, the AVP influence on the corticosterone release is observed when AVP antagonist is injected into the DMH, but not when AVP antagonist is injected in the VMH. Furthermore, high levels of corticosterone are particularly evident when injections in the DMH/PVN area are followed by a novelty stressor paradigm, associating the DMH/PVN not only with circadian corticosterone release but also with the stress response. Most interesting, the study of Kalsbeek (Kalsbeek et al., 1996) identifies as the main source of AVP in the DHM as originating from the SCN rather than intra-nucleus transmission within DMH itself (Hoorneman and Buijs, 1982; Kalsbeek et al., 1992; Kalsbeek et al., 1993; Kalsbeek et al., 1995). Altogether these results support the idea of a dual role of AVP. AVP released by the PVN in the median eminence works together with the CRH for the release of ACTH acting on the corticotropes, while the AVP released by the SCN in the DMH acts as a break in the rising phase of the corticosterone during the rest phase of the circadian cycle. Thus, the study also raises the possibility of the existence of another factor that acts as a stimulus, rather than a break, to induce the rising phase of plasma corticosterone (Kalsbeek et al., 1996).
All these results indicate that both SCN^{AVP} and SCN^{VIP} neurons work as break for the corticosterone release during the rest phase.

Furthermore, the SCN-PVN^{CRH} communication has been indirectly explored by Mukai *et al*. (Mukai et al., 2020) using calcium imaging recording, revealing that CRH neurons do not respond to SCN peptides such as VIP, AVP or NMS. While this study demonstrates a clear lack of response, it remains possible that some CRH neurons may respond to AVP, although these responses may be considered outliers from the median Z-score. Despite the AVP response, the inefficacy of SCN peptides in generating a response on the PVN^{CRH} neurons, suggests that their regulation of corticosterone release, may acts indirectly, perhaps through the SPZ, as conceivable by the results of the present research, or through the DMH, as reported elsewhere.

SCN and the autonomic control of corticosterone release.

The neurosecretory pathway for circulating glucocorticoids is under the circadian control of both the SCN and the HPA axis. Its final goal is to release factors that modulate motivational behaviors, food intake, energy metabolism, rest and sleep. Indeed, this pathway is not sole determinant of the circadian control of corticosterone release. Several evidence indicate how the

SCN can indeed influence the adrenal gland, not only via the endocrine system, but also working upon the autonomic nervous system.

As we have already explained circadian rhythms are the results of the activity of different oscillators, including central and peripheral ones, with the adrenal glands belonging to the latter group. Specifically, the circadian clock machinery operates within the adrenal glands, and it is regulated by the SCN through the autonomic nervous system. This regulatory mechanism controls corticosterone rhythms by influencing adrenal cell sensitivity to ACTH (Ungar and Halberg, 1962; Ungar, 1964; Torress-Farfan et al., 2006) The TTFL genes active in the adrenal gland of rodents can indeed be entrained by the photic input conveyed by the SCN to the autonomic system. The denervation of the adrenal gland halted the photic induction of Per1 in the gland (Bittman et al., 2003). Furthermore, Oster *et al.* (Oster et al., 2006) have proven that the adrenal gland TTFL "*gates the physiological response of this organ to ACTH stimulation via the control of genes encoding proteins of the complex steroidogenic network*". Specifically, the TTFL directs the transcriptional regulation of key components such as the steroidogenic acute regulatory protein (StAR) and 3-β-hydroxysteroid dehydrogenase (3-β-HSD), thereby controlling the corticosterone secretion. The concepts can be summarized as follows. The circadian corticosterone release initiates with photic input, which contacts the SCN and internal neuronal networks. From there, through a hormonal and neuronal pathway, this signal reaches the adrenal gland, where the molecular asset of the TTFL creates a final regulatory level for rhythmic control.

Specifically, the SCN exert influence through this secondary pathway by communicating with the autonomic portion of the PVN. The PVN contains pre-autonomic neurons that project to the sympathetic preganglionic column of the spinal cord, which in turn innervate the adrenal gland. In this way the SCN/PVN axis controls the adrenal gland's sensitivity to corticosterone release (Buijs et al., 1999; Ueyama et al., 1999). An observation clarified by Ishida *et al.* (Ishida et al., 2005) where they show that the light input fail to entrain the adrenal gland activity in the SCN-lesioned animals. Conversely, in wild-type animals the adrenal gland TTFL response correlates with light intensity and corticosterone release rather than ACTH concentration, suggesting the exclusion of HPA axis involvement in the process.

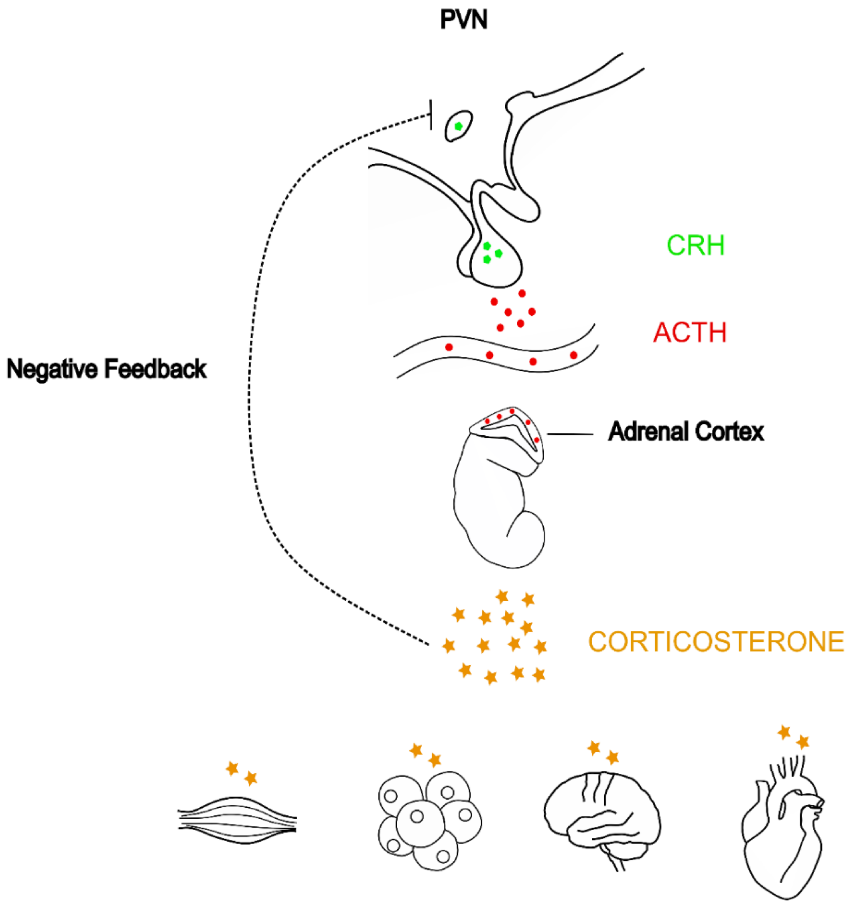

Figure 1.7: schematic representation of the HPA axis for the corticosterone release.

While the autonomic pathway of SCN influence on glucocorticoid rhythms appears relatively well understood, the involvement of high-order multisynaptic circuits within the CNS, which ultimately modulate CRH neurons and the HPA axis, remains a topic of ongoing investigation. It is evident that both the SCN and the PVN play crucial roles, but the extent to which SCN-PVN communication alone is sufficient to determine the rhythm is still uncertain, especially considering the limited SCN→PVN projections. Indeed, other nuclei are proposed as potential mediators in this process, notably the SPZ and the DMH. These nuclei may contribute to the intricate network involved in the regulation of glucocorticoid rhythms and warrant further investigation.

The predominant termination of SCN fibers occurs in the regions of the SPZ, with projections to the PVN and DMH being comparatively weaker. This suggests that the SPZ likely serves as an effective mediator in corticosterone release (Vujovic et al., 2015). The corticosterone rhythm is disconnected from SCN oscillation until the formation of connections between SCN^{VIP} neurons and the SPZ, which relay SCN output to other brain areas (Ban et al., 1997). Notably, the DMH connections with ventral SPZ neurons are established early in the life of rats (Gall et al., 2012).

Additionally, the involvement of the SPZ in various circadian outputs has been previously addressed or suggested (for references, see Lu et al., 2001; Buijs et al., 2003; Engeland et al., 2005; Todd et al., 2018).

The DMH serves as another major output target of the SCN. As previously described, the SCN-derived vasopressin profoundly inhibits corticosterone fluctuations by modulating the activity of DMH neurons. Additionally, studies involving DMH ablation in rats, conducted using both electrolytic lesions and cell-specific lesions, have demonstrated a lack of circadian fluctuations in corticosterone levels (Bellinger et al., 1976; Kalsbeek et al., 1996; Chou et al., 2003). Furthermore, corticosterone injection into the DMH acts as a negative feedback mechanism to attenuate the increase in glucocorticoids following stress restraint, suggesting a role in the negative feedback loop associated with the HPA axis and the ultradian rhythm of plasma ACTH and corticosterone (Stamper et al., 2015).

To date, the prevailing notion is that the SPZ serves as a pivotal relay nucleus for the circadian control exerted by the SCN. With the present study, we have delved into novel aspects concerning the communication between the SCN and SPZ, as well as elucidating the role of the SPZ in corticosterone release.

1.4 THEORETICAL ASPECTS OF THE TECHNIQUES USED IN THE PRESENT STUDY.

1.4.1 Patch clamp technique.

Developed by the Nobel Prize's B. Sakmann and E. Neher during the '70 (Neher and Sakmann, 1976, Neher and Sakmann, 1976), the patch clamp is the principle modern electrophysiological technique to study the electrical properties of excitable cells, such as neurons (Molleman, 2003). The patch clamp technique is built upon fundamental contribution from various scientists operating in different fields. These include the conceptualization of the membrane theory by J. Bernstein and E. Overton; the anatomical description of the squid giant axons by J.Z. Young and L.W. Williams; the first electrophysiological recordings of the squid giant axon by K.S. Cole; the genesis of the ionic theory by Nobel Prize's A.F. Huxley, A.L. Hodgkin and B. Katz and the use of microelectrodes by of R.W. Gerard, Judith Graham and N. Ling (Carmeliet, 2019).

The technique, with its different configuration including cell-attached, inside-out, outside-out and whole cell **[Figure 1.8]**, enables the recording of single ion-channel-based currents (pA resolution) and membrane potential variation (mV resolution). Recordings are conducted using a glass pipette with a very small opening (1-3 micrometer in diameter) (Brown et al., 2008). The pipette is carefully positioned to establish a tight contact with the cell membrane, resulting in a

formation of a high-resistance seal (GΩ) which is fundamental for recording the electrical activity of the cell arising from the ionic flow across the cell membrane. The cell membrane works as an insulator that maintain the different ion accumulation between the extracellular and intracellular compartments. These ion gradients, produced by the activity of specific ionic transporter and channels, generates an electrochemical field across the membrane that create the force for charged particle to move according to their electrochemical gradients. The circuital model representing these components including the membrane, two compartments (extra- and intracellular) and the ions transporter can be depicted as a resistance and a capacitor in parallel as illustrated in **Figure 1.8.**

In the voltage-clamp configuration, patch-clamp allows for a precise control of the membrane potential (Vm), by clamping it at a desired value. This modality allows to record the membrane currents, which are directly amplified by a differential amplifier and digitized by a digital-analog/analog-digital converter. The digitized signals are conveyed to a computer software controller for further visualization, storage and analysis. On the other hand, current-clamp configuration recordings measure the resting membrane potential variations in response to specific injected current. This setup provides insights into the intrinsic electrical properties of the cell, including its ability to generate action potentials and respond to synaptic input. All the patch-clamp experiments in the present study were conducted using the whole-cell configuration. Briefly, a silver chloride electrode used for the recordings is contained within a borosilicate glass patch pipette, filled with an isosmotic intracellular solution. Upon formation of the giga-seal between the patch pipette and cell membrane, a mild suction is applied to break the membrane patch providing low-resistance electrical access. This process allowed the cytoplasm to become continuous with the solution inside the pipette where is located the silver-wire recording electrode. The main advantages of this configuration include to record the electrical activity of the entire cell while controlling the cytosolic and extracellular environment. Additionally, the intracellular solution can be customized to include compost of interest, such as intracellular antagonist (i.e. lidocaine) or biosensor (i.e Fura-2) or labeling molecule (i.e. Alexa-Fluor). However, due to relatively larger volume of the pipette solution in respect to the cytoplasm, over time, the cytoplasm will be replaced by the pipette solution, causing a washout of unknown cytosolic factors, potentially altering the physiology of the cell and its responses.

We have specifically employed the patch clamp technique in whole-cell configuration to assess the electrophysiological responses, by recording from mouse brain slices.

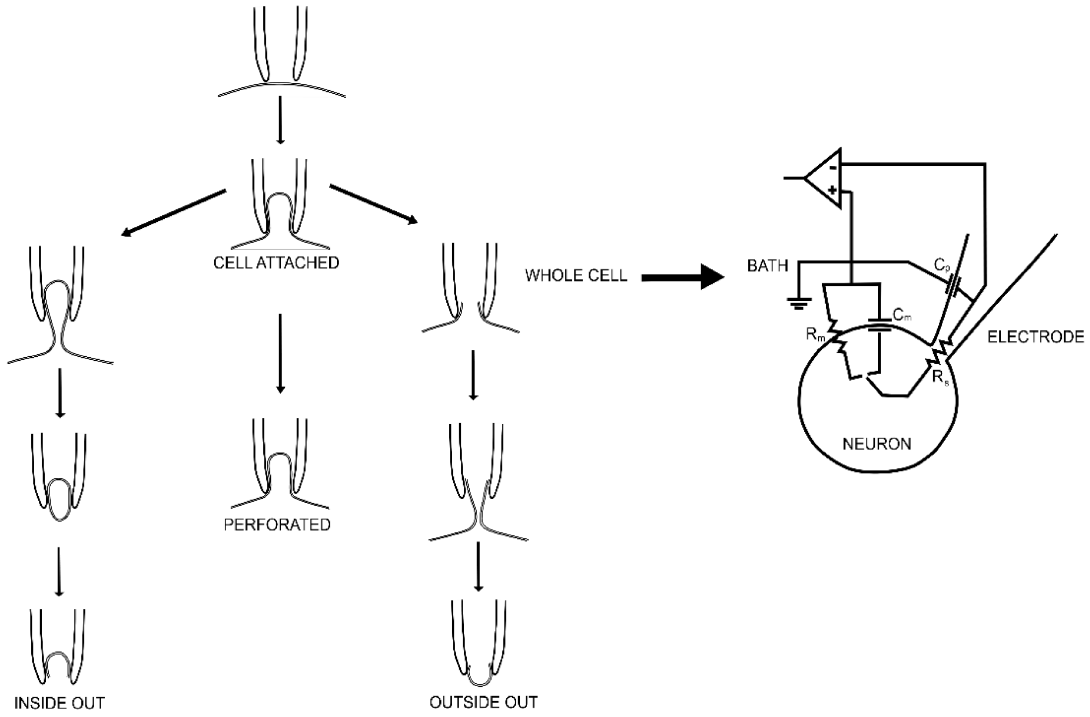

Figure 1.8: patch clamp configuration on the *left* and electronic model of the whole cell configuration on the *right*. *Rm*, membrane resistance; *Cm*, membrane capacitance; *Cp*, pipette capacitance; *Rs*, series resistance. [Adapted from (Molleman, 2003)].

1.4.2 Optogenetic stimulation technique.

To understand the relationship between neuronal population within a network or to assess the *sufficiency* of a group of cells in generating a behavior with a stimulation (gain-of-function), or its *necessity* through its inhibition (loss-of-function) (Carter and Shieh, 2015), it is necessary to manipulate the activity of the components of that specific circuit or cell group (Luquet et al., 2005; Oikonomou et al., 2019). Achieving this necessitates manipulation strategies with both high spatiotemporal resolutions (Crick, 1979) and reversibility to define the contribution of specific components to the generation of functional outcomes. Optogenetic pioneered by E. Boyden and K. Deisseroth (Boyden et al., 2005), meet these requirements by exploiting the optical properties of specific channels which can modulate the neuronal activity within milliseconds, combined with the specificity provided by genetic engineering to express these light sensitive channels (opsins) exclusively in targeted cells. This approach enables a high-throughput strategy in terms of spatial, temporal and reversibility resolution. In this system the light-gated molecular complex is represented by the engineered microbial opsins proteins.

In the present study we only used Channelrhodopsin-2 (ChR-2) opsin to perform the channelrhodopsin-assisted circuit mapping (CRACM) studies. The ChR2 derives from the green

unicellular alga *Chlamydomonas reinhardtii* and functions as a light-gated non-specific cationic channel (permeable to Na+, H+, K+, Ca2+) (Nagel et al., 2002; Nagel et al., 2003) **[Figure 1.9].** The ChR2 is composed of a Type I opsin, a seven-transmembrane light-responsive protein which can respond to specific light wavelength when bound to the vitamin-A-related organic cofactor or retinal. In this bound-state the complex is defined "rhodopsin". Retinal serves as biochemical light sensor of the protein, specifically when exposed to a specific light wavelength, the rhodopsin undergoes conformational changes where 11-cis-retinal is transformed to all-trans-retinal. This process causes the opening of ion pore allowing ions to pass through the membrane. In the absence of the specific light source, retinal switch back to its 11-cis status and the pore closes (Mahmoudi et al., 2017). For different purpose, there are different types of opsins capable of either silencing or activating neurons. Within them, ChR2 is typically used to depolarized neurons (Yizhar et al., 2011; Klapoetke et al., 2014). Responding with a good fidelity in generating a current in a range of photon source between 460-475nm, ChR2 determines a depolarization by cationic net influx determined by the electro-chemical gradient for ions (Na+, H+, K+, Ca2+). ChR2 is able to depolarize and generate action potentials in a range of photostimulation frequency typical of neuronal firing rate and showing high spike-fidelity and photostimulation response-fidelity in different types of neurons, demonstrating a high level of versatility. Notably, these effects are achieved without altering the electrical properties and the health of the ChR2-positive neurons, and without producing shunt current effect in the absence of light (Boyden et al., 2005).

One of the most important advantages of the optogenetic stimulation, the principal strategy used in this study, is the possibility to perform CRACM recordings (Petrenau et al., 2007; Petrenau et al., 2009). This type of recording allows the dissection of connectivity between neurons, elucidating the components of a specific circuit and validating the functional state of short and long-range projections. Opsins are expressed in the membrane of the entire compartment, including the cell bodies, dendrites, axons and synaptic terminals. Consequently, in a brain slice is possible to obtain a photo-evoked events even when the neuronal somata is not present in the sample. This feature allows CRACM recordings to provide quantitative and functional evidence to complement anatomical tracing studies (Goyer et al., 2020) or electron microscopy investigation, which completely lack for a proof of neurotransmitter communication.

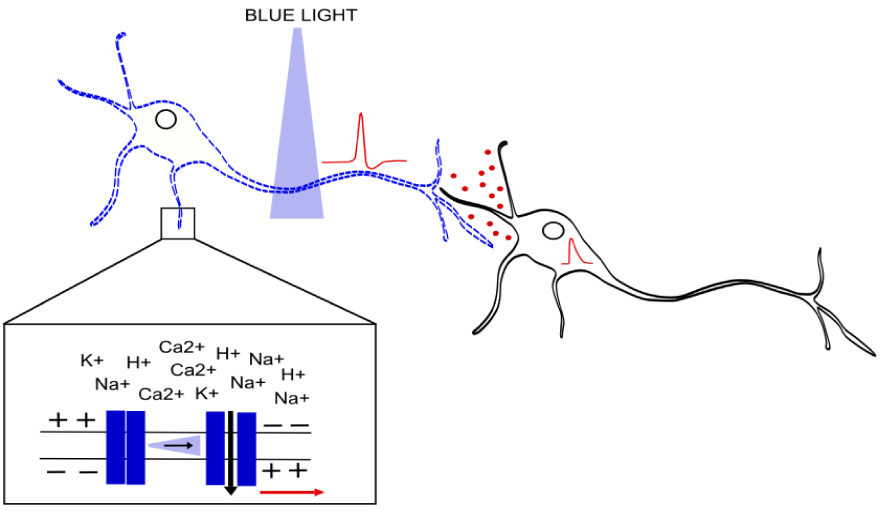

Figure 1.9: the opsin can control the neuronal activity. The Channelrhodopsin-2, *in blue*, is expressed along the entire neuronal plasmatic membrane. When exposed to blue light (~475nm), the channel allows a non-selective cationic current to flow into the cell, resulting in the generation of action potentials and neurotransmitters release. The signal, *in red*, is then transmitted to the postsynaptic neurons.

1.4.3 Calcium imaging technique.

Calcium imaging is an extremely informative technique that allows the simultaneous monitoring of neuronal activity in multiple neurons (tens to hundreds) providing a comprehensive temporal and spatial perspective. The calcium flow from and to the intracellular compartments, is a direct proof of neuronal response, offering insights into changes in electrical activity, alterations in synaptic inputs or sub-threshold firing events, and the activation of intracellular signaling pathway (Ross, 2012). Thus, calcium imaging allows us to detect and monitor any interference caused by a specific trigger on intracellular calcium dynamics. These intracellular calcium variations are detected using specific biosensors that change fluorescence properties when they bind or unbind calcium ions.

In the present study, we utilized the latest advancements in calcium imaging by employing the genetically encoded calcium indicator (GECIs) which can be expressed through transgenic delivery system with high cellular specificity (Muto et al., 2011; Oh et al., 2019). Specifically, we employed a single-fluorophore GECI that belongs to the GCaMP family (Tian et al., 2009). GCaMPs are large proteins composed by three components: the calcium-binding protein calmodulin, the calmodulin-binding protein peptide M13 flanking the central molecular core which consists in a circularly permuted enhanced green fluorescent protein (cpEGFP). Four calcium ions bind to the EF hands of the calmodulin. This binding induces a conformational change which allows the formation of a tight molecular ring between the CaM and the CaM-binding protein **[Figure 1.10]**. The new complex imposes conformational changes of the entire GECI creating a new domain interface and ultimately triggering excitation of the fluorescent

components, that in this activated state emits more photons (Nakai et al., 2001; Nagai et al., 2001).

In the present study, we employed GCaMP7f which is one of the fastest GECI available on the market, indicated for cytoplasmic free calcium in neurons with high sensitivity and brilliance upon binding to calcium as well as faster decay time, which is an important property when investigating fast events (Chen et al., 2013; Ding et al., 2014). It is worth noting that, in our study, we were not primarily concerned with the kinetic properties of the sensor, as we were investigating slow changes in calcium dynamics.

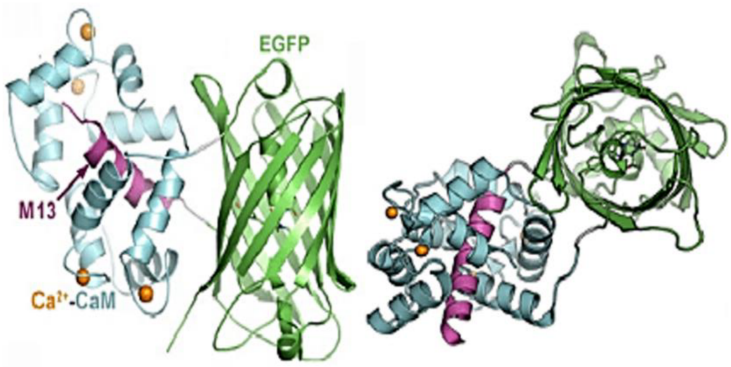

Figure 1.10: crystal structure of the GCaMP sensor in the calcium-binding state on the *left* and in the unbound state on the *right* [from (Akerboom et al., 2009)].

1.4.5 Conditional recombinant rabies virus tracing technique.

Anatomical tracing studies are instrumental in elucidating the connections between neuronal nuclei, delineating the underlying components of specific brain functions. While these studies lack functional proof of synaptic connectivity, they offer compelling evidence of nuclei interaction at both long and short-range level. In the present study we employed the recombinant rabies virus for monosynaptic neuronal tracing to understand the first order input connection of the CRH neurons in the PVN.

The rabies virus (RABV) is a replication-competent virus capable of retrogradely traveling more than one synapse from the initially infected neurons. Thus, it can trans-neuronal infect neurons without specificity. To achieve cell infection, the rabies virus encodes for the *rabies envelope glycoprotein* (RG) which is fundamental for the assembling and the infectivity of the native virus during its life cycle. This virus has been used to generally understand input to a specific nucleus, that can be both monosynaptic and polysynaptic. To avoid this low specificity, the long range spread of the virus, and to focalize the tracing only to the monosynaptic input, the virus has been manipulated by I.R. Wickersham (Wickersham et al., 2006; Wickersham et al., 2007) to obtain a high specific and mono-trans-synaptic tracing tool. Specifically, the genetic sequence for the

RG is removed and substituted with a fluorescent marker such EGFP, transforming the RABV in the named RABVΔG-EGFP. This recombinant virus has then lost the native infectivity, but it can regain its infectivity property in the presence of exogenous RG. However, because the recombinant RABVΔG-EGFP cannot express RG, it cannot spread further when it reaches the second order neuron. As a result, the tracing is restricted only between the starter neuron, infected by the recombinant RABVΔG-EGFP and the exogenous RG, and the monosynaptic contacting neurons. In this way by injecting the RABVΔG-EGFP together with the RG, is possible to obtain a one order synaptic spread, without the possibility to select the starter neurons. Therefore, Wickersham *et al.* (Wickersham et al., 2007) have improved the recombinant RABVΔG-EGFP by adding the *envelope glycoprotein* EnvA (RABVΔG-EGFP-(EnvA)). The EnvA protein forms the envelope of the avian sarcoma and leukosis virus and it recognizes the TVA receptor on the avian cell membranes. This receptor that is not present in mammalian cells, therefore, restricts the infectivity of RABVΔG-EGFP-(EnvA) to the cells that express the TVA receptor.

Is possible to deliver the TVA receptor with traditional transgenic tool (see paragraph 1.4.7), such as the adeno-associated virus (AAV) read by the Cre recombinase. In this manner the TVA will be expressed only by the Cre positive cells. The TVA injection is accompanied also by the Cre dependent expression of the glycoprotein RG, that ensures the RG to be specifically expressed in the starter neurons. Finally, the injection of the modified RABVΔG-EGFP-(EnvA). In this way the RABVΔG-EGPF-(EnvA) can infect only the cells which expressed the TVA receptor together with the RG, and from these neurons can retrogradely migrate to the second order neurons, where the lack of the RG will block the rabies spread.

In this method, the presence of the RABVΔG-EGPF-(EnvA) is indicated by the EGFP fluorescent tag both in the starter neuron and in the second order neurons. While the expression of TVA is indicated by another tag, usually mCherry, which is fused with the TVA gene in the AAV vector. Therefore, the starter neurons expressing the TVA and infected by the recombinant rabies, will exhibit a final tag signal that results from both the EGFP and mCherry. In the context of the figure and the present work where TVA is fused with mCherry, whereas the rabies virus is EGFP marked, the starter neurons will appear yellow (due to the combination of EGFP and mCherry fluorescent signals) while the neurons connected to them will appear green (due to EGFP fluorescence alone) **[Figure 1.11]**.

.

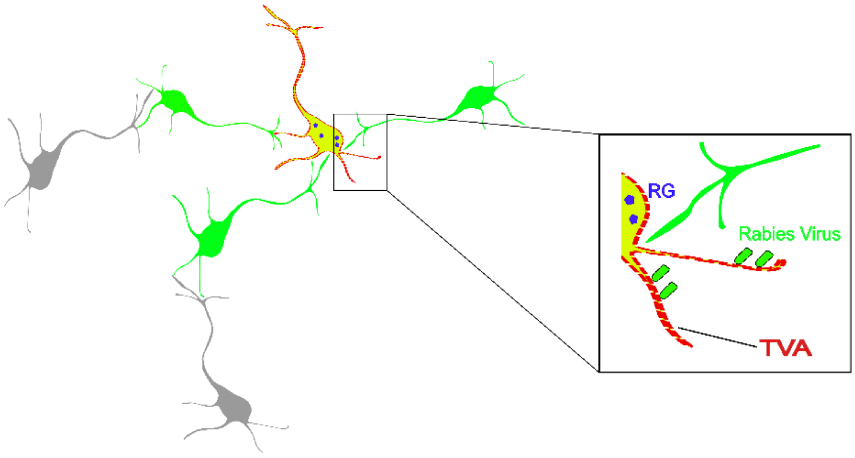

Figure 1.11: schematic representation of the RABVΔG-EGPF-(EnvA) mechanism of infection. The yellow neuron is the starting neuron infected both by the recombinant rabies virus (*in green*), the TVA receptor (*in red*) and RG protein (*in blue*). The neurons monosynaptically connected are then marked by the GFP signal, while the second order neurons remain unlabeled and uninfected by the virus (*in gray*).

1.4.6 Conditional diphtheria toxin A ablation.

The ablation study performed using different strategies (i.e. cut knife, ibotenic acid, electrical damage, radiofrequency etc.) represent an extremely important approach to study the role of a brain region in a specific function, despite the numerous disadvantages associated with them. Ablation is rarely limited solely to the targeted area, the elimination of a brain portion affects several circuits and networks simultaneously, leading to different outcomes. However, it has proven to be essential for several crucial discoveries, including those related to the suprachiasmatic nucleus as a circadian regulator.

The lack of specificity which is one of the most problematic aspects of older ablation techniques, can be addressed through the conditional expression of the diphtheria toxin A (DTA). This tool is widely used to achieve tissue specific ablation of cells. The diphtheria toxin is an exotoxin secreted by the gram-positive bacterial strain of *Corynebacterium diphtheriae*. The toxin, in the presence of its specific receptor on sensitized host cells, is internalized into a clathrin-coated vesicle and converted then in an early endosome. Acidification of the endosome lumen induces the formation of a pore on the vesicle membrane, allowing the toxin to enter the cytosol of the cell. Once inside, it acts as an enzyme catalyzing the NAD^+-dependent ADP-ribosylation of elongation factor 2 (EF-2), thereby inhibiting the cellular protein synthesis and ultimately leading cells to death by apoptosis (Murphy et al., 2011).

The toxin is composed by two fragment, fragment A and fragment B. Fragment B is responsible for receptor binding and internalization, while fragment A alone catalyzes the fatal biochemical reaction. In this study, the diphtheria toxin has been targeted to the neurons of interest using a

viral vector that encodes directly for fragment A of the toxin. The viral vector is expressed into the cells of interest by the Cre/LoxP genetic system. Consequently, the cells are not sensibilized for the diphtheria receptor activation, but directly express the fragment A of the diphtheria toxin. This means that in the absence of fragment B, the released fragment A from dying cells cannot interfere with the vitality of the surrounding cells **[Figure 1.12]**. This approach leads to the specific ablation of a subpopulation of neurons where the Cre recombinase is expressed and its reliability has been validated by several groups, (for references see Kaur et al., 2017; Anaclet et al., 2018; Todd et al., 2020).

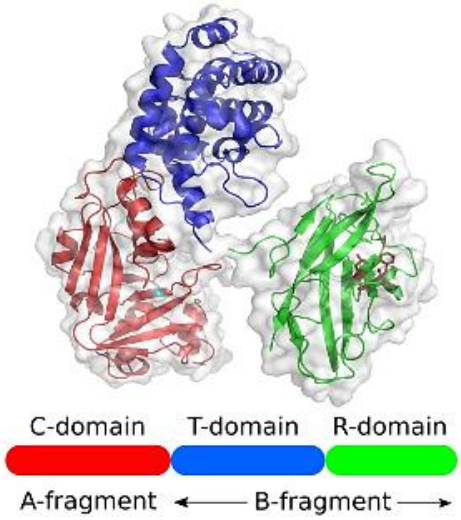

Figure 1.12: biochemical structure of the diphtheria toxin fragment A and fragment B. [From (Wenzel et al., 2020)].

1.4.7 Tools for gene delivery.

In the present study we used specific genetic strategies to obtain a high specificity level in neuronal manipulation, aimed to achieve detailed scientific goal. Particularly we employed transgenic mice that express Cre-recombinase in specific neuronal populations along with cre-dependent viral vectors to drive the expression of bio-molecule of interest, such as ChR2, GCaMP7f, TVA receptor or diphtheria toxin A (DTA) exclusively in neurons expressing the Cre-recombinase.

For all these goals, we used vectors based on adeno-associated virus (Naso et al., 2017). The AAV carrying the gene of interest, is microinjected through a stereotaxic injection in the mouse brain following the anatomical coordinates of the target area. The AAVs are known for their high transduction efficiency of mitotic or post-mitotic cells, long-term stable expression and low immune reactivity, and high safety. Engineered AAVs do not incorporate into the genome but persist as stable episomes within the cell nucleus (Ahmed et al., 2004; Zincarelli et al., 2008).

To achieve cell-specific viral expression, we used engineered mice for the Cre/LoxP site-specific recombinases tool (Madisen et al., 2012). Cre (**c**yclization **re**combinase) gene derived from P1 bacteriophage encodes a 38-kDa enzyme, a DNA recombinase, that catalyzes site-specific recombination between LoxP (**l**ocus **o**f **x**(cross)-over, in **P**1 bacteriophage) sites. LoxP sites are composed of 34bp sequence that include a 13bp inverted and palindromic repeats separated by an asymmetric 8bp core sequence (Kim et al., 2018). Depending on the orientation of the core sequence, LoxP site possesses directionality properties that guides the action of Cre-recombinase. When LoxP sites have opposite orientation and reside on the same DNA strand, the enzyme operates an inversion recombinant event of the sequence resulting in the reversal of the DNA-region between LoxP sites. The reversed DNA can now be read by the transcriptomic apparatus of the host cells leading to the expression of the exogenous bio-molecule **[Figure 1.13]**.

For our experimental purposes the gene encoding the tool of interest is inverted and flanked by two opposite LoxP sites, and engineered in an AAV virus to obtain a viral vector. The vector can then be recognized by the Cre-recombinase enzyme that is expressed constitutively under the control of a promoter specifically targeting a subtype of neuronal cells under investigation. This targeted approach ensures that only the subtype of cells expressing Cre-recombinase, can recombine the viral recombinant DNA and transcript the gene of interest. It is important to note that while the virus can infect all neuronal cells surrounding the injected region, only the cells expressing Cre-recombinase will effectively express the gene of interest (Packer et al., 2013). Most of our transgenic mice have the gene for the Cre recombinase inserted after the internal ribosome entry site (IRES) which is an RNA sequence that facilitates the recognition by the ribosome apparatus and the expression of more proteins from a single mRNA. This configuration ensures that the host gene expression occurs together with the exogenous enzyme expression providing a method for selective targeting and expressing gene of interest within specific neuronal subtypes (Kim et al., 2018).

The Cre/LoxP system is widely used in the neuroscience field, although there are some limitations. For example, Cre-recombinase can be expressed not only in the neuron of interest, especially during developmental stage, leading to ectopic expression and potentially confounding observations. The expression of the protein of interest depends on the expression and the activity of the Cre recombinase in the cell giving a low reproducibility (variable level of expression of Cre-recombinase). The reliance on a viral brain injection also raises concerns about the potential involvement of neurons from other nuclei in the study (spread of the expression). Despite these challenges to be taken into account during data interpretation, the advantages of this system are

remarkable and have given the possibility to explore scientific questions that would otherwise remain underexplored.

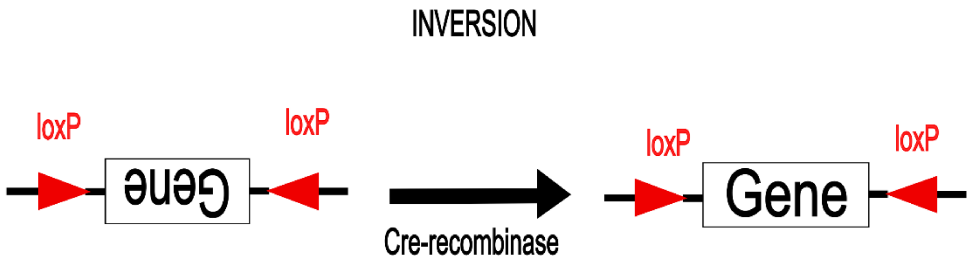

Figure 1.13: schematic representation of the Cre recombinase inversion recombinant mechanism.

2. AIMS

The SCN plays a central role in regulating daily physiological rhythms, yet to date many gaps in our understanding of its function remain. The scientific work dedicated to the comprehension of the SCN is extremely vast, going from the molecular and genetical analysis, the single cells activity, the intra-nuclei integration, the circuital connections, the systemic physiology until the computational modeling. However, there is still much to learn about how specific behaviors and functions are orchestrated by the SCN.
Principal in this scenario is the downstream control of the SCN over its principal projecting nuclei, first the SPZ, which receives the majority of the SCN fibers.

In the present study we have focused our scientific analysis on three main aims dedicating to the exploration of the SCN-SPZ communication and the role of the SPZ in the circadian control of corticosterone release:

1. evaluation of the synaptic connectivity between the SCN neuronal subpopulations and the SPZ subregions,

2. evaluation of the neuropeptidergic modulation of the SPZ subregions,

3. evaluation of the consequence of the SPZ ablation in the corticosterone physiology, focusing on the interplay connectivity with the DMH nucleus.

3. METHODS

3.1 CIRCUITAL AND MODULATORY STUDIES.

3.1.1 Animals.

The animals used in this study are transgenic mice for the Cre recombinase, aged 4-12 months, of both sexes. All mice were treated in accordance with guidelines from the National Institute of Health (NIH – U.S.A.) Guide for the Care and Use of Laboratory Animals. All protocols were approved by Beth Israel Lahey Center Institutional Animal Care and Use Committee. The animals were housed in cages with food and water *ad libitum* in a controlled environment with a 12-hour light/dark (LD) cycle (lights on at 6:00 AM and off at 6:00 PM).

Animal models and brain microsurgery procedures

To study the SCN^{NMS}→SPZ projections, we used NMS-Ires-Cre mice, where the Cre recombinase is expressed under the control of the NMS promoter. The selective expression of ChR2 in SCN^{NMS} neurons was achieved by the stereotaxic injection of the Cre-dependent AAV8-Efla-FLEX-ChR2-EYFP viral vector (30 nl) (Addgene, Watertown, MA, USA) into the SCN (AP = - 0.4mm, ML = ± 0.1mm, DV = - 5.5mm) of NMS-Ires-Cre mice.

To study the SCN^{VIP}→SPZ projections, we used VIP-Ires-Cre mice where the Cre recombinase is expressed under the control of the VIP promoter. The selective expression of ChR2 in SCN^{VIP} neurons was achieved by the stereotaxic injection of the AAV8-Ef1a-DIO-hChR2(H134R)-mCherry viral vector (30 nl) (Addgene, Watertown, MA, USA) into the SCN (AP = - 0.4mm, ML = ± 0.1mm, DV = - 5.5mm) of VIP-Ires-Cre mice.

To study the SPZ^{VGAT}→DMH^{VGAT} projections, we used Vgat-Ires-Cre mice where the Cre recombinase is expressed under the control of the Vgat promoter. The selective expression of ChR2 in SPZ^{VGAT} neurons was achieved by the stereotaxic injection of the Cre-dependent AAV8-Ef1a-DIO-hChR2(H134R)-mCherry viral vector (6 nl) (Addgene, Watertown, MA, USA) into the SPZ (AP = 0mm, ML = ± 0.17mm, DV = - 5.35mm) of Vgat-Ires-Cre mice. To recognize the DMH^{VGAT} neurons we also injected in the DMH (AP = - 1.6 mm, ML = ± 0.2mm, DV = - 3.5mm) the Cre-dependent AAV-hSyn-DIO-EGFP viral vector (100nl) (Addgene, Watertown, MA, USA) which drives expression of GFP in the GABAergic neurons that express Cre-recombinase. We recorded from fluorescently labeled DMH GABAergic neurons, while optogenetically stimulating the SPZ input fibers.

To study the SPZ neuronal activity with calcium imaging, we used Vgat-Ires-Cre models mice expressing Cre recombinase under the control of the Vgat promoter. The Cre-dependent AAV8-hSyn-FLEX-jGCaMP7f-WPRE viral vector (6.5 nl) (Addgene, Watertown, MA, USA)

encoding the Ca^{2+} indicator was stereotaxically injected into ventral SPZ (AP = 0mm, ML = ± 0.17mm, DV = -5.35mm) or dorsal SPZ (AP = - 0.36 mm, ML = ± 0.17 mm, DV = - 5.35 mm) of Vgat-Ires-Cre mice.

All the viruses have been delivered using a compressed air system. For the entire microsurgery procedure, mice were maintained under 3% isoflurane anesthesia. Before recovering from anesthesia, animals were injected with 4 mg/kg meloxicam-SR (pain reliever) and visually monitored until they start moving around the cage. After 2 to 4 weeks followed the AAV injection coronal slices containing SCN-SPZ or SPZ alone or DMH could be prepared for optogenetic stimulation or calcium imaging recordings.

Ex vivo sample preparation for optogenetic and calcium imaging recordings.

Mice were euthanized by decapitation between 9:30 AM and 12:30 PM. Before euthanasia, mice were anesthetized with isoflurane by inhalation in an induction chamber. Once they exhibited slow breathing frequency and absence of movement, they were transcardially perfused with cold artificial cerebrospinal fluid (ACSF) containing N-methyl-D-glucamine (ACSF-NMDG). The mouse was then decapitated using sharp scissors, the brain extracted, and coronal brain slices (250 µm thick) were prepared at +4°C in ACSF-NMDG using a vibratome (VT1200S, Leica, Bannockburn, IL, USA). For solution composition see next paragraph.

For patch clamp/optogenetic recording the sections containing the SPZ, SCN or DMH were incubated for 5 minutes in warm ACSF-NMDG (+37°C) and then transferred to warm normal Na-based ACSF for patch clamp/optogenetic recording (ACSF-Na) (+35°C) in an incubation chamber, where they were kept for at least 10-15 minutes to restore optimal conditions after the cutting process. Sections were left at room temperature for 1 hour, and then brain slices were transferred to a recording chamber, immersed, and perfused with ACSF-Na. The recording solution was continuously enriched with a gas mixture (95% O2 and 5% CO2) providing oxygen and stability in terms of temperature (+23°C) and pH (7.3).

For calcium imaging recording the sections containing the ventral or the dorsal SPZ were incubated for 10 minutes in warm ACSF-NMDG (+35°C) and then transferred to HEPES-Na-based ACSF (Ting et al., 2014; Asrican and Song, 2021) at room temperature where they were kept for at least 1h to restore optimal conditions after the cutting process. After the recovery the brain sections were transferred to a recording chamber, immersed, and perfused with Na-based-ACSF. The recording solution was continuously enriched with a gas mixture (95% O2 and 5% CO2) providing oxygen and stability in terms of temperature (+23°C) and pH (7.3).

3.1.2 Solutions and drugs.

- ACSF-NMDG (in mM): 100 NMDG, 2.5 KCl, 1.24 NaH2PO4, 30 NaHCO3, 25 glucose, 20 HEPES, 2 thiourea, 5 Na-L-ascorbate, 3 Na-pyruvate, 0.5 CaCl2, 10 MgSO4 (310-320 mOsm, pH 7.3 with HCl, and carboxygenated with 95% O2 and 5% CO2).
- ACSF-Na for patch clamp/optogenetic recording (in mM): 120 NaCl, 2.5 KCl, 1.3 MgCl2, 10 glucose, 26 NaHCO3, 1.24 NaH2PO4, 4 CaCl2, 2 thiourea, 1 Na-L-ascorbate, 3 Na-pyruvate (pH 7.4 when carboxygenated with 95% O2 and 5% CO2).
- ACSF-HEPES for calcium imaging recording (in mM): NaCl 92, KCl 2.5, HEPES 20, Glucose 25, $NaHCO_3$ 30, NaH_2PO_4 1.25, $CaCl_2$ 2, Thiourea 2, Na-Ascorbate 5, Na-Pyruvate 3, $MgSO_4$ 2, N-acetyl-L-cysteine 6 (carboxygenated with 95% O_2 / 5% CO_2; pH 7.24-7.3; 330 mOsm)
- ACSF-Na for calcium imaging recording (in mM): NaCl 122.5, KCl 3.5 or 11, HEPES 10; Glucose 15, NaHCO3 26, NaH2PO4 1.25, CaCl2 2, and MgCl2 1.3 (carboxygenated with 95% O2 / 5% CO2; pH 7.24-7.3; 335-350mOsm).
- K-gluconate-based pipette solution (in mM): 120 K-Gluconate, 10 KCl, 3 MgCl2, 10 HEPES, 2.5 K2-ATP, 0.5 Na-GTP (pH 7.2 adjusted with KOH; 280 mOsm).
- Cs-methane-sulfonate-based pipette solution (in mM): 125 Cs-methane-sulfonate, 11 KCl, 10 HEPES, 0.1 CaCl2, 1 EGTA, 5 Mg-ATP, and 0.3 Na-GTP (pH regulated to 7.2 with CsOH, 280 mOsm).

Drugs

- Arginine-Vasopressin (AVP), 1 µM, purchased from Sigma-Aldrich (Saint Louis, Missouri, USA).
- BAY 55-9837, 0.5 µM, purchased from Tocris Cookson (Bristol, UK). VPAC2 receptor specific agonist.
- Charbachol (Cch), 50 µM, purchased from Sigma-Aldrich (Saint Louis, Missouri, USA). Cholinergic receptors agonist.
- Galanin 1.29 (Gal), 1 µM, purchased from Tocris Cookson (Bristol, UK).
- Vasoactive Intestinal Peptide (VIP), 1 µM, purchased from Bachem (Bubendorf, Switzerland).
- Neuromedin S (NMS), 100-200 nM, purchased from USA-Canada Phoenix Phamaceuticals (USA-Canada).
- Cs-methane-sulfonate, 125 mM, purchased from Sigma-Aldrich (Saint Louis, Missouri, USA). It is a potassium channel blocker. It is added in the pipette recording solution to block action potentials. It is used to record GABAergic synaptic activity at a holding potential of 0 mV.

- 4-Aminopyridine (4-AP), 250 μM, Sigma Aldrich (Saint Louis, Missouri, USA). Selective blocker of potassium channels responsible for the repolarization phase of the membrane.
- Bicuculline (BIC), 20 μM, purchased from Sigma-Aldrich (Saint Louis, Missouri, USA). Bicuculline is a selective antagonist of $GABA_A$ receptors.
- Tetrodotoxin (TTX), 1 μM, purchased from Tocris Cookson (Bristol, UK); it is a selective blocker of voltage-dependent Na+ channels. TTX is added to the extracellular solution to prevent the generation of action potentials in the entire slice.
- Kinurenic Acid, 1 mM, purchased from Sigma-Aldrich (Saint Louis, Missouri, USA). Antagonist of the glutamatergic transmission.

3.1.3 Patch clamp and optogenetic set-up.

To identify the cells of interest in the brain slices containing the SCN and the SPZ or the DMH, we employed a combination of fluorescence and infrared light in differential interference contrast video microscopy (IR-DIC). The set-up comprised a fixed vertical tabletop microscope (BX51WI, Olympus America Inc.) equipped with a water immersion Nomarsky objective (Olympus 40X/0.8 NA) and an infrared-sensitive CMOS camera (Thorlabs, Newton, NJ, USA, DCC3240C). These experimental components are placed on a vibration-isolating table to ensure stability during data acquisition, and a Faraday cage was used to suppress external electrical effects. For the electrophysiological experiments we performed the whole-cell configuration recordings using a Multiclamp 700B amplifier, a Digidata 1440A interface, and Clampex 9.0 software for instruments control (Molecular Devices, Foster City, CA, USA). To reach the whole-cell configuration the recording pipette was prepared from borosilicate glass tubes (Sutter Instruments, CA,USA) using a horizontal puller (P-97, Sutter Instruments CA, USA) for about a final resistance of ~5-6MOhm and filled with iso-osmotic solution. We placed the recording pipette into the head-stage of the preamplifier where an Ag/AgCl electrode maintains the electrical contact between the cell and the electronic devices. Using micromanipulators, the patch pipette was oriented through the tissue to the cells and in proximity of the cell of interest suction was applied to create a high resistance seal (>1GOhm) between the pipette tip and the cell membrane, as described previously. Subsequently, a mild suction was applied to rupture the membrane seal, allowing continuity between the recording pipette and the intracellular compartment.

For optogenetic stimulation, full-field stimulation with LED light sources was employed. LEDs, specifically a 5W LUXEON blue LED (470 nm wavelength; #M470L2-C4; Thorlabs, Newton,

NJ, USA), coupled to the epifluorescence pathway of the microscope, was used to stimulate the soma and synaptic terminals of ChR2-expressing SCN^{VIP}, SCN^{NMS} and SPZ^{VGAT} neurons.
To assess the post-synaptic photo-evoked effect, patch clamp technique in whole-cell configuration was used both in the voltage clamp and current clamp configuration, studying the photo-evoked current events and the effect of stimulation on the membrane potential and firing frequency in SPZ or DMH neurons.

3.1.4 Calcium imaging set-up.

Calcium imaging recordings were performed to analyze the activity of neuronal populations by measuring changes in intracellular calcium. In this study, GECI GCaMP7f was stereotaxically injected via Cre-dependent viral infection into the cells of interest. To identify the GABAergic cells in the brain slices contained in the ventral and the dorsal SPZ, we employed a combination of a fluorescence and infrared light in differential interference contrast video microscopy (IR-DIC). The set-up comprised a fixed stage upright microscope (BX51WI, Olympus America Inc.) equipped with a water immersion lens (Olympus 10X / 0.3 NA) and an infrared-sensitive CMOS camera (Thorlabs, Newtons, NJ, DCC3240C). A 5W LUXEON blue light-emitting diode (470 nm wavelength; #M470L2-C4; Thorlabs) and a standard set of filters for GFP were used to excite the GCaMP7f and to collect the cpEGFP emitted photons. Imaging was carried out using the sensitive CMOS camera controlled by a customized software (PCCAM 0.2.254 Software) to synchronize the photostimulation and the acquisition, thus limiting the photobleaching. Exposure time was set at 40-400ms and the images were acquired at low frequency 0.2Hz (0.8-8% duty cycle) and saved as frame stack in *.tif* format.

3.1.5 Analysis and statistics for patch clamp recordings.

All data were acquired using Clampex 9.0 software (Molecular Devices) and sampled at 20 kHz. The recorded traces were analyzed offline using Clampfit 10 software (Molecular Devices Foster City, CA, USA). Statistical analysis and graphs were conducted using Microsoft Office Excel (Microsoft 2010), OriginLab (OriginLab Corporation 2018), Prism (GraphPad Software 9.0 2019) and costume made script in Python (Python 3.5.8 Centrum voor Wiskunde en Informatica Amsterdam). All results are represented as mean ± standard error (SEM) or standard deviation (SD); "n" indicates the number of neurons per group, “N” indicates the number of animals. Significance set at $*p < 0.05$; $**p < 0.01$;$***p < 0.001$.

Analysis of the membrane potential.

We evaluated the effect of SCN^{NMS} and SPZ^{VGAT} input stimulation at different frequencies on the membrane potential of ventral SPZ neurons and DMH^{VGAT} neurons respectively. Traces were recorded in current clamp, maintaining the membrane potential closed to the neuron's firing threshold. The mean value of the membrane potential (Vm), under pre-stimulus, during stimulation, and post-stimulus conditions, is calculated by defining an all-point histogram of the membrane potential values in the three different conditions. We selected 10-seconds interval for each condition. For each interval, we created a histogram comprising all the points by inserting Vm values on the X-axis and Vm potential occurrences on the Y-axis. The reported values show a normal distribution and can be interpolated with a Gaussian function. The mean value of the distribution, corresponding to the peak of the distribution, correlates with the mean V_m of the interval. Points representing events such as action potentials fall in the proximal tails of the distribution, allowing for a more precise analysis unaffected by rapid and brief changes in membrane potential. For statistical analysis of the data, we normalized the membrane potential values to the pre-stimulus condition and applied an ANOVA test to compare the three conditions or a Student's T-test to compare two conditions.

Analysis of the firing rate.

We evaluated the effect of SCN^{NMS} and SPZ^{VGAT} input stimulation at different frequencies on the firing rate of ventral SPZ neurons and DMH^{VGAT} neurons respectively.

Traces were recorded in current clamp, maintaining the membrane potential at the activation firing threshold. The mean frequency value was calculated over a 10-seconds window under pre-stimulus, stimulus, and post-stimulus conditions. For statistical analysis of the data, we normalized values to the pre-stimulus condition and applied an ANOVA test to compare the three conditions or a Student's T-test to compare two conditions.

Analysis of the opto-evoked post-synaptic current (oPSC).

We recorded spontaneous inhibitory postsynaptic current events in SPZ or DMH^{VGAT} cells at a voltage of 0mV for 5 minutes by stimulating ChR-expressing fibers of SCN or SPZ neurons every 10 second with a single 10ms stimulus pulse (30 total stimuli). The spontaneous and opto-evoked postsynaptic currents were detected off-line using MiniAnalysis Program (Synaptosoft Inc. – Software for Neuroscientists). We have analyzed the probability of spontaneous inhibitory postsynaptic events over the minutes of recordings and during the stimulation. Cells that, during optogenetic stimulation, exhibit a release probability greater than 50% compared to the baseline

probability, are considered connected. We analyzed oPSCs amplitude, analyzing the peak averaged value obtained from the 30 averaged stimuli. We calculated the latency of the averaged oPSCs, defining it as the time between the onset of the blue light pulse and the onset of oPSC.

3.1.6 Analysis and statistics for calcium imaging recordings.

Fiji software has been used for the initial imaging processing (Schindelin et al., 2012). Image registration, semi-automatic cell detection ROI (region of interest) and neuropil fluorescent signal calculation were done using Suite2P software (Pachitariu et al., 2016). Using MATLAB software (R2019a, MathWorks, Natick, MA, USA), the ROIs fluorescence signal has been corrected for the background contribution, subtracting 70% of the neuropil signal **(Equation 3.1)**, and for photobleaching trend.

$$F_{corrected}(i,t) = F_{raw}(i,t) - (F_{neuropil}(i,t) * 0.7)$$

Equation 3.1

Where F_{raw} is the signal of the single ROI *i* before correction at time *t;* $F_{neuropil}$ is the signal of the neuropil corresponding to the ROI *i* at time *t*.
The final $F_{corrected}$ is then normalized to the Z-score by the equation **(Equation 3.2)**

$$\text{Z-score}(i,t) = [F_{corrected}(i,t) - \mu] / SD$$

Equation 3.2

Where $F_{corrected}$ is the corrected signal of *i* at time *t*; *mu*, the mean, and *SD*, the standard deviation, correspond to the mean value and SD of fluorescent corrected signal during the 5 min recording before the drug application.
Z-score values ≤ -2 was used to define inhibiting drug or inhibited cells; Z-score value $\geq +2$ for activating drug or activated cells; and the $-2 < \text{Z-score} < +2$ has been used to define a drug with no effect on the cell activity. The analyzed Z-score is the average value obtained during the last 2.5 minutes of compounds application.

3.2 SYSTEMIC STUDY

3.2.1 Animals.

The animals used in this study were male transgenic mice for the Cre recombinase, aged 3-4 months. All mice were treated in accordance with guidelines from the National Institute of Health (NIH – U.S.A.) Guide for the Care and Use of Laboratory Animals. All protocols were approved by Beth Israel Lahey Center Institutional Animal Care and Use Committee. The animals were housed in cages with food and water *ad libitum* in a controlled environment with a 12/12 hour light/dark (LD) cycle, unless otherwise specified (lights on at 6:00 AM and off at 6:00 PM), and stable humidity and temperature (22°C).

Animal models for tracing study.

The monosynaptic tracing study of the CRH neurons in the PVN has been explored using the CRH-Ires-Cre mice (Krashes et al., 2014), where the Cre recombinase is expressed under the control of the CRH promoter. The selective expression of TVA receptor and optimized rabies glycoprotein in the PVN^{CRH} neurons was achieved by stereotaxically injecting the AAV8-CMV-FLEX-TVAmCherry-2A-oG (45nl) viral vector (Addgene, Watertown, MA, USA) into the PVN (AP = - 0.8 mm, ML = ± 0.2 mm, DV = - 4.85 mm) of 5 CRH-Ires-Cre mice. After 3 weeks the same mice have been treated for a second brain microsurgery using the same coordinates and injecting 55nL of EnvA G-deleted Rabies-EGFP (Salk Institute). For the surgery procedure the mice have been equally treated as described for the *in vitro* procedures in paragraph 3.1.1.
After 7 days post-surgery, mice are treated for histology procedure and anatomical validation.

Animal models for corticosterone monitoring study after SPZ nuclei deletion.

The DTA ablation has been performed in a Vgat-Ires-Cre::L10 mouse model. Vgat-Ires-Cre (Jackson Laboratory, Bar Harbor, ME, USA) were crossed with a Cre-dependent GFP reporter transgenic line (Jackson Laboratory, Bar Harbor, ME, USA), obtaining a Vgat-Ires-Cre:R26-loxSTOPlox-L10-GFP mice for experimental purposes. The model has been used to better identify the area of the lesion induced by the DTA, since the SPZ is a GABAergic nucleus.
In the SPZ of 7 Vgat-Ires-Cre::L10 the virus AAV-mCherry-DIO-DTA (30nl) (Addgene, Watertown, MA, USA) has been bilaterally stereotaxically injected (AP = - 0.35 mm, ML = ± 0.25 mm, DV = - 5.1 mm). The control cohort, formed by the Vgat-Ires-Cre or Vgat-Ires-Cre::L10 received a bilateral injection in the SPZ for the Cre-dependent AAV-hSyn-EGFP viral vector (30nl) (Addgene, Watertown, MA, USA). After four weeks post-surgery the corticosterone sampling is began.

3.2.2 Histology.

After 7 days the CRH-Ires-Cre mice injected with the rabies virus have been treated for tissue fixation.

After the corticosterone recordings the Vgat-Ires-Cre::L10 mice injected with the DTA have been treated for tissue fixation.

Mice were euthanized by decapitation. Before euthanasia, mice were anesthetized with isoflurane by inhalation in an induction chamber. Once they exhibited slow breathing frequency and absence of movement, they were transcardially perfused with 30ml of PBS 1X solution (Thermo Fisher Scientific, US) to eliminate any trace of blood followed by the perfusion of 30ml of formalin 10% (Thermo Fisher Scientific, US). The mouse was then decapitated using sharp scissors and the brain has been carefully extracted and resuspended in formalin 10% at +4°C. After 24h the dehydration has been performed immersing the brain in a solution of PBS 1X – 25% sucrose at +4°C. The brain is then cut on the microtome at ideal temperature of ~ – 80°C in dry ice. Coronal sections of 30µm of thickness are then stored at +4°C in PBS 1X enriched with the antimycotic sodium-azide. The slices are then prepared to be mounted on positive charged slides (Epredia USA) with Vectashield antifade mounting medium (catalog #H-1400, Vector Laboratories) and imaged on confocal microscope (Zeiss LSM 5 Pascal).

3.2.3 Corticosterone circadian monitoring.

The corticosterone level has been measured via blood samples collected at 4 time points every 30h (5 days of recording for 4 points per animal) at zeitgeber time ZT1, ZT7, ZT13, ZT19 during the LD cycle. After 5 days of recording in LD we placed the animals in constant darkness condition and with dim red light we sampled the blood starting on the third day in DD at circadian time (CT) 13. Mice were recorded in DD for other 5 days.

Blood samples were obtained from mice's tail. Animal were restrained at the base of the tail and puncture of the tail permits to collect ~30µl of blood stored in a tube (CB300, Sarstedt, US). The blood was then centrifuged at 10.000rpm for 10 min, and the plasma were separated and stored at -20°C. Duplicate samples have been analyzed with ELISA assay for corticosterone detection following the manufacturer guidelines (ADI-901-097, Enzo life science, US). Quantification has been made through 405nm filter (iMark, Bio-Rad, US).

3.2.4 Analysis and statistics.

For the conditional rabies tracing study, neurons marked both with TVA-mCherry and EGFP were classified as starter neurons. Each EGFP positive neurons has been counted for each nucleus

at least at three anatomical levels in coronal sections of 30µm and registered to the mouse atlas Paxinos and Franklin (Paxinos & Franklin 2001). The afferent inputs are presented as the total counted number of EGFP expressing neurons in the specific brain region and the SEM between animals.

For corticosterone monitoring parametric criteria have been assessed for Brown-Forsythe (homoscedasticity and heteroscedasticity) and Shapiro Wilk (normal distribution) test. Two-way ANOVA with a factor for group and a factor for time followed by the post-hoc Sidak test, have been then applied to analyze the corticosterone plasma levels.
The circadian index (CI) for corticosterone is calculated as the difference between ZT13/CT13 and ZT1/CT1 levels normalized by the average control group value at ZT1/CT1, in both the groups (control and ablated) and in both the conditions (LD and DD). Significance for CI values were obtained with two-way ANOVA with a factor for group and a factor for time followed by a post-hoc multiple comparisons Sidak test.
Statistical analyses were made with GraphPad Prism (GraphPad Software 9.0 2019) software. Data are represented as mean ± standard error (SEM) and significance is set at $p < 0.05$* or $p < 0.01$** or $p < 0.001$***.

4. RESULTS

4.1 CHAPTER ONE

Subparaventricular zone input: *ex vivo* study of the SCN → vSPZ projections.

In this study, optogenetic stimulation was employed to activate neurons expressing excitatory ChR2 opsin in combination with whole-cell patch-clamp recordings performed on vSPZ neurons. Experiments were conducted on brain slices (250µm thickness) containing both the SCN and vSPZ obtained from VIP-Ires-Cre transgenic mice (N = 3 animals) and NMS-Ires-Cre transgenic mice (N = 2 animals). Prior to the experiments these mice underwent stereotaxic injection of AAV viral vectors encoding ChR2 (see **Figure 4.1 panel A and Figure 4.4 panel A**).

4.1.1 vSPZ neurons respond to the optogenetic photostimulation of the SCN^{NMS} input.

We assessed the presence of ChR2 in the biological preparation through visualization of the EYFP (enhanced yellow fluorescent protein) transfection tag, as evidenced through confocal acquisition post-fixation in 10% formalin (**Figure 4.1 panel B**). The activity of inhibitory postsynaptic events in SPZ neurons was recorded at a holding potential of 0mV. For intracellular recording a solution containing cesium-methanesulfonate, the potassium channel blocker, was used. The mouse brain slices were continuously perfused with ACSF-Na solution for patch-clamp recordings, carboxygenated with 95% O2/5% CO2. Additionally, 1mM of dissolved kynurenic acid was added to isolate the inhibitory input.

We performed photostimulation of SCN^{NMS} input using full-field stimulation through a 470 nm LED and concurrently recording the presence or absence of photo-evoked events synchronized with the stimulus. The SCN^{NMS} input was photostimulated with a 10ms light pulse given every 10 seconds for a total of 5 minutes (30 trials). Notably, this protocol did not affect spontaneous inhibitory synaptic activity between stimuli (considering a 600ms window of time, ANOVA one-way, Bonferroni post-hoc $p > 0.05$), (**Figure 4.1 panel F**). 10 out of 17 recorded neurons (59%, **Figure 4.1 panel C**) exhibited a response to optogenetic stimulation displaying an opto-evoked inhibitory postsynaptic current (oIPSC). Neurons with a release probability greater than 50% compared to the baseline (pre-stimulus) were considered connected. The average probability was 113 ± 4.3%, suggesting a potential plasticity phenomenon following stimulation or a polysynaptic contribution (**Figure 4.1 panel D**). Importantly, we observed no significant variation in the baseline probability of the spontaneous IPSCs (sIPSCs) between connected and non-connected cells (considering a 2s window of time, unpaired T-test $p > 0.05$), (**Figure 4.1 panel G**).

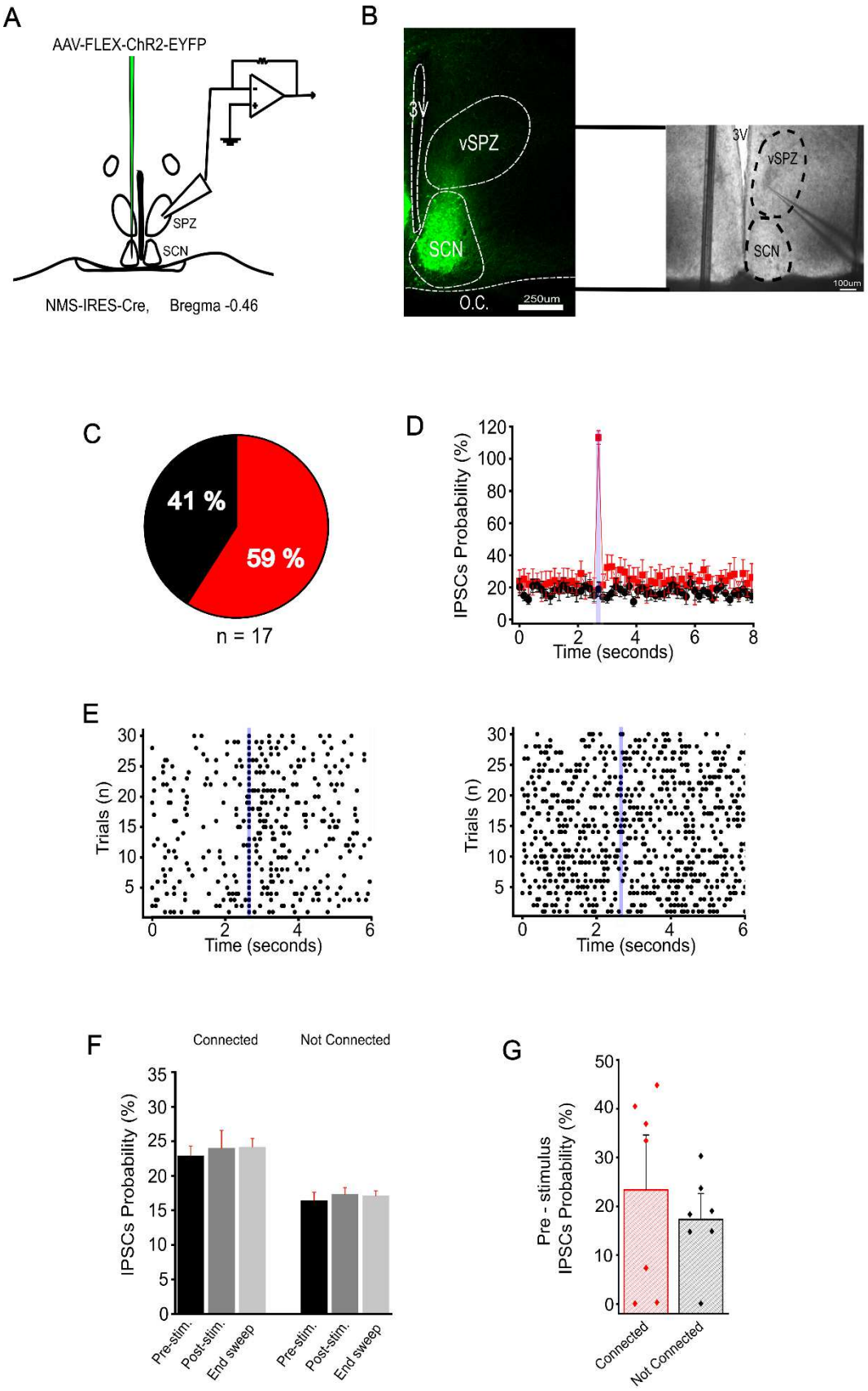

Figure 4.1: vSPZ neurons respond to the optogenetic photostimulation of the SCN^{NMS} input. A) Schematic model representing the experimental design used to investigate the SCN input of the SPZ region. AAV-FLEX-ChR2-EYFP was injected into the SCN of NMS-Cre mice.

Patch-clamp recordings were made from vSPZ unlabeled neurons. **B)** Confocal acquisition post-formalin fixation of the ChR2-EYFP native fluorescence (*scale bar* 200µm) combined with a 4X infrared acquisition of the recorded SPZ area, with an example of the patch capillary position (*scale bar* 100µm). **C)** Photostimulation of SCN^{NMS} neurons evoked oIPSCs in 59% of the recorded vSPZ neurons (n = 17) **D)** Average probability of the oIPSCs in the connected cells (*red*, n = 10/17) and non-connected cells (*black*, n = 7/17) **E)** Raster plot of the IPSCs events of a connected cell (*left*) and non-connected cell (*right*) **F)** Average variation of the IPSCs probability in the connected and non-connected cells pre-stimulus (pre-stim.), post-stimulus (post-stim.) and before the following stimulus (end-sweep) (considering a 600ms window of time, ANOVA one-way $p > 0.05$). **G)** Average of the IPSCs probability pre-stimulus of the connected and non-connected cells (considering a 2s window of time, unpaired T-test $p > 0.05$). (10ms photostimulation is indicated by the *blue bar*). *SPZ*, subparaventricular zone; *SCN*, suprachiasmatic nucleus.

The average amplitude of the photo-evoked events was 141 ± 67pA, with an average latency of 6.8 ±1.2ms (calculated based on n = 7/10 connected cells, **Figure 4.2 panel A**). To further investigate the nature of connection, a pharmacological combination of 1µM TTX and 250µM 4-AP was applied to 2 out of 7 connected cells recorded at 0mV. This approach aimed to assess the monosynaptic nature of the connection, as suggested by the average latency. Notably, both photo-evoked events in the two recorded cells showed resistance to the pharmacological treatment, confirming the monosynaptic nature of the connection between SCN^{NMS} cells and a population of vSPZ region. Subsequently, in one of these two cells, bicuculline at 20µM was bath applied. Remarkably, bicuculline completely abolished the photo-evoked event after 25 minutes of administration, indicating that this connection is primarily mediated by $GABA_A$ ionotropic receptors (**Figure 4.2 panel B**).

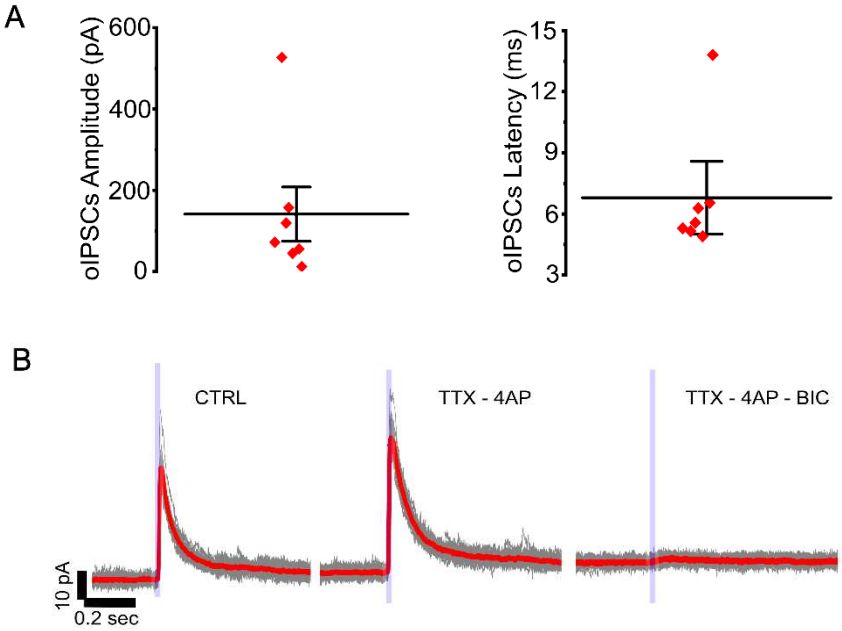

Figure 4.2: nature of the SCN^{NMS}→vSPZ input. **A)** Average amplitude and latency of the vSPZ neurons responding to the ChR2 photostimulation (n = 7, mean ± SEM) **B)** Representative whole-

cell recording at 0mV of the oIPSCs in a control condition (CTRL), during the pharmacological TTX-4AP (TTx-4AP) (n = 2) treatment and after bicuculline application (TTX-4AP-BIC) (n = 1). Average trace in *red*, single trace in *light grey*. (10ms photostimulation is indicated by the *blue bar*).

Using an intracellular solution of K-gluconate, we recorded in current clamp modality the effect of photo-stimulation on the firing frequency and membrane potential of three vSPZ neurons assessed as connected cells based on the study of opto-evoked inhibitory event in voltage clamp at -40 mV (3 out of 10 of the connected cells). Subsequently photo-stimulation at 2Hz or 5Hz, all cells exhibited a significant change in firing frequency (ANOVA one way, Bonferroni post-hoc $p < 0.01$**, $n = 3$), while no significant alteration was observed in membrane potential (ANOVA one way, Bonferroni post-hoc $p > 0.05$, $n = 3$). One cell underwent treatment with 20µM bicuculline following a positive control recording where photo-stimulation abolished firing. Remarkably, the pharmacological treatment completely abolished the effect of the photo-stimulation (**Figure 4.3 panels A, B** and **C**).

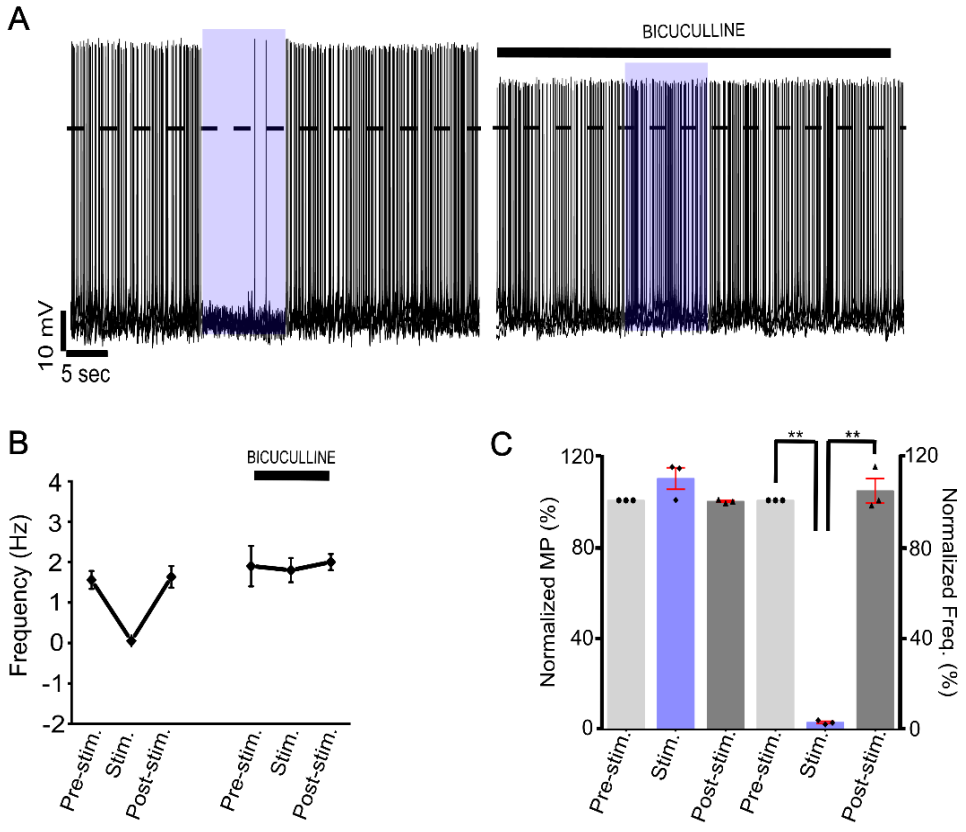

Figure 4.3: SCN^{NMS} → vSPZ input modulation on the membrane potential and firing rate. **A)** Representative whole-cell recording in current clamp modality during photostimulation of the SCN^{NMS}→vSPZ input before and after bicuculline application. *Dotted line*, 0mV **B)** Dot-line graph of the same cell represented in A during the control and bicuculline application. **C)** Normalized membrane potential (ANOVA one way, $p > 0.05$) and firing rate (ANOVA one way,

$p < 0.01$**) pre-stimulus (pre-stim.), during the stimulus (stim.) and post-stimulus (post-stim.) (n = 3, mean ± SEM).

4.1.2 vSPZ neurons respond to the optogenetic photostimulation of the SCN^{VIP} input.

We confirmed the presence of ChR2 in the biological sample by visualizing the mCherry transfection tag, as demonstrated by confocal acquisition post-fixation in 10% formalin (**Figure 4.4 panel B**). The activity of postsynaptic inhibitory events in SPZ neurons was recorded using the same conditions described in paragraph 4.1.1 and we applied the same protocol of photo-stimulation as described for the SCN^{NMS}→vSPZ circuit. Among the 8 recorded neurons, 4 cells (50%, **Figure 4.4 panel C**) responded to optogenetic stimulation with oIPCSs. Neurons showing during the stimulation a release probability greater than 50% compared to the baseline (pre-stimulus) were considered connected. The average probability of the connected cells was determined to be 90 ± 2% (**Figure 4.4 panel D**). We did not find a significant variation in the baseline probability of the spontaneous IPSCs (sIPSCs) between the connected and non- connected cells (considering a 2s window of time, unpaired T-test $p > 0.05$), (**Figure 4.4 panel F**).

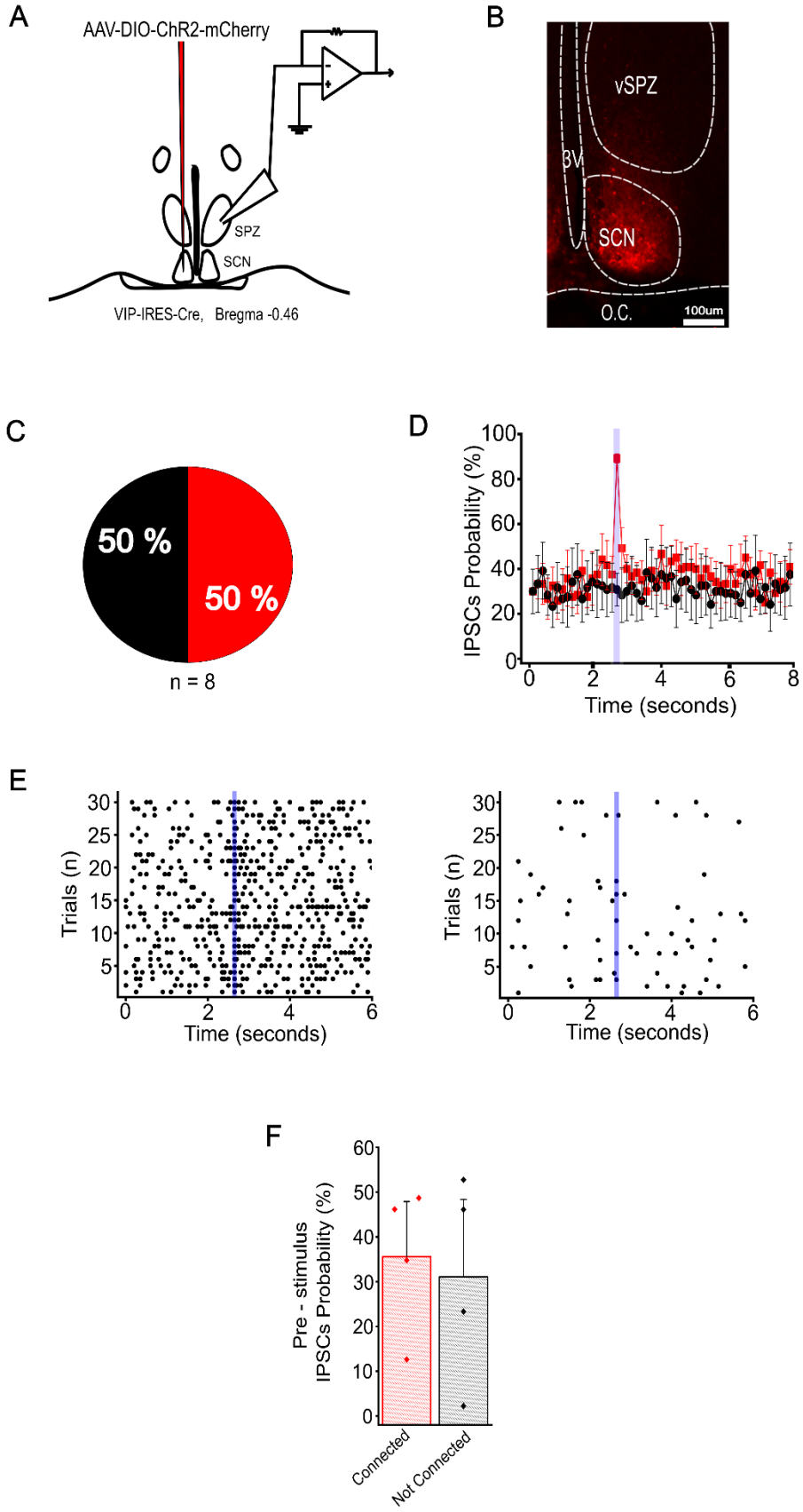

Figure 4.4: vSPZ neurons respond to the optogenetic photostimulation of the SCN^{VIP} input. **A)** Schematic model representing the experimental design used to investigate the SCN^{VIP} connectivity with the SPZ region. AAV-DIO-ChR2-mCherry was injected into the SCN of VIP-Cre mice. Patch-clamp recordings were made from vSPZ unlabeled neurons. **B)** Confocal

acquisition post-formalin fixation of the ChR2-mCherry native fluorescence (*scale bar* 100µm). **C)** Photostimulation of SCN^{VIP} neurons evoked oIPSCs in 50% of the recorded vSPZ neurons (n = 8) **D)** Average probability of the IPSC in the connected cells (*red*, n = 4/8) and non-connected cells (*black*, n = 4/8) **E)** Raster plot of the IPSC events of a connected cell (*left*) and non-connected cell (*right*) **(F)** Average of the IPSCs probability pre-stimulus of the connected and non-connected cells (considering a 2s window of time, unpaired T-test $p > 0.05$). (10ms photostimulation is indicated by the *blue bar*). *SPZ*, subparaventricular zone; *SCN*, suprachiasmatic nucleus.

The average amplitude of the photo-evoked event was 72 ± 31pA, with an average latency of 7 ± 1.7ms, suggesting a monosynaptic connection (**Figure 4.5 panel A**). In one connected cell, bicuculline at 20µM was applied. Bicuculline completely abolished the oIPSCs, indicating that this connection is primarily mediated by $GABA_A$ ionotropic receptors (**Figure 4.5 panel B**). The postsynaptic spontaneous activity and the photo-evoked event are recovered after washing out the antagonist confirming the model of an inhibitory synaptic connection between the SCN^{VIP} and SPZ neurons.

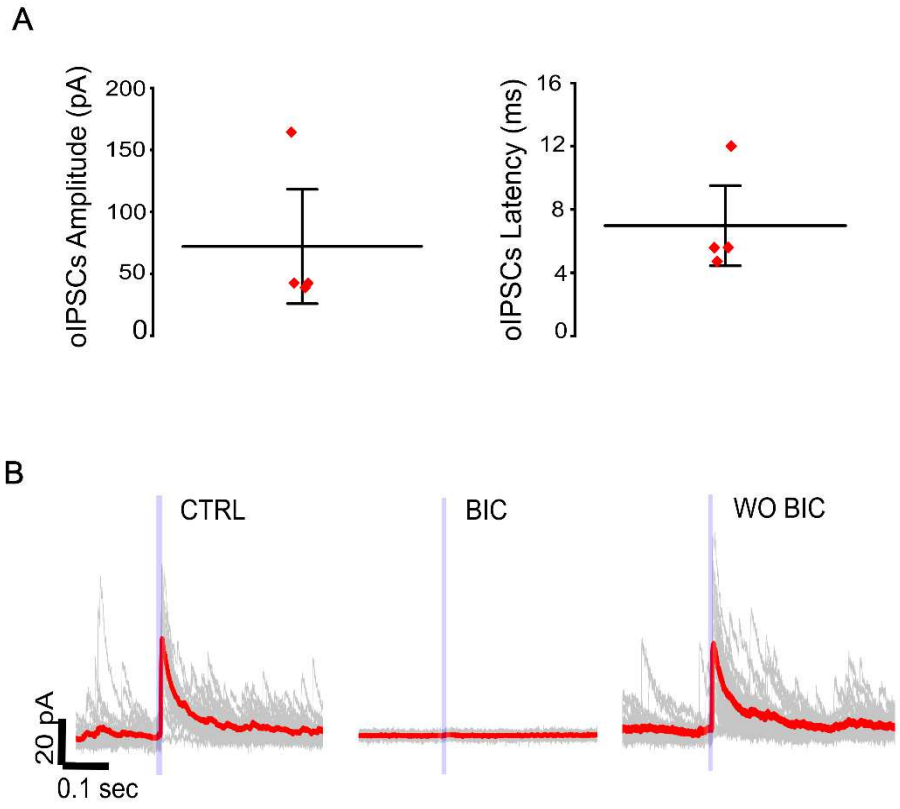

Figure 4.5: oIPSC characteristics of the SCN^{VIP}→vSPZ input. **A)** Average amplitude and latency of the vSPZ neurons responding to the ChR2 photostimulation (n = 4, mean ± SEM). **B)** Representative whole-cell recording at 0mV of the oIPSC in a control condition (CTRL), during bicuculline application (BIC) and after the bicuculline wash-out (WO BIC) (n = 1). Average trace in *red*, single trace in *light grey*. (10ms photostimulation is indicated by the *blue bar*).

4.1.3 DISCUSSION: the SCN neurons are monosynaptically connected to the vSPZ neurons through a GABAergic transmission.

The suprachiasmatic projections to the subparaventricular zone have been well established through several anatomical studies where tracing results highlight how the SCN fibers densely innervate the ventral and dorsal SPZ. In rats Vujovic *et al.* (Vujovic et al., 2015) demonstrated that SCN^{AVP} neurons mainly project to the medial SPZ whereas the SCN^{VIP} neurons to the lateral SPZ. Although anatomical studies are extremely important to understand the possible relation between neuronal nuclei, they do not confirm the functional nature of the connection. CRACM studies serve as crucial role in demonstrating the presence and activity of these connections. Through various pharmacological strategies, these studies aim to unveil the nature of the synapse and elucidate how the incoming input modulate the activity of the target or how opto-evoked events themselves may be influenced by other input mimicked by drugs perfusion. Thus, CRACM studies play a pivotal role in bridging the gap between anatomical connectivity and functional interactions within neural circuits.

The link between the SCN^{VIP} output and the SPZ neurons has been elucidated in a study of Paul *et al*. (Paul et al., 2020) conducted in nocturnal animal. They show that optogenetic activation of the SCN^{VIP} resulted in the inhibition of neurons in the vSPZ as observed through MEA recordings. Although the study did not specifically isolate these neurons, it explored the entire region innervated by the SCN^{VIP} neurons in the recorded slice. Single cells responses revealed that the predominantly response of these neurons, termed *"VIP^{in}"*, was a reduction in firing rate. Conversely, when SCN^{VIP} neurons were optogenetically stimulated with Archaerhodopsin-3, it correlated with an increase in the firing rate of VIP^{in} cells. Moreover, they have shown how these neurons change their firing rate over the 24h period, displaying a clear antiphase circadian rhythm compared to the SCN^{VIP} neurons. This finding aligns with *in vivo* MUA recordings (Nakamura et al., 2008), suggesting that part of the low and cyclic activity in the SPZ may be directed by and correlated with the cyclic neuronal activity of the SCN^{VIP}.

Furthermore, in brain slices of nocturnal mice functional synaptic connections between SCN^{VIP} neurons and the SPZ has already been assessed. Todd *et al*. (Todd et al., 2018) demonstrated that 55% of neurons in the dorsal SPZ projecting to the VMH receive monosynaptic input from SCN^{VIP} neurons. In the same work they found that the ventral SPZ mainly projects to the DMH, and in a subsequent study (Todd et al., 2020) they have shown that approximately 30% of SCN^{VIP} neurons have functional connection with vSPZ→DMH projecting neurons. The first case (Todd et al., 2018) elucidated a circuit involved in the circadian control of aggressive behavior, while in the second (Todd et al., 2020) the manipulation of the SCN^{VIP} neurons drastically impaired the

locomotor activity rhythm. They proposed a circuital model where SCN^{VIP} neurons through a polysynaptic circuit involving the SPZ as the second node, contact the VMH and DMH neurons. Notably, lesions in the DMH area known to result in impaired locomotor activity (Chou et al., 2003).

The present CRACM recordings of the SCN^{VIP}→vSPZ circuit reaffirm the presence of a functional $GABA_A$-mediated connection between the SCN^{VIP} and the vSPZ neurons mirroring the percentage observed in previous studies (50% in the present study, 55% by Todd *et al*. 2018, 30% by Todd *et al*. 2020). None of these studies, including the present one, specifically conducted experiments to establish the monosynaptic nature of this connection. The high opto-evoked probability to obtain a synaptic response of approximately 90%, strongly suggests a monosynaptic connection, as polysynaptic circuits are typically characterized by more failures. However, the key observation supporting the monosynaptic connection comes from the mean latency time. It is well-established experimental criterion that when the opto-evoked events have a latency time < 10ms (Petranau et al., 2007, Petrenau et al., 2009, Cho et al., 2013, Ferrari et al., 2018), the connection is highly likely to be monosynaptic and resistant to TTX treatment (Petrenau et al., 2009). Thus, with a mean latency of 7 ± 1.7ms presented in this study we conclude that SCN^{VIP} monosynaptically contact vSPZ neurons. Additionally, the contacted neurons show no specific difference in spontaneous inhibitory post synaptic currents compared to non-contacted neurons (Figure 4.1 panel G). Finally, we have reconfirmed the GABAergic nature of this connection through the $GABA_A$ antagonist application.

Knowing the SCN efferences, the results from CRACM recordings performed by stimulating the SCN^{NMS} neurons are not surprising. SCN^{NMS} neurons constitute approximately 40% of the nucleus and encompass a large percentage of the AVP and VIP positive neurons (Lee et al., 2015). Here for the first time, we show evidence that SCN^{NMS} neurons monosynaptically contact a subpopulation of vSPZ neurons (59% or the recorded neurons) through a $GABA_A$ mediated mechanism. Notably, very low frequency stimulation proved effective in abolishing the firing of post-synaptic neurons. Cells which show minimal variation in membrane potential were stimulated at 2Hz. Therefore, probably just the rising in the photostimulation frequency could result in a significant variation in membrane potential.

While the real firing frequency of the stimulated neurons remains unknown, previous studies indicate that SCN fires in antiphase to the SPZ (Nakamura et al., 2008, Paul et al., 2020). Considering these results, we can hypothesize that when the SCN^{NMS} are active, the SPZ neurons are likely inhibited, similar to the SCN^{VIP} effect.

While CRACM recordings are important to delineate the presence of a connection, they do not confirm the absence of neuronal modulation. The present recordings suggest that the input from the SCN is either monosynaptically present or absent, indicating the absence of polysynaptic circuit at this anatomical level. However, it remains possible that SCN neurons could modulate the activity of the non-connected neurons through alternative mechanism, such as peptides release. So, we cannot exclude other pathway of communication (long range polysynaptic circuit or peptidergic modulation) between SCN^{VIP}/SCN^{NMS} and the vSPZ neurons. The controlled and artificial optogenetic release of peptides remains a challenge in brain slices, and we did not investigate the effect on the opto-evoked event by perfusing exogenous compound for VIP or NMS transmission.

Finally, to gain a more comprehensive understanding, additional recordings are required. Following the anatomical division of the SPZ, studying of the transcriptome of connected and non-connected neurons could offer new insight into the organization of the SPZ area. Furthermore, exploring how photo-evoked input may be modulated by exogenous application of peptides could unveil novel mechanisms in SCN-SPZ communication. Lastly, given limited evidence regarding a glutamatergic source in the SCN, it might be interesting to replicate these experiments in a Vglut2-Ires-cre mice to confirm past findings or the more recent work of Harding *et al*. (Harding et al., 2020). This recent study proposed that the glutamatergic contribution may be attributed to passing fibers originating from the optic chiasm, a known glutamatergic input for both the SCN and the SPZ, rather than to the SCN neurons.

4.2 CHAPTER TWO

Subparaventricular zone modulation: *ex vivo* study of the neuropeptidergic modulation in the SPZ subregions.

4.2.1 SPZ neurons responses to the SCN neuropeptides.

In *ex vivo* experiments releasing endogenous peptides through optogenetic stimulation presents challenges due to distinct mechanisms governing peptide release compared to fast neurotransmitter such as GABA and glutamate (Arrigoni and Saper, 2014). Even if a specific experimental protocol would be established for a particular connection, the combination of optogenetic stimulation with patch-clamp technique, would provide crucial insights into the nature of synapses and communication phenomena. However, this approach necessitates numerous recordings to comprehensively understand the distribution of responses along the anatomical axis. In this context, imaging techniques offer a very good option for researcher seeking to explore whether a specific neuronal population responds to a specific compound. Imaging helps discern the anatomical distribution of response, whether they are indirect or direct, and investigates the presence of functional receptor in the area. To assess whether peptides, which are predominant in the SCN, can influence the neuronal activity of the SPZ, whether released by the SCN itself or other neuronal sources, we employed calcium imaging techniques.

As described in the methods paragraph, in our study we employed a Cre-dependent AAV encoding the calcium fluorescent biosensor GCaMP7f. This AAV was injected in a transgenic mouse model expressing the Cre recombinase under the Vgat promoter. This choice was based on literature indicating that the majority of SPZ neurons are GABAergic. The study was conducted with a cohort of 6 mice of both sexes, aged over 5 months.

Following viral injection, brain slices containing the SPZ were prepared as described in the methods. The SPZ is anatomically divided into distinct regions. Based on the Paxinos-Franklin mouse brain atlas (Paxinos and Franklin, 2001) the ventral portion is primarily located at Bregma –0.46mm level, while the most dorsal and caudal region extends to Bregma -0.94mm. A central transitional region lies between the two main divisions. Slices were prepared from Bregma -0.46mm to Bregma -0.94mm resulting in three slices each with a thickness of 250µm. This allowed us to separately record the ventral (vSPZ), the central (cSPZ) and the most dorsal (dSPZ) regions of the SPZ, as illustrated by the schematic representation in **Figure 4.6**. In this representation, the ventral SPZ corresponds to the top-left slice, the central SPZ to the top-right slice, and the dorsal SPZ to the region at the bottom.

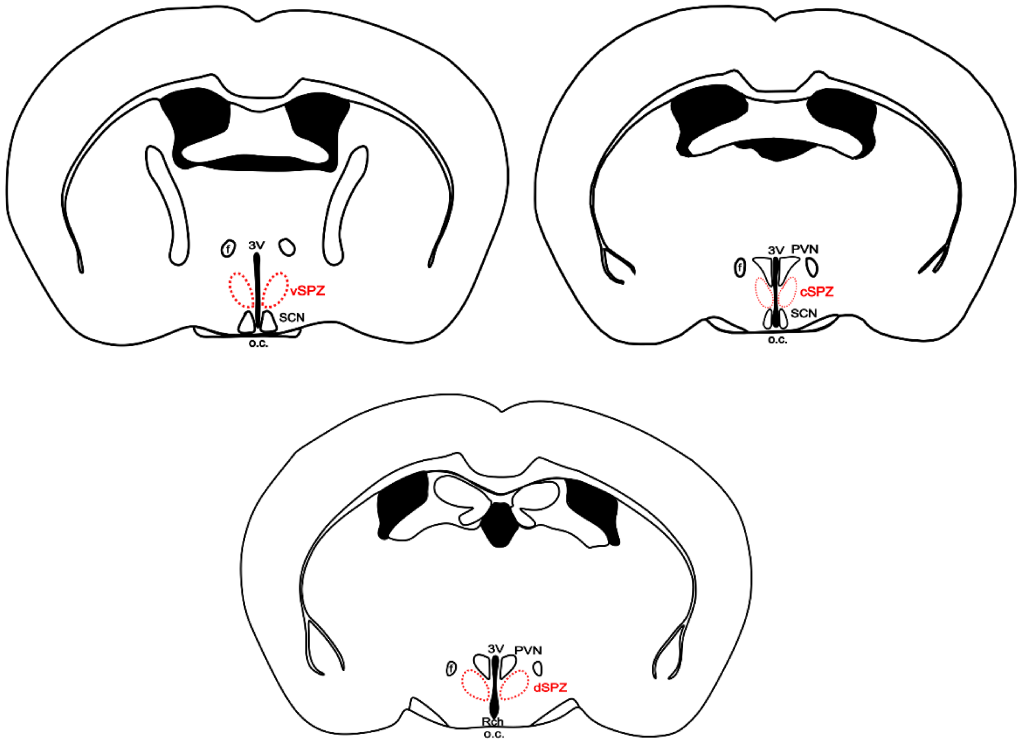

Figure 4.6: schematic representation of the SPZ subregions. Calcium imaging recordings have been performed in ventral SPZ, *top left*, central SPZ, *top right*, and dorsal SPZ, *bottom center*. *vSPZ*, ventral subparaventricular zone,; *cSPZ,* central subparaventricular zone; *dSPZ*, dorsal subparaventricular zone; *PVN*, paraventricular nucleus; *SCN*, suprachiasmatic nucleus; *Rch*, retrochiasmatic area; *o.c.*, optic chiasm; *f*, fornix.

The presence of the GCaMP7f calcium biosensor in the biological preparation was assessed by visualizing the fluorescent signal using an epifluorescence microscopy system. Prior to initiating recordings, we ensured that the viral vector injection was localized to the SPZ, particularly avoiding the SCN.

Recording sessions were conducted by monitoring changes in GCaMP7f fluorescence over time while perfusing the mouse brain slice with ACSF-Na^+ solution for calcium imaging recordings, carboxygenated with 95% O2/5% CO2. To isolate the direct responses, we added TTX (1µM). This approach allowed us to assess the direct effect of the drug on the SPZ population silencing the circuital contribution. In the presence of TTX we applied the drugs detailed in **Table 4.1** below.

DRUG	MOLARITY µM
Neuromedin s	0.1-0.2
Arginine Vasopressin	1
Vasoactive intestinal polypeptide	1
BAY – 55-9837	0.5
Galanin	1
Carbachol	50

Table 4.1: the table reports the drugs used in the present study with the relative concentration used in µM.

The peptides NMS, AVP and VIP represent the main peptides produced by the SCN and were selected for application to assess their effect on the SPZ population. The goal was to understand how and where they might modulate SCN-SPZ communication, particularly if released by the SCN through synaptic or paracrine mechanisms. Notably, the release of these peptides into the SPZ is not exclusively sourced from the SCN, as other inputs remain elusive and are currently under investigation through tracing study, filling an information gap existing in literature.
About peptide receptors, insights were gathered from the Allen Institute *in situ* hybridization data (Allen Institute for Brain Science, 2004**)**. Specifically,

- *in situ* hybridization for NMS receptors, NMUR1 and NMUR2, is only in sagittal slices of the mouse brain, posing interpretational challenges for the SPZ area;
- *in situ* hybridization for AVP receptors indicates a robust signal for AVPR1b and a modest signal for the AVPR1a, suggesting the presence of AVP receptors in the area. However, AVPR2 analysis is limited to sagittal slices;
- *in situ* hybridization for VIP receptors shows practically no signal for the principal VIP receptor, the VPAC2; VPAC1 has been evaluated only in sagittal sections; conversely *in situ* hybridization for a secondary VIP receptor, PAC1, exhibits a high signal.

Then, since there are in literature some proofs about the expression in the SPZ of VPAC2 receptor, especially in the most ventral SPZ (Kallò et al., 2004; Hermes et al., 2009), we applied the BAY 55-9837, a synthetic specific agonist for VPAC2R.
Given the lack of information regarding input to the SPZ and potential modulators of this area, we explored additional factors. Evidence supports the presence of the galanin receptor, GAL1R, as well as galanin-fibers and even galanin mRNA signal in the SPZ (Skofitsch and Jacobowitz, 1985;

Allen Institute for Brain Science, 2004). Additionally, a robust signal for cholinergic transmission mediated by M1 and M4 receptors was identified. Consequently, we applied both galanin (GAL) and the general cholinergic agonist carbachol (Cch) to further investigate their impact on SPZ activity. The role of galanin and carbachol will not be discussed in their general physiologic role, but their effect is used to highlight the different anatomical distribution and the diversity of the SPZ neuronal responses to the principal SCN neuropeptides. By utilizing these two compounds, we aimed to observe distinct pattern of neuronal calcium variation, thereby enhancing the reliability of the responses, and minimizing potential association with technical issues. Moreover, these findings contribute novel information to the field, paving the way for future experiments.

The experiments reported in this study have been conducted applying the compounds in sequence as reported in **Table 4.2**. Each drug was administered following 5-6 minutes of stable baseline, ensuring a total duration sufficient to retain a stable mean plateau variation for at least 2.5 minutes. This approach aimed to extract the maximum response from the slice. The wash-out period extended until mean fluorescence signal reverted to baseline. Subsequently, an additional waiting period of 5 minutes was observed before the application of the second compounds. To minimize the risk of crossed effects between agonists, the sequence was altered in different recordings.

Compound's sequence application

vSPZ	**cSPZ**	**dSPZ**
BAY NMS AVP VIP GAL Cch	BAY AVP NMS VIP GAL Cch	Cch BAY GAL AVP NMS
Cch NMS GAL VIP BAY	Cch AVP NMS BAY GAL	BAY NMS AVP
AVP VIP		
BAY		

Table 4.2: the table shows the sequence of drug applications in the different regions of the SPZ. Each delimited section represents a different mouse brain slice that was recorded.

In each subregion, we aggregated the recorded effects of individual compound. The results are shown in the following pages.

The initial analysis involved the assessment of the mean effect of each compound on the SPZ subregions. As reported in red in **Table 4.3** below, NMS, VIP and BAY 55-9837 in the vSPZ, NMS in the cSPZ and Cch in the dSPZ, did not demonstrate a mean response surpassing the Z-score thresholds. This suggests that these areas are insensitive to these drugs.

	vSPZ		cSPZ		dSPZ	
Drug	**Mean**	**± SEM**	**Mean**	**± SEM**	**Mean**	**± SEM**
NMS	-0.02	0.2	1.2	0.2	4.5	0.3
AVP	2.3	0.3	4.4	0.6	5.5	0.6
VIP	1.7	0.3	4.2	1.6	NaN	NaN
BAY 55-9837	1.6	0.4	4.1	0.4	4.4	0.3
GAL	-4.3	0.3	-3.5	0.3	-3.3	0.5
Cch	4.5	0.9	13	1.6	-0.03	1.6

Table 4.3: the table reports the mean ± SEM Z-score values of the effect exerted by each drug grouped by the SPZ subregions. *NaN*, missing data.

Upon inspecting the distribution of the values in the box-normal plots in **Figure 4.7** remains possible to observe that in all cases there are several Z-score points which fall over the Z-score threshold. This indicates the potential existence of smaller clusters in the area that behave differently from the mean. Particularly noteworthy is the response to Cch in the dorsal SPZ, where the mean value of -0.03 ± 1.6, as shown below, highlights how the resulting mean is essentially the arithmetic summation of cells activated by Cch and cells that are inactivated or non-responding. This could lead the erroneous conclusion that Cch does not exert any effect on the dSPZ.

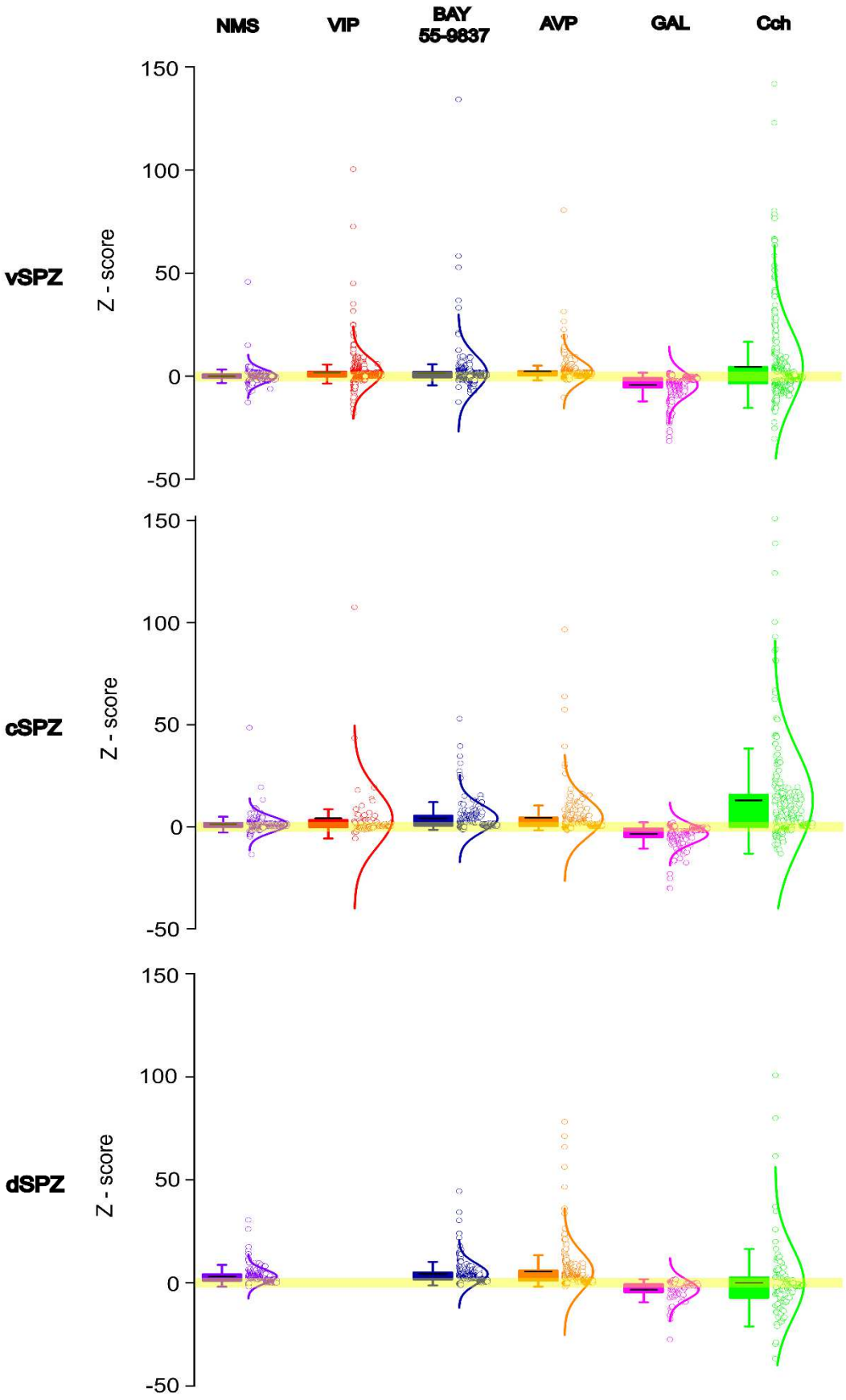

Figure 4.7: compound mean effect observed on the SPZ subregions. Box-normal plots of the mean Z-score values, represents the overall effect of the drugs in the SPZ subregions. *Black bar*, average; *whiskers*, outliers limit.

Subsequently, based on the Z-score threshold and the tendency to wash-out after drug application, we categorized the responses of single cells into three groups:

- activated cells,
- inactivated cells,
- non-responding cells.

These results are reported in **Figure 4.8, Figure 4.9** and **Figure 4.10.**

For each subregion we display the Z-score time course of all the activated, inactivated or not responding cells in light gray, with the average response highlighted in black. The inset of the average responses is depicted on the right side, together with the relative percentages (*right bottom*). The relative mean ± SEM of the Z-score, along with the number of cells (*n*) and the number of brain slices/animals (*N*) considered for the analysis are summarized in the table on the right (*right top*).

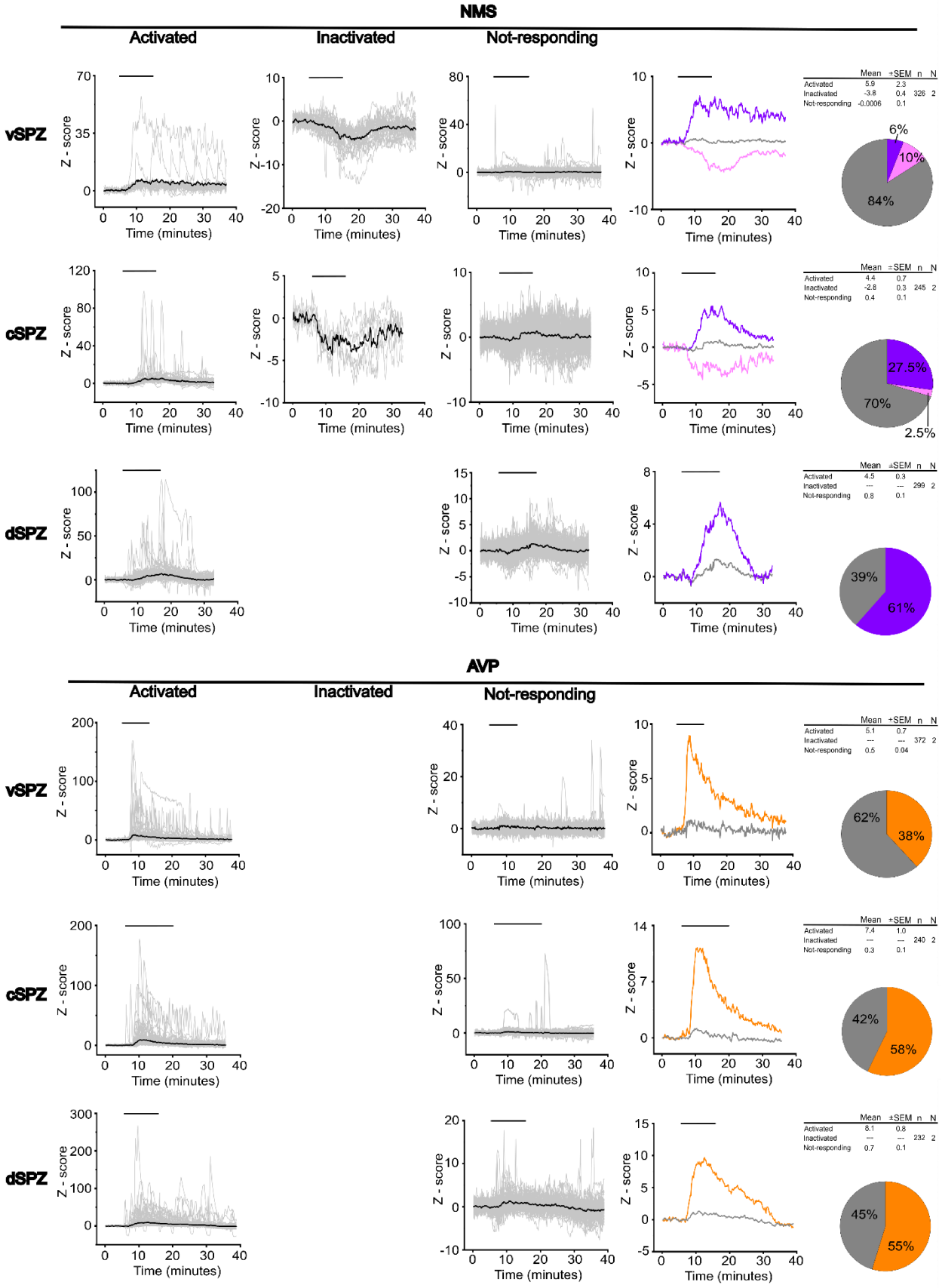

Figure 4.8: vSPZ, cSPZ and dSPZ neurons respond to the NMS and AVP applications.

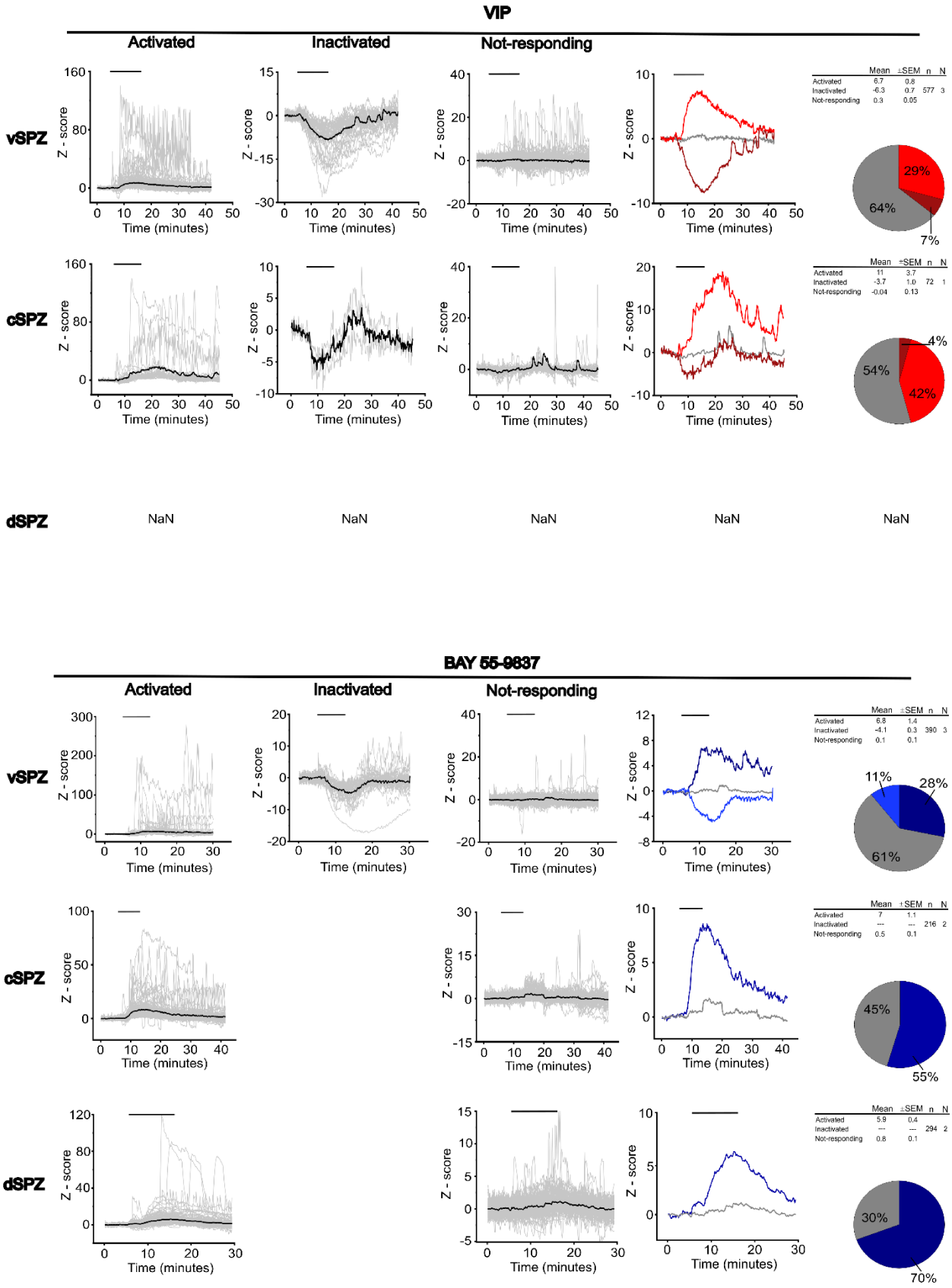

Figure 4.9: vSPZ, cSPZ and dSPZ neurons respond to the VIP and BAY 55-9837 applications.

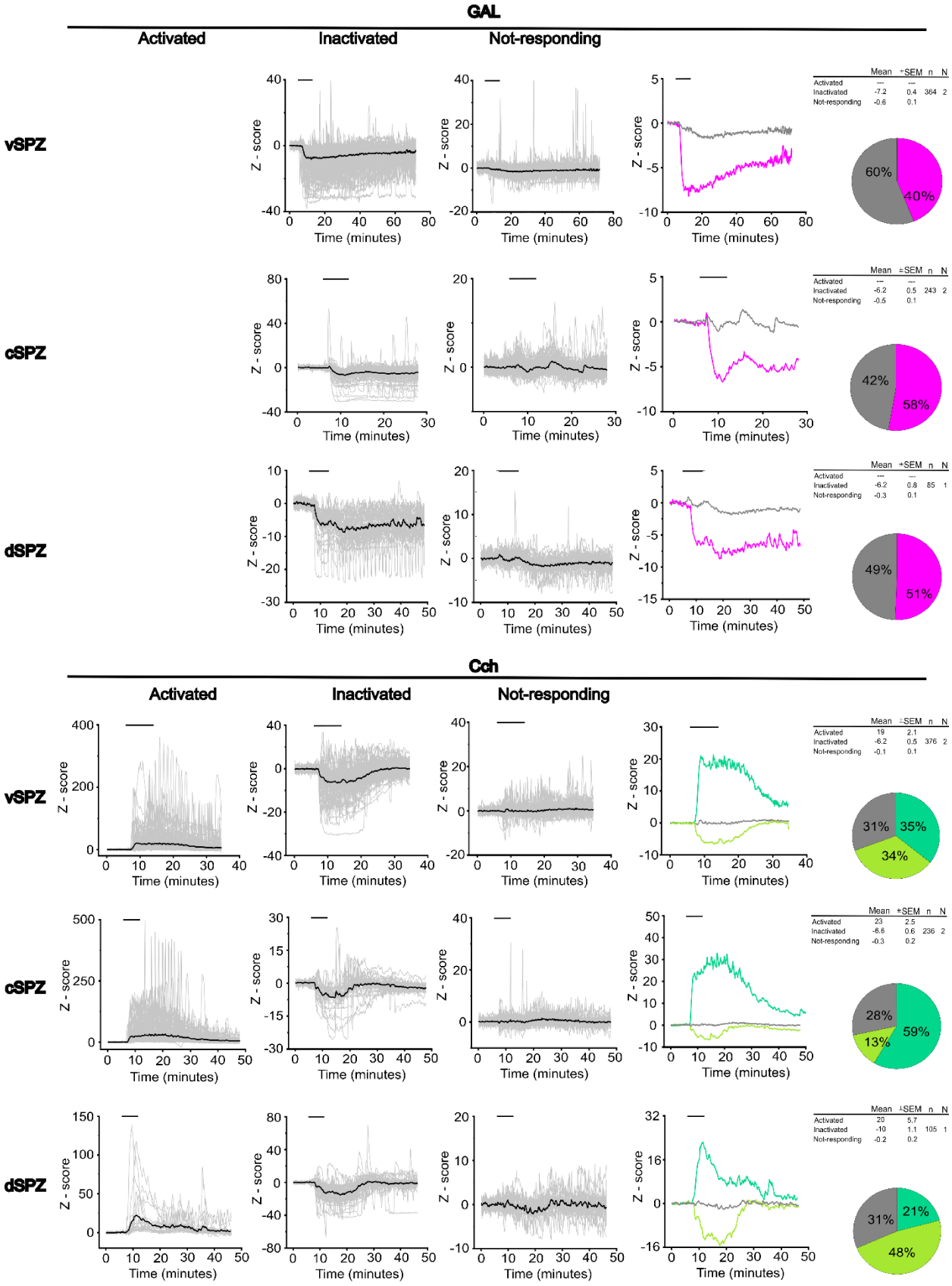

Figure 4.10: vSPZ, cSPZ and dSPZ neurons respond to the GAL and Cch applications.

4.2.2 DISCUSSION: SPZ neurons respond to the SCN neuropeptides with an anatomical organization.

The neuromedin S effect on the SPZ subregions.

The results from the present study indicate that neuromedin S can elicit diverse responses in the cells of the SPZ, suggesting the presence of NMS receptors on the membrane cells of the SPZ neurons. Interestingly the response to NMS appears to vary along the rostro-caudal axis of the SPZ nucleus. Specifically, cells responding to NMS application range from 16% in the vSPZ, to 30% in the cSPZ (chi-square test $p < 0.001$*** comparing vSPZ vs cSPZ responding cells/non-responding cells), reaching the 60% in the dSPZ (chi-square test $p < 0.001$*** comparing cSPZ vs dSPZ responding cells/non-responding cells). More interesting in the vSPZ the predominant response to NMS is an inactivation of neurons in terms of calcium changes, while from the central SPZ to the dorsal SPZ the prevalent response is activation. This dual response to NMS may be explained by the fact that NMS signaling can be mediated by NMUR1 and NMUR2 receptors, both of which have been associated with inhibitory and excitatory GPCR-mediated pathways. While there is not much information about the expression of NMS receptors in the SPZ area, this study suggests that NMS may serve as neuromodulator in the SCN-SPZ transmission with a potential anatomical organization that varies along the axis of the SPZ nucleus.

The arginine vasopressin effect on the SPZ subregions.

The application of AVP induces a response in neurons of the SPZ subregions indicating the presence of AVP receptors on the membrane of these neurons. Additionally, like the NMS study, is possible to recognize an anatomical distribution of the response along the rostro-caudal axis. The response is relatively homogeneous in the central SPZ and dorsal SPZ, with 58% and 55% of responding cells, respectively (chi-square test $p > 0.05$ comparing cSPZ vs dSPZ responding cells/non-responding cells). However, the ventral SPZ shows a slightly lower effect, with 38% of responding cells (chi-square test $p < 0.001$*** comparing vSPZ vs cSPZ responding cells/non-responding cells).

Another aspect to be considered is that AVP seems to induce a transient change of the intracellular calcium levels, suggesting a probable mechanism of receptor adaptation. The response does not reach a stable plateau during the application and the analysis has been performed around the midpoint of the application due to the peculiar effect of AVP on calcium dynamics. These findings shed light on the potential role of AVP in modulating neural activity in the SPZ and suggest the need for further investigations to identify the mechanisms underlying the transient calcium changes induced by AVP. Regarding this attenuation phenomenon in response to AVP,

characterized by a transient change in intracellular calcium levels that does not reach a stable plateau during the application, there are evidence for an uncoupling from the internal pathway and also for an internalization process of the receptor. A study in *Xenopus* oocyte where the cRNA for the AVPR1a is expressed, has proved that the activation of the PKC induces receptor desensitization (Ancellin et al., 1998). Additionally, imaging study in HEK cells has provided evidence for an acute and reversible process of receptor internalization leading to the formation of cytoplasmatic endosomes (Innamorati et al., 2001). Notably the vasopressin receptor 1a has proven to be affected also by heterologous desensitization, particularly mediated by M3 and M5 muscarinic receptors, but in both studies (Ancellin et al., 1998, Ancellin et al. 1999) the activation of the muscarinic pathway occurs in a very short time (less than 5 minute between drug application). In contrast, in this study, the intervals between drug applications are at least 20 minutes. The stable response observed between different areas and sequences of drug application suggests that the attenuation of the AVP response may be primarily due to homologous internal desensitization or receptor internalization rather than a heterologous mechanism. Further investigation into the internal processes underlying this phenomenon would provide valuable insights into regulatory mechanisms of AVP receptors in the SPZ. Finally, in all the SPZ regions we did not detect a possible inactivation mechanism caused by the AVP.

The vasoactive intestinal polypeptide effect on the SPZ subregions.

The effect of the VIP on SPZ neurons has been previously studied by Hermes *et al.* (Hermes et al., 2009) with the patch-clamp technique. In their paper is not specified the anatomical level in which they have recorded, but it seems that the study was concentrated in the vSPZ/cSPZ. They described a post-synaptic depolarization current mediated by VPAC2, and a presynaptic facilitation phenomenon for SCN GABAergic transmission induced by VIP. These, opposite effects occur in two different subtypes of SPZ neurons. Moreover, Reed *at al*. in the SCN neurons have found that VIP can induce both an increase and a decrease in the firing rates. They proposed that the decrease might be modulated by the GABAergic transmission, but bicuculline treatments in some cells, did not completely block it (Reed et al. 2002). In our study, the decrease in the intracellular calcium mediated by VIP application, as shown in **Figure 4.9**, which characterizes a small cluster of the vSPZ and cSPZ can be attributed to VIP-mediated effects. Understanding the diverse responses to VIP in different subregions and cell types contributes to a more comprehensive view of its modulatory role in the SCN-SPZ circuitry.

The inhibitory action mediated by BAY 55-9837, a VPAC2R agonist, presents some interesting aspects. VPAC2R is usually associated with Gs signaling, which usually implies excitatory

responses. Then an inhibitory action by VPAC2R activation probably implies different unknown mechanisms. The observation that higher inhibitory response was obtained in experiments where BAY 55-9837 has been added after the washing out of VIP, adds complexity to the signaling relationship, and its precise mechanisms are unclear. Possibly explanations for this observation includes a strong presynaptic effect on the GABA-terminals (potentially from SCN or other sources), or the existence of a cluster of vSPZ neurons where the VPAC2R is associated with an inhibitory internal signaling.

Then our results are coherent with Hermes *et al*. (Hermes et al., 2009) work and provide evidence for the presence of a VIP signaling pathway, likely mediated by VPAC2R, in the SPZ subregions. Even if the VIP application experiment has not been performed in the dSPZ, rostro-caudal development of response across SPZ subregions using BAY 55-9837 (chi-square test $p < 0.001$*** comparing vSPZ vs cSPZ responding cells/non-responding cells; chi-square test $p < 0.001$*** comparing cSPZ vs dSPZ responding cells/non-responding cells) suggests a broad influence of VIP modulation, extending to the dorsal SPZ. Moreover, these results are in contrast to those of Paul *et al*. (Paul et al. 2020), because they did not find a significant change in the firing rate of the VIP^{in} neurons (the group of cells that receives the innervation of SCN^{VIP} and to which the SPZ neurons belong) after the application of exogenous VIP. One plausible explanation for that apparent discrepancy between the results of this study and those of Paul *et al*., is because they employed MEA recordings that probably could not detect VIP effect. The sensitivity of recordings techniques plays a crucial role in detecting neuronal responses, especially if the modulation induced by a substance, in this case, VIP, is subtle or requires a specific threshold for firing. If the depolarizing transmembrane current generated by VIP is not strong enough to initiate firing from the membrane's resting potential, it might go undetected in certain recording setups. Patch-clamp recordings might provide a more detailed view of the modulation of SPZ neurons. Additionally, the concentration of VIP used in this study and in the study by Hermes *et al.* (Hermes et al., 2009) (between 0.5µM and 1µM) might have been more effective in eliciting responses compared to the lower concentration (100nM) used by Paul *et al.* (Paul et al., 2020). Hence, it is crucial to consider factors like peptide concentration, neuronal subtypes, and anatomical regions when comparing results across studies.

In conclusion, VIP is capable of modulating SPZ neurons through a VPAC2 receptor mechanism, and this modulation spread from the vSPZ to the cSPZ and dSPZ (Kallò et al., 2004, Lein et al., 2007).

The galanin and carbachol effect on the SPZ subregions.

As anticipated in the present study the galaninergic and cholinergic role in the circadian rhythmicity is not discussed. The consistent response to galanin and carbachol in all SPZ regions provides valuable insights into the overall modulation of SPZ neurons by these neurotransmitters. Hence, these two transmitters have served to validate the results of the NMS, AVP and VIP influence considering that we were initially exploring how to perform this study with the calcium imaging technique.

The clear signal for the expression of the GALR1 receptor associated with the Gi pathway (Jiang and Zheng 2022), aligns with our recordings that define an inactivation of the SPZ neurons with a long-lasting effect. More interesting when comparing the effect of galanin with those of NMS, AVP and VIP action, it appears that galanin affects SPZ neurons with same proportions between subregions in a manner similar to AVP (chi-square test $p < 0.001$*** comparing vSPZ vs cSPZ responding cells/non-responding cells; chi-square test $p > 0.05$ comparing vSPZ vs dSPZ responding cells/non-responding cells). This consistency strengthens the validity of the observed responses to different modulators in the SPZ population.

Acetylcholine acts through many different receptors belonging to the nicotinic and muscarinic families. While interpreting the expression of the nicotinic receptor in SPZ is difficult, the *in situ* hybridization data from Allen Institute reports a high signal for M1 and M4 muscarinic receptors. The signaling associated with these two receptors is complex and can depend on the concentration used. For example, the M4 activated by a 100µM of agonist can switch the response from the predominant coupling to the Gi/o to the stimulation of the Gs with the consequent production of the cAMP, usually correlated with neuronal activation. M1 receptors are predominantly associated with the Gq pathway, but responses involving Gi and Gs responses have also been described (van der Westhuizen et al., 2021). Consistent with the expressions of M1 and M4 receptors in the SPZ and their main signaling pathway, we have found two distinct clusters responding to the Cch application in the SPZ. There is indeed a clear group of neurons inhibited by cholinergic transmission and another group that is activated. Interestingly, the activated cells are more prevalent in the rostral SPZ, while the inhibited group characterize the dorsal SPZ. This finding provides important insights into the differential effects of cholinergic transmission in distinct subregions of the SPZ, however, this observation requires further experimental sessions. Notably, cholinergic transmission influences the SPZ with approximately the same proportion of affected neurons (~70%) across different subregions (chi-square test $p > 0.05$ comparing vSPZ vs cSPZ responding cells/non-responding cells; chi square test $p > 0.05$ comparing cSPZ vs dSPZ responding cells/non-responding cells).

These results gave us more confidence in the observed results obtained using the NMS, AVP and VIP peptides agonist. Hence, calcium imaging recordings have provided valuable proof of principle for the ongoing study. The consistent and region-specific responses observed with these neuropeptides suggest the presence and involvement of specific receptors in the SPZ.

4.3 CHAPTER THREE

Subparaventricular zone in the systemic physiology: the SPZ involvement in the corticosterone circadian release.

The results regarding the conditional rabies tracing and the corticosterone monitoring followed by SPZ ablation of the present chapter, are kindly provided by Ph.D. Oscar Ramirez Plascencia (Beth Israel Lahey Health - Harvard Medical School, Boston, MA).

4.3.1 Conditional ablation of the SPZ^{VGAT} neurons and corticosterone monitoring.

The more traditional ablation techniques lack of specificity. Therefore, we pursued a conditional ablation method to chronically disrupt the SPZ^{VGAT} neuronal function. For this experiment we used an AAV that expresses diphteria toxin subunit A in neurons expressing Cre recombinase and the mCherry protein in neurons that do not express Cre recombinase. This virus permits to better mark the extension of the injection. The virus has been injected in the SPZ nucleus of 7 Vgat-Ires-Cre::L10-GFP mice (**Figure 4.11 panel A**). The expression of mCherry marked the injection site and highlights the reduced L10 signal in the ablated SPZ animal. The post-formalin fixation of the tissue revealed comprehensive deletions that characterized the entire SPZ nucleus as depicted in **Figure 4.11 panel B**. The reliability of the extension of the ablation to the targeted area is shown by the heat map of the injection site **Figure 4.11 panel C**. This methodology allows for a precise and specific disruption of the SPZ^{VGAT} neuronal function for further investigation into its role.

After 4 weeks post-surgery, we have collected blood samples to measure the corticosterone concentration in the ablated mice, paralleled with sampling in the non-ablated cohort. Blood collection (described in paragraph "3.2.3 Corticosterone circadian monitoring") has been performed at zeitgeber time (ZT) 1,7,13,19 in light/dark cycle condition (with lights ON corresponding to the ZT12) and at circadian time (CT) 1,7,13,19 in DD condition. The ablated and not-ablated animals after the sampling in the LD condition have been subjected to 3 days of constant darkness condition to permit adaptation to the change in the zeitgeber absence, before to start the corticosterone sampling in DD conditions.

ELISA assay has been performed and the results in **Figure 4.12 panels A** and **B** illustrate the distinct corticosterone profiles between the ablated and non-ablated cohorts in both LD and DD conditions. In non-ablated mice corticosterone levels exhibited a characteristic circadian rhythm with a peak before the dark/active phase, consistent with the natural diurnal pattern both in LD and DD photoperiods. Notably, the absence of the SPZ^{VGAT} neurons completely abolishes the typical circadian peak of corticosterone suggesting the SPZ^{VGAT} neurons play a crucial role in

regulating the circadian release of corticosterone. Specifically, in LD photoperiod the two-way ANOVA indicated significant effect of Time ($F_{(3,64)} = 13.49$, $p < 0.001$***) and Time*Group interaction ($F_{(3,64)} = 2.88$, $p = 0.042$*), but no for Group factor ($F_{(1,64)} = 0.09$, $p = 0.76$). In the DD photoperiod the significance is for all the variables: Time ($F_{(3,64)} = 15.73$, $p < 0.001$***), Group ($F_{(1,64)} = 4.85$, $p = 0.03$*) and Time*Group interactions ($F_{(3,64)} = 19.46$, $p < 0.001$***).

Circadian index analysis (**Figure 4.12 panel C**) also confirmed the loss of the circadian rhythmicity in the corticosterone release at ZT13 both in the LD, with a reduction of 39.31% ±13.86 (unpaired T-test: $T_{(16)} = 2.83$, $p = 0.011$*) and DD conditions, with a reduction of 80.29% ±13.42 (unpaired T-test: $T_{(16)} = 5.98$, $p < 0.001$***).

A stable rhythm for the corticosterone is instead confirmed both in LD and DD conditions in non-ablated animals, indicating the internal control of the rhythm itself.

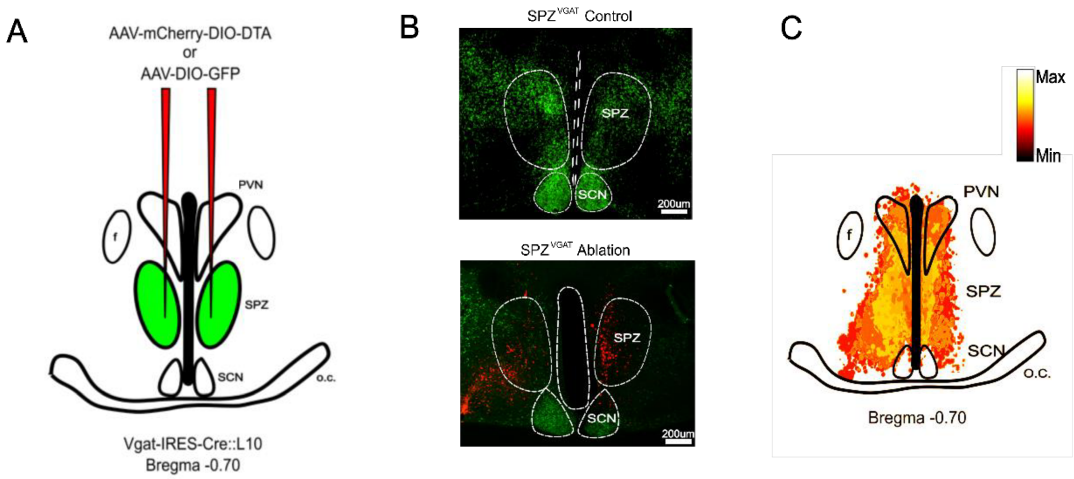

Figure 4.11: SPZ^{VGAT} conditional DTA ablation. A) Schematic representation of the bilateral AAV-mCherry-DIO-DTA injection in the SPZ nucleus of Vgat-Ires-Cre:L10 mice. **B)** Confocal acquisition images showing the L10:GFP (control) and the L10:GFP with the AAV-mCherry-DIO-DTA signal (ablation) of one injected animal, demonstrating the loss of the SPZ^{VGAT} neurons. **C)** Averaged heat map of the area affected by the DTA ablation (n = 7). (For copyright reasons, not all the SPZ anatomical levels are represented). *SPZ*, subparaventricular zone; *PVN*, paraventricular nucleus of the hypothalamus; *SCN*, suprachiasmatic nucleus; *o.c.*, optic chiasm; *f*, fornix.

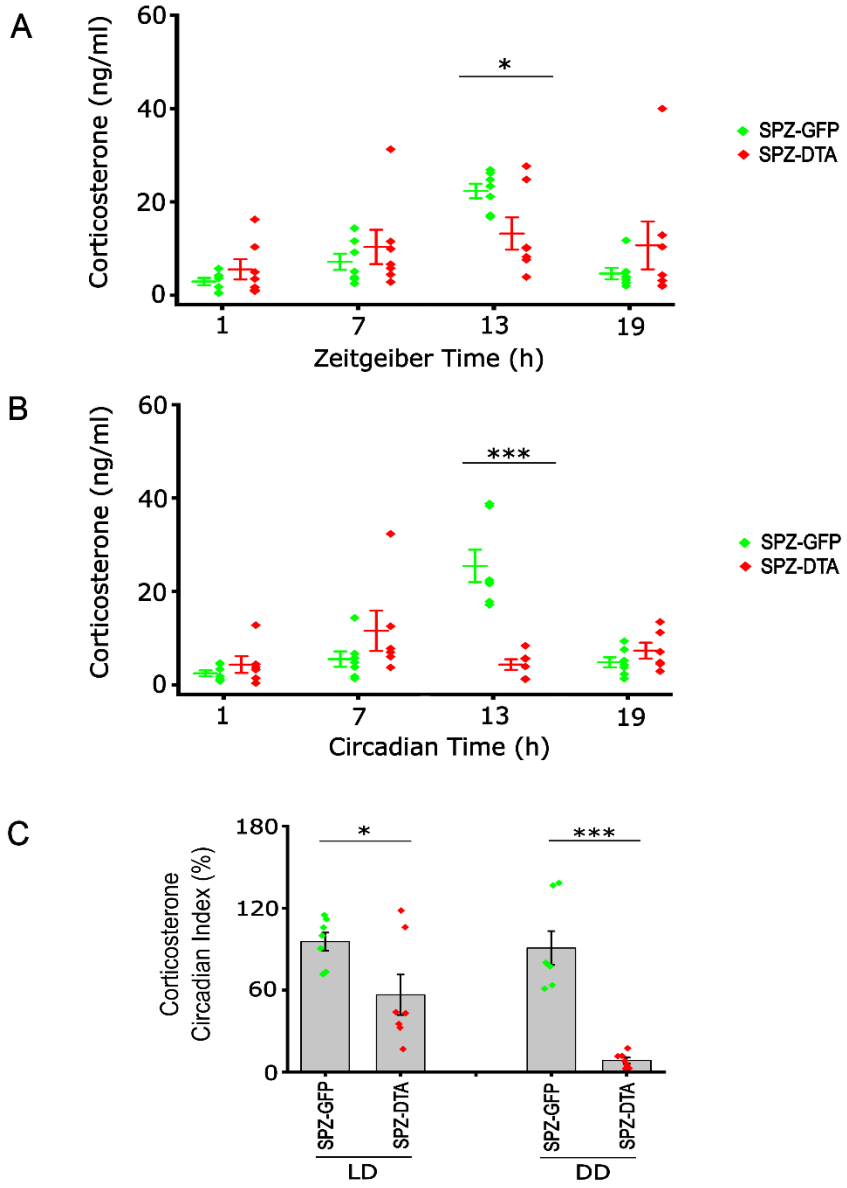

Figure 4.12: conditional DTA ablation of SPZ^{VGAT} neurons results in loss of the corticosterone circadian release. **A-B)** Scatter interval grouped plots showing the change in blood corticosterone level in the ablated Vgat::L10 mice (*red*, n = 7) and non-ablated Vgat::L10 mice (*green*, n = 7), in the LD (A) and DD (B) conditions. Values are represented as mean ± SEM. (ANOVA two-way, LD $p < 0.05$* and DD $p < 0.001$***) **C)** Bar grouped graphs displaying the circadian index results, showing a significant variation for ablated animal (SPZ-DTA) in LD (*left*, n = 7) and DD (*right*, n = 7) compared to the circadian index of non-ablated animals (SPZ-GFP), (ANOVA two-way, LD $p < 0.05$* and DD $p < 0.001$***) .

4.3.2 Conditional rabies tracing of the PVN^{CRH} neurons.

Knowing the limits of the traditional tracing study we aimed to define the synaptic input to the PVN^{CRH} neurons using conditional monosynaptic retrograde rabies tracing.

Using a stereotaxic apparatus for mouse brain microsurgery the injection of the conditional virus for the TVA and RG was initially targeted at the PVN in CRH-Ires-Cre mice (n = 5). After 21 days post-surgery a second injection was performed in the PVN of the same animals with the RABVΔG-EGFP-(EnvA) (**Figure 4.13 panel A**). This approach allowed for the selective targeting of CRH-expressing neurons in the PVN for monosynaptic retrograde rabies tracing. After 7 days post second injection, histological analysis was carried out as described in "paragraph 3.2.2 Histology". In the hypothalamic regions the CRH is mostly expressed in the PVN, making the injection highly specific to the PVN^{CRH} neurons with no leakage in the surrounding areas. Approximately 90% of the TVA transfected starter cells colocalized with the rabies signal, indicating a high degree of viral infection and successful targeting of the CRH neurons in the PVN (**Figure 4.13 panel B**). This technique provides a valuable tool for mapping the synaptic inputs to PVN^{CRH} neurons.
With the employed conditional strategy, the PVN^{CRH} neurons expressing the TVA receptor were recognized by the mCherry transfection tag, while the neurons infected by the rabies virus were labeled with the EGPF transfection tag. Colocalization of these two signals resulted in a yellow signal (**Figure 4.13 panel C**). This double-labeling approach helps distinguish between PVN^{CRH} neurons expressing the TVA receptor and those infected with rabies virus, providing clearer visualization of monosynaptic inputs to PVN^{CRH} neurons.
Many retrogradely EGFP labeled neurons were found in the bed nucleus of the stria terminalis in the forebrain and in the Reuniens thalamic nucleus (*data not shown*). The majority of the afferent inputs to the PVN^{CRH} neurons originates from the hypothalamus. **Figure 4.13 panel D** illustrates an important monosynaptic input to the PVN^{CRH} neurons from the preoptic area (MPA, VLPO, VMPO, MnPO) indicating an important role of these nuclei in regulating the PVN^{CRH} activity. A consistent inter-connectivity is also observed within a high number of rabies positive cells in the PVN that are no starter cells. Additional projections arise from the arcuate nucleus, the lateral hypothalamus and retrochiasmatic area. Notably are the projections from the SPZ and DMH (**Figure 4.13 panel E**). In the previous paragraph "4.3.1 Conditional ablation of the SPZ^{VGAT} neurons and corticosterone monitoring*"* it is demonstrated that the SPZ is crucial for maintaining a normal circadian rhythm in corticosterone release. The DMH has been proved to be important to regulate the PVN^{CRH} activity**.** Interestingly no EGFP signal was detected in the SCN, suggesting that the circadian control exerted by the SCN for the corticosterone release is not direct. Instead, it likely occurs through a polysynaptic circuit, possibly involving the SPZ which relays information to the DMH nuclei. Indeed is shown that the DMH has stronger input to the PVN^{CRH} than the SPZ and comes out as a key player in the regulation of circadian corticosterone release (Chou et al., 2003; Saper et al., 2005; Saper, 2013).

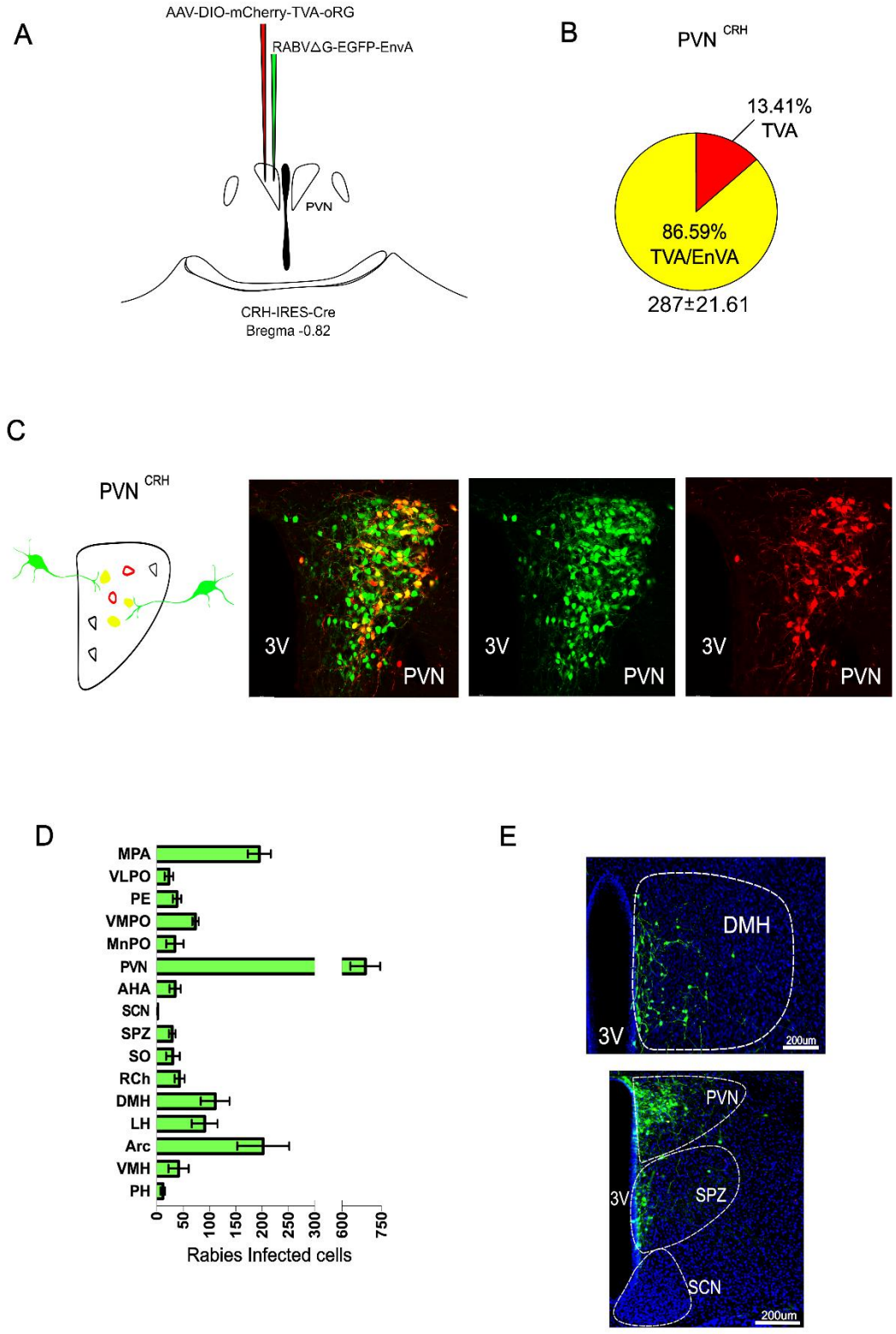

Figure 4.13: monosynaptic input to the PVN^{CRH} neurons originates from areas involved in the corticosterone circadian release. A) Schematic representation of the conditional rabies injection in the PVN^{CRH} neurons of the CRH-Ires-Cre mice. **B)** Pie chart of the TVA-Rabies positive PVN^{CRH} neurons (86.59%, n = 287±21.61 **C)** Confocal images of TVA-mCherry (*red*) and rabies-EGFP (*green*) signal in the PVN^{CRH} neurons. Colocalizing signals result in a yellow color as indicated also in the schematic representation on the left. **D)** Bar graph representing the counted cells ± SEM in the hypothalamic nuclei of the injected mice **E)** Confocal images of the

rabies-EGFP (*green*) signal in the DMH (*top*) neurons and SPZ (*bottom*) neurons. *MPA*, medial preoptic area; *VLPO*, ventrolateral preoptic area; *PE*, periventricular nucleus; *VMPO*, ventromedial preoptic area; *MnPO*, median preoptic area; *PVN*, paraventricular nucleus; *AHA*, anterior hypothalamus; *SCN*, suprachiasmatic nucleus; *SPZ*, subparaventricular zone; SO, supraoptic nucleus; *RCh*, retrochiasmatic area; *DMH*, dorsomedial nucleus; *LH*, lateral hypothalamus; *Arc*, nucleus arcuate; *VMH*, ventromedial hypothalamus; *PH*, posterior hypothalamus.

4.3.3 DMH^{VGAT} neurons respond to the optogenetic photostimulation of the SPZ^{VGAT} input.

To unravel the connectivity nature of the SPZ input to the DMH neurons, the following investigation was prompted by the findings of the present study and literature. Preliminary data (*data not shown*) demonstrated that PVN^{CRH} neurons receive both a direct glutamatergic input and an indirect GABAergic input from the DMH. The DMH^{GABA} input, in particular, diminishes the inhibitory spontaneous currents of the PVN^{CRH} neurons (*data not shown*, *Ramirez Plascencia and De Luca et al. in preparation*). Given the GABAergic nature of the SPZ, we decided to firstly investigate potential indirect SPZ modulation of the PVN^{CRH} neurons through the DMH, indagating the SPZ modulation of the DMH GABAergic neurons. This question has also given us the possibility to use a single transgenic mouse. The idea in this regard is that the SPZ inhibiting the DMH GABAergic neurons, induces the inhibition of the PVN^{CRH} neurons, synergizing probably together with a direct inhibitory effect as suggested by our rabies study.

To analyze the modulation operated by the SPZ on DMH neurons, we employed optogenetic stimulation of neurons expressing the excitatory ChR2 opsin combined with whole-cell patch clamp recordings. Experiments were conducted on brain slices (250μm thickness) containing DMH neurons. We have injected Vgat-Ires-Cre mice in the SPZ with the ChR2 and in the DMH with a Cre-dependent GFP to label the GABAergic population (**Figure 4.14 panels A** and **C**). The following present results are derived from experiments collected from a sample size N = 4.

We assessed the presence of ChR2 in the biological preparation through visualization of the mCherry transfection tag. The specificity of the injection site to the SPZ was then confirmed. More specifically, our injections were more concentrated in the vSPZ (as shown by the compiled map of the injection site), a region that has been described (Chou et al., 2003; Vujovic et al., 2015; Todd et al., 2020**)** to send a robust innervation to the DMH (**Figure 4.14 panel B**). While the DMH injection was verified by the GFP tag and the injection has been considered satisfactory even if other areas were involved. In this case the tag was important only to recognize specific cells and did not have a functional meaning.

The activity of inhibitory postsynaptic current events in DMH^{VGAT} neurons were recorded while maintaining stable the membrane voltage at 0mV using an intracellular recording solution

containing the potassium channel blocker cesium-methanesulfonate. The brain slice was continuously perfused with ACSF-Na solution for patch clamp recordings carboxygenated with 95% O2/5% CO2, where we added 1mM of kynurenic acid to isolate the inhibitory input. Full-field stimulation of SPZ^{VGAT} input was achieved through a 470nm LED and the presence or absence of the photo-evoked events synchronized with the stimulus were recorded. The SPZ^{VGAT} input was photostimulated with a 10ms light pulse given every 10 seconds for a total of 5 minutes (30 trials). Firstly, we have evaluated if there was a specific anatomical difference in the SPZ→DMH input by recording 5 cells in the most anterior DMH and 5 cells in the most medial DMH from each animal. The data indicate that 65% of the recorded neurons (n = 40) responded to the activation of the SPZ input. However, this connection rate did not show specific difference between the anterior (66.6% connected cells, 33.4% non-connected cells, n = 18) and medial (63.6% connected cells, 36.4% not connected cells, n = 22) DMH (**Figure 4.14 panel E**, chi-square test $p > 0.05$). Either the amplitude (average of 53.03 ± 9.26pA n = 12/18 for the anterior DMH, and average of 31.73 ± 8.45pA n = 14/22 for the medial DMH) and latency (average of 8.02 ± 0.5ms n = 12/18 for the anterior DMH, and average of 9.06 ± 0.98ms n = 14/22 for the medial DMH) of the connected cells show significant differences (**Figure 4.14 panel F**, unpaired T-test $p > 0.05$). All the recorded cells were then treated together, and the average probability of the connected cells was 109.35 ± 6.5% (n = 26/40). No difference in spontaneous IPSCs was detected between the connected and non-connected cells (2s window of time considered, unpaired T-test $p > 0.05$), (**Figure 4.15 , panels A** and **B**).

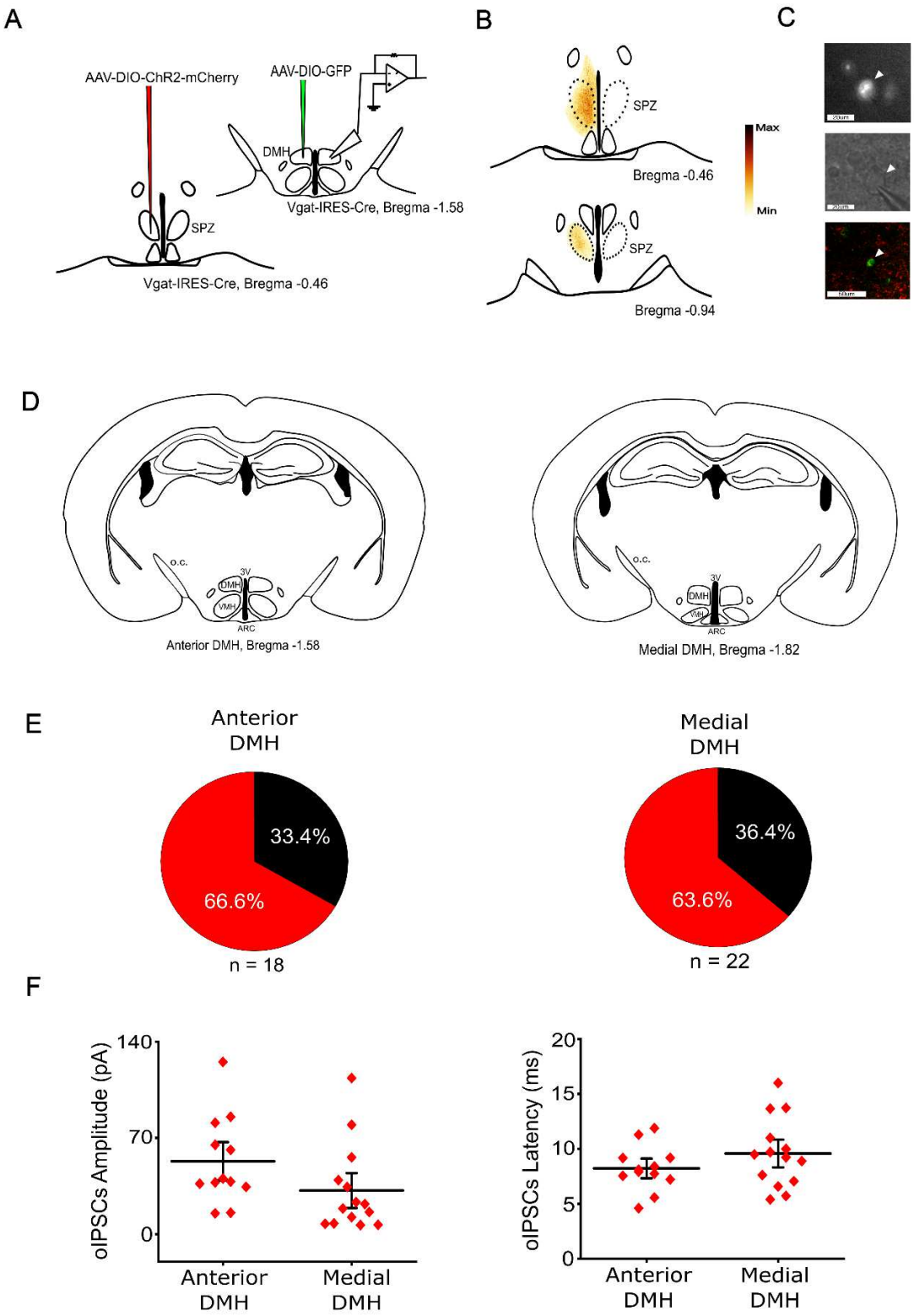

Figure 4.14: optogenetic stimulation of the SPZ^{VGAT}→DMH^{VGAT} input. **A)** Schematic model representing the experimental design used to investigate the SPZ input to the DMH region. AAV-DIO-ChR2-mCherry was injected into the vSPZ of Vgat-Ires-Cre mice. Patch clamp recordings were made from GFP labeled DMH^{VGAT} neurons in the anterior and medial DMH. **B)** Mapping of the injection site for the ChR2 expression in the SPZ. Glow LUT (**l**ook **u**p **t**able) applied. **C)** *Top*, fluorescence determination of the DMH^{VGAT} GFP-positive recorded neuron. *Center*, infrared picture of the DMH^{VGAT} recorded neuron (*scale bar*, 20µm). *Bottom*, confocal images post-formalin fixation of the DMH^{VGAT} neuron GFP-marked and surrounded by the SPZ mCherry fibers (*in red*). (This acquisition is random, is not the same neuron of the top and the

center) (*scale bar*, 50µm). **D)** Schematic representation of the anatomical level considered to define the anterior DMH, on the *left*, and the medial DMH, on the *right*. **E)** Pie charts of the connected and not connected cells of the anterior and medial DMH. Photo-stimulation of SPZ^{VGAT} neurons evoked post-synaptic currents in 65% of the recorded DMH^{VGAT} neurons (n = 26/40) **F)** Average amplitude and latency time of the opto-evoked IPSCs in the anterior and in the medial DMH. *SPZ*, subparaventricular zone*; DMH,* dorsomedial hypothalamic nucleus*; VMH,* ventromedial hypothalamic nucleus*; ARC,* arcuate nucleus*; o.c.,* optic chiasm; *3V*, third ventricle.

In 4 out of 26 connected cells recorded at 0mV, the pharmacological combination of 1µM TTX and 250µM 4-AP was applied to assess the monosynaptic nature of the connection, as already suggested by the average latency. The recorded cells showed resistance to the pharmacological treatment, indicating the monosynaptic nature between SPZ^{VGAT} and the DMH^{VGAT} cells. Two of these cells, have been also treated with bicuculline at 20µM. Bicuculline completely abolished the photo-evoked event after 25 minutes of administration, indicating that this connection is primarily mediated by $GABA_A$ ionotropic receptors (**Figure 4.15 panel C**).

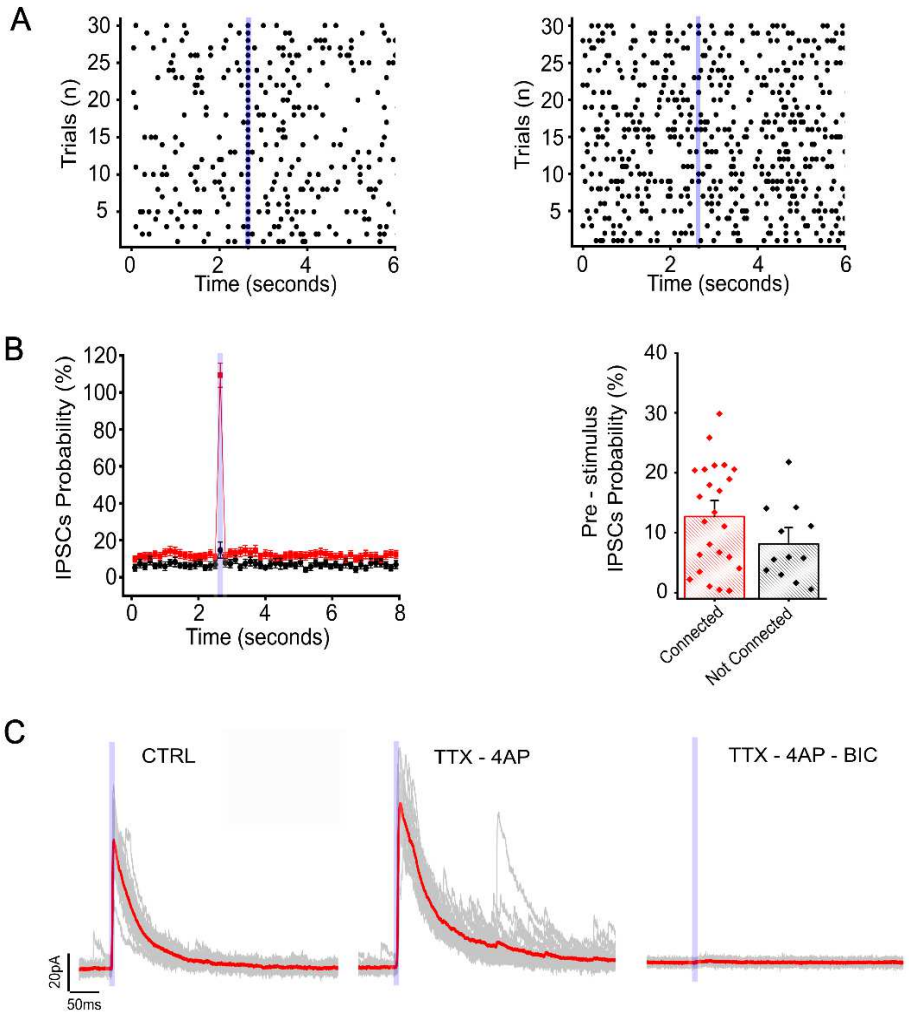

Figure 4.15: nature of the SPZ^{VGAT}→DMH^{VGAT} input. **A)** Raster plot of the IPSCs events of a connected cell (*left*) and not connected cell (*right*) **B)** *On the left*, average probability of the IPSCs in the connected cells (*red*, n = 26/40) and not connected cells (*black*,

n = 14/40). *On the right*, average of the IPSCs probability pre-stimulus of the connected and not connected cells (2s window of time considered, unpaired T-test p > 0.05). **C)** Representative whole cell recording at 0mV of the oIPSC in a control condition (CTRL), during the pharmacological TTX-4AP (TTx-4AP) (n = 4) treatment and after bicuculline application (TTX-4AP-BIC) (n = 2). Average trace in *red*, single trace in *light grey*. (10ms photostimulation is indicated by the *blue bar*).

Whole-cell recordings in current clamp mode were conducted using an intracellular solution of K-gluconate, to assess the effect of photo-stimulation on the firing frequency and the membrane potential of DMH^{VGAT} neurons. These neurons were identified as connected cells based on the study of the opto-evoked inhibitory event in voltage clamp at -40 mV. In 3 out of 6 recorded neurons, we have applied a range of photostimulation frequencies of the SPZ terminals (1Hz, 2Hz, 5Hz, 10Hz, 20Hz). Qualitatively, our data show that the higher inhibitory effect in the membrane potential and in the firing rate of the DMH^{VGAT} neurons occurred between 2Hz and 10Hz of photo-stimulation. However, only at 10Hz of photostimulation the variations of the firing frequency and the membrane potential result significant (paired T-test p < 0.05*, n = 3), (**Figure 4.16 panels A** and **B**). The photostimulation of the SPZ fibers influences the active state of the DMH^{VGAT} cells.

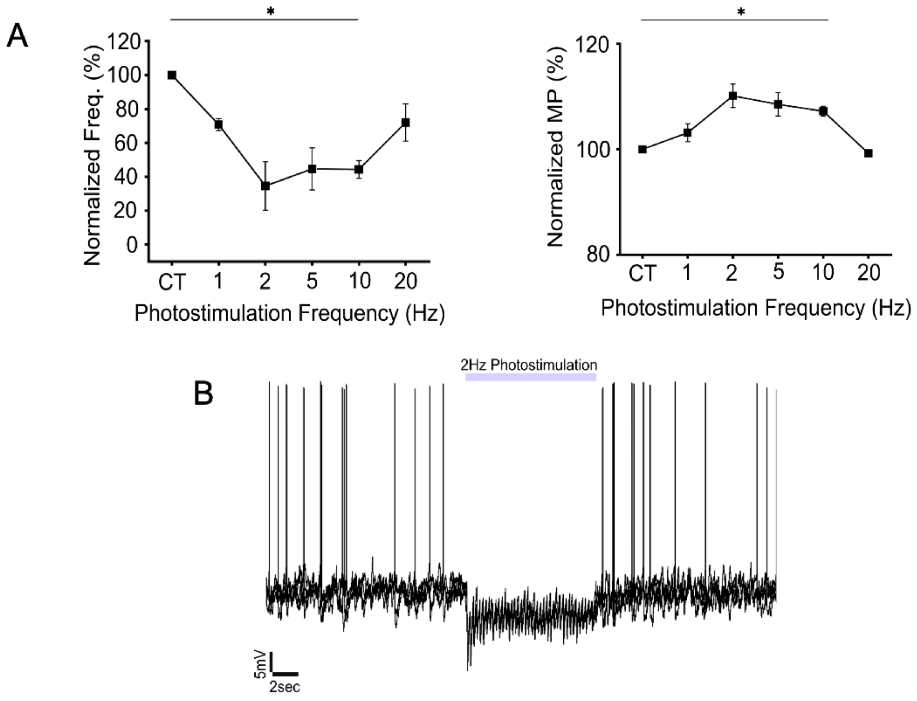

Figure 4.16: SPZ^{VGAT}→DMH^{VGAT} input modulation on the membrane potential and firing rate. A) Dot-line graph of the normalized membrane potential and firing rate (paired T-test p < 0.05* CT vs 10Hz photostimulation, n = 3) at pre-stimulus (CT) and at different frequencies of SPZ^{VGAT} terminals photostimulation (1Hz, 2Hz, 5Hz, 10Hz, 20Hz) (mean % variation ± SEM) **B)** Representative whole-cell recording in current clamp modality during photostimulation of the SPZ^{VGAT}→DMH^{VGAT} input.

DISCUSSION: **the SPZ represents a critical node of the central polisynaptic circuit that governs the corticosterone circadian rhythm.**

From the rabies tracing study of Ph.D. O. Ramirez Plascencia, emerges that the principal hypothalamic areas that monosynaptically project to the PVN^{CRH} neurons include the MPA, LH, ARC and DMH and notably the SPZ. The MPA exerts an inhibitory control over CRH neurons activity during acute stress events (Herman et al., 2016). The interaction between LH neurons and PVN^{CRH} neurons is well known, with Orexin-A and Orexin-B influencing CRH release at CNS level in a dose-response manner (Jászberényi et al., 2000). Moreover, CRH neurons project to the neurons of LH and bath application of CRH in LH brain slices stimulates the depolarization of a group of orexin-positive neurons (Winsky-Sommerer et al., 2004). Additionally, tracing studies verified that CRH neurons monosynaptically contact the LH neurons (Füzesi et al., 2016). This PVN-LH communication is primarily associated with the control of arousal induced by stress triggers. Our findings suggest that this interplay, focused on PVN^{CRH} output, could also be modulated by feedback transmission from LH neurons directly onto PVN^{CRH} neurons. Furthermore, PVN^{CRH} neurons play a pivotal role in orchestrating the systemic release of glucocorticoids in response to different stimuli to cope with stress. Our rabies tracing studies have revealed a dense monosynaptic input from the ARC nucleus, a hypothalamic region where agouti-related protein (AgRP) positive neurons are associated with the synthesis of CRH during fasting (Fernandes et al., 2022). Moreover, the ARC AgRP-positive neurons seem to regulate the CRH neurons synaptically, contacting their terminals at the median eminence level, where they stimulate CRH release through an excitatory action mediated by GABA, dependent on the Na^+-K^+-$2Cl^-$ cotransporter-1 (NKCC1) (Kakizawa et al., 2016; Yesmin et al., 2022).

All these connections form the basis of circuits that regulate the CRH neurons activation and, subsequently, the release of CRH, in response to stressors. Instead, in the context of circadian regulation of the HPA axis, the key structures contacting the CRH neurons are represented by the DMH and SPZ.

The circadian release of corticosterone is under the control of the SCN through an autonomic pathway that involves the autonomic division of the PVN and through a multisynaptic circuit that acts on top of the HPA axis. In the latter case, the connections of the SCN with downstream nuclei play a necessary and crucial role. The SCN serves as core for circadian rhythms, and its lesions completely abolish the circadian changes in corticosterone release. Interestingly, this circadian rhythm, differently to others, is not recovered with SCN transplantation, indicating that the SCN needs to synaptically contact other centers.

SCN^{AVP} neuronal ablation stimulates the ACTH release (Gomez et al., 1997) and the SCN^{VIP} chemogenetic and optogenetic manipulation inhibits the corticosterone level in a time-manner (Paul et al., 2020; Jones et al., 2021). The more known SCN populations act then as inhibitor regulators. However, which are the complete circuits involved is still unsolved.

A first candidate circuit could involve a direct modulation of the PVN. The PVN nucleus contains the CRH producing neurons that stimulate the production of the ACTH. But data regarding the SCN connections with the CRH neurons are still primarily anatomical and they are describing weaker innervation. Noteworthy our rabies studies delineate the absence of a direct projection from the SCN. Functionally, there are some evidence regarding the SCN modulation of the PVN activity performed in brain slices (Ono et al., 2020; Paul et al., 2020; Jones et al., 2021) but despite all of them show a correlation between the activities of the two nuclei, where the activation of the SCN neurons induces a reduction in the PVN activity, none of them have shown functional $SCN \rightarrow PVN^{CRH}$ monosynaptic connectivity, leaving this question still open to date.

The second candidate nucleus proposed is the DMH (Saper et al., 2005). The DMH is known to be a principal SCN output and plays different roles in circadian rhythmicity, including the regulation of locomotor activity, feeding behavior and wakefulness, and lesions of the DMH abolish the circadian rhythm of corticosterone (Chou et al., 2003; Todd et al., 2020). Moreover, administration of AVP in the DMH diminishes the peak rise in corticosterone release before the onset of the active phase, and most probably the AVP source is represented by the SCN^{AVP} neurons. Additionally, CRH administration in the DMH drives the negative feedback hormonal control in the corticosterone release. Taken together, all these information indicate the involvement of the DMH in the corticosterone circadian rhythms.

With this study, we are adding another circuital node in the circadian regulation of corticosterone release, the SPZ. Firstly, the conditional DTA ablation of the SPZ^{VGAT} neurons completely abolishes the circadian rhythms of corticosterone release in nocturnal mice. Secondly, we have found proof that justifies the SPZ as negative regulator in the release of the CRH both directly, through a monosynaptic connection to the PVN^{CRH} neurons, as shown by the recombinant rabies study, and indirectly diminishing the activation of the DMH GABAergic neurons. The second observation is explained by recent studies (*data not shown, Ramirez Plascencia and De Luca et al. in preparation*) that highlight how the DMH^{VGAT} projections to CRH neurons act mainly inhibiting their spontaneous inhibitory activity. Then the inhibition of the GABAergic DMH population through the SPZ, leave stable the spontaneous inhibitory tone on the CRH neurons. Moreover, it is likely that the monosynaptic connection found by our rabies study between the DMH and PVN^{CRH} neurons, is not represented by the GABAergic DMH population, but by other

source, most probably glutamatergic. This supports the idea that the DMH can act as a positive regulator, while the SPZ represents, together with the SCN, an inhibitory regulator in corticosterone release. In this way the SPZ becomes part of the polysynaptic circuit that starts from the SCN and reaches the PVN in controlling hormone daily variation, with the DMH serving as a key relay (Saper et al., 2005).

5. CONCLUSIONS

Circadian rhythms are present in neuronal and non-neuronal cells throughout the body and they are generated primarily at molecular level. The circadian system is then consistently present in influencing and determining human functions and behaviors. In humans, the genetically determined familial advanced sleep phase syndrome (FASPS) is characterized by an early sleep time and early awakening and it is caused by a mutation in casein kinase I binding domain of PER2 gene. Single nucleotide polymorphism onto the PER2 gene are driving pathologies such as the delayed sleep-wake phase disorder (DSWPD), sleep paralysis and rem sleep behavior disorder. And many other mutations at the level of the TTFL elements are associated with the insurgence of other conditions such as neurodegenerative diseases, alcoholic behaviors, depression, bipolarism, metabolic dysfunctions and cardiovascular diseases. Other than the genetic roots of circadian related pathologies, the circadian system can be altered at different levels by various factors like social pressure, work pressure (i.e. shift-work, jet-lag), high level of stress etc. All these cues impose changing in the circadian asset and its disruption can primarily aggravate pathological state of diabetes, cancer, obesity, neurodegenerative disease and so on (Xu et al., 2005; Pavithra et al., 2023). In all this pathological scenario, the SCN and its related nuclei play a central role. Dissecting the circuit of the circadian timing system represents a key step to understand how this system works and where it fails.

The circadian control of behavior involves the synergistic action of different components spanning from the molecular level to various neuronal structures and peripheric organs. Here we have focused our questions on one of the first neuronal nodes of this intricate network, the SPZ.
Firstly, our studies demonstrate that the vSPZ neurons receive monosynaptic input from the SCN^{NMS} and the SCN^{VIP} neurons, involving a $GABA_A$ mediated transmission. This communication aligns with the antiphase activity observed between the two nuclei in the LD cycle, as found both *in vivo* (Nakamura et al., 2008) and *ex vivo* (Paul et al., 2020). Thus, the SCN directly influences the active and inactive state of the SPZ **(Figure 4.17).**
Secondly, as reported in **Figure 4.18**, our findings from calcium imaging recordings reveal the presence of different receptors for the SCN peptides signaling mostly leading to the activation of SPZ neurons, with a suggested anatomical organization along the rostro-caudal axis. These results then indicate the existence of a potential anatomical organization also in the connectivity between SCN and SPZ that should be explored. Moreover, since these peptides primarily induce direct neuronal activation, their actions have to be interpreted as a modulatory rather than representing

the principal effect of the SCN on the SPZ neurons. The GABAergic transmission is likely the major effect of the SCN onto SPZ neurons, while peptides serve as specific messages delivered in a timed manner. Notably, not all of them follow the same producing time. AVP and NMS are mainly produced during the light phase, while VIP is highly produced during the dark phase. This suggests that they could be released under specific input that evolve at different times. Furthermore, the opposite effect of VIP and NMS in the vSPZ, suggests the presence of two distinct groups of cells associated with opposite intracellular pathway. This question should be investigated with patch clamp recordings, exploiting the functional mapping emerged from the present study. Despite the novelty of our work, there are still several experiments that need to be performed. Our recordings should be refined with a larger number of animals and the use of specific antagonists is fundamental step to confirm the receptors mainly implicated in genesis of responses to different peptides. Additionally, the tracing study of the SPZ input would open up new questions such us identifying the source of these peptides. Indeed, it is important to note that not only the SCN could release VIP, NMS and AVP. Furthermore, delineating the main sources of galanin and cholinergic inputs, could be extremely interesting to understand the role of the SPZ in other circadian and related functions. The inhibitory action of galanin on the SPZ neurons could correlate with a VLPO input. Indeed the SPZ activity is in phase with the active phase and high locomotor activity of the animal, while the galaninergic neurons of the VLPO are primarily associated with an inhibition of the components of the wake system, such the orexin neurons in the LH. The role of the cholinergic system, however, is more complicated since the action of carbachol has been shown to inhibit and activate two different SPZ neuronal populations. It is likely that the source of a cholinergic projection are not the basal regions of the forebrain (Agostinelli et al., 2019). Perhaps, a cholinergic input could come from the brainstem nuclei typically associated with wakefulness. It may therefore be extremely interesting to understand to which cells and nuclei the carbachol-inhibited SPZ cells and carbachol-activated SPZ cells project, in order to better delineate the role of acetylcholine in modulating the SPZ outcome.

The presented study demonstrates that the SCN not only contacts and modulates the SPZ neurons, but also highlights the importance of the SPZ in the circadian release of corticosterone in nocturnal animals. The DTA ablation of the SPZ resulted in the loss of the circadian peak of corticosterone release before the onset of the active phase. Buildings on previous evidence (Chou et al., 2003; Saper et al., 2005), on our preliminary data (*data not shown, Ramirez Plascencia and De Luca et al. in preparation*) on the relationship between the DMH excitatory/inhibitory populations and the PVN^{CRH} neurons, and on the rabies results of the present work, we hypothesized that the SPZ might indeed function by directly inhibiting the PVN^{CRH} neurons and

indirectly relying on DMH^{VGAT} neurons. We have proven here that SPZ^{VGAT} neurons monosynaptically contact the anterior and medial DMH^{VGAT} neurons and they modulate their firing and membrane potential at very low levels of photostimulation. Consequently, the SPZ may serve as an inhibitory regulator in corticosterone release together with SCN^{AVP} and SCN^{VIP} neurons.

In this scenario emerges a hypothetical model for the circadian control of corticosterone which take into account several observations regarding the implicated nuclei and their relations. During the light phase the SCN^{AVP} and SCN^{VIP} neurons are mainly responsible for the slow rising phase of the corticosterone acting as inhibitor factor (Kalsbeek et al., 1996; Kalsbeek et al., 2006; Paul et al., 2020; Jones et al., 2021). As these neurons tend to lose their activation throughout the light phase, mainly due to the regulation of the core molecular clock mechanism and the loss of the zeitgeber signal, they gradually reduce their inhibitory effect on the PVN^{CRH} over time. Consequently, the rising phase of the corticosterone release could be the result of the SCN deactivation accompanied by a stronger yet unidentified positive regulator that can act on both DMH glutamatergic population (that we know to highly project directly to the PVN^{CRH} neurons, *data not shown, Ramirez Plascencia and De Luca et al. in preparation*) or PVN^{CRH} neurons directly. In the meantime, while the SCN is reaching its nadir point of activity, the SPZ starts to fire at a higher frequency, likely contributing to the descending phase of corticosterone after the peak. Presumably in doing so the SPZ is acting both directly on the PVN^{CRH} neurons and indirectly deactivating the DMH^{VGAT} neurons which could not anymore diminish the inhibitory input onto the CRH neurons. This, together with other negative regulator factors, as the hormonal negative feedback of the corticosterone itself onto the central structures of the HPA axis, suggests that both SCN and SPZ are acting as negative modulators, while the DMH serves as a positive controller (**Figure 4.19**). However, the identification of the necessary positive driver for the corticosterone peak remains unknown.

Much work remains to be done to understand all the components of these polysynaptic circuits and where they intersect to drive behaviors. *In vivo* photostimulation of SPZ^{VGAT} terminals in the anterior-medial DMH to address how much this input is essential for hormonal regulation, and other circuital studies between the SPZ and the DMH glutamatergic population, as well as between the SCN and the DMH populations, will be future experiments.

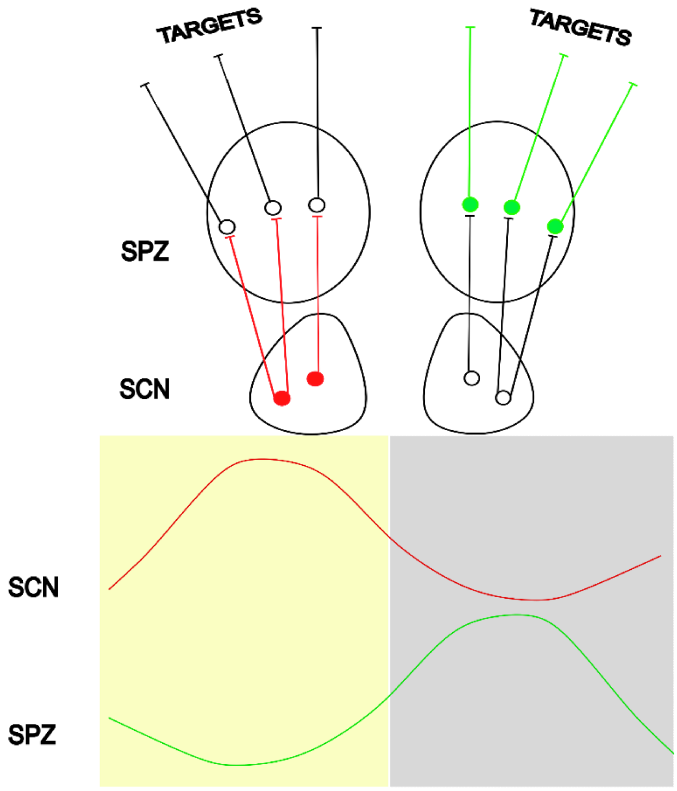

Figure 4.17: schematic representation of the SCN-SPZ communication. The SCN neurons monosynaptically contact the SPZ neurons. When the SCN neurons are active, during the light phase (*red curve, acrophase point*), they inhibit the SPZ neurons (*green curve, nadir point*). During the night, the SCN is at its nadir point (*red curve*), while the SPZ reaches its acrophase (*green curve*) regulating the downstream targets determining the active state of the nocturnal animal. *Yellow rectangle*, light phase; *gray rectangle*, dark phase.

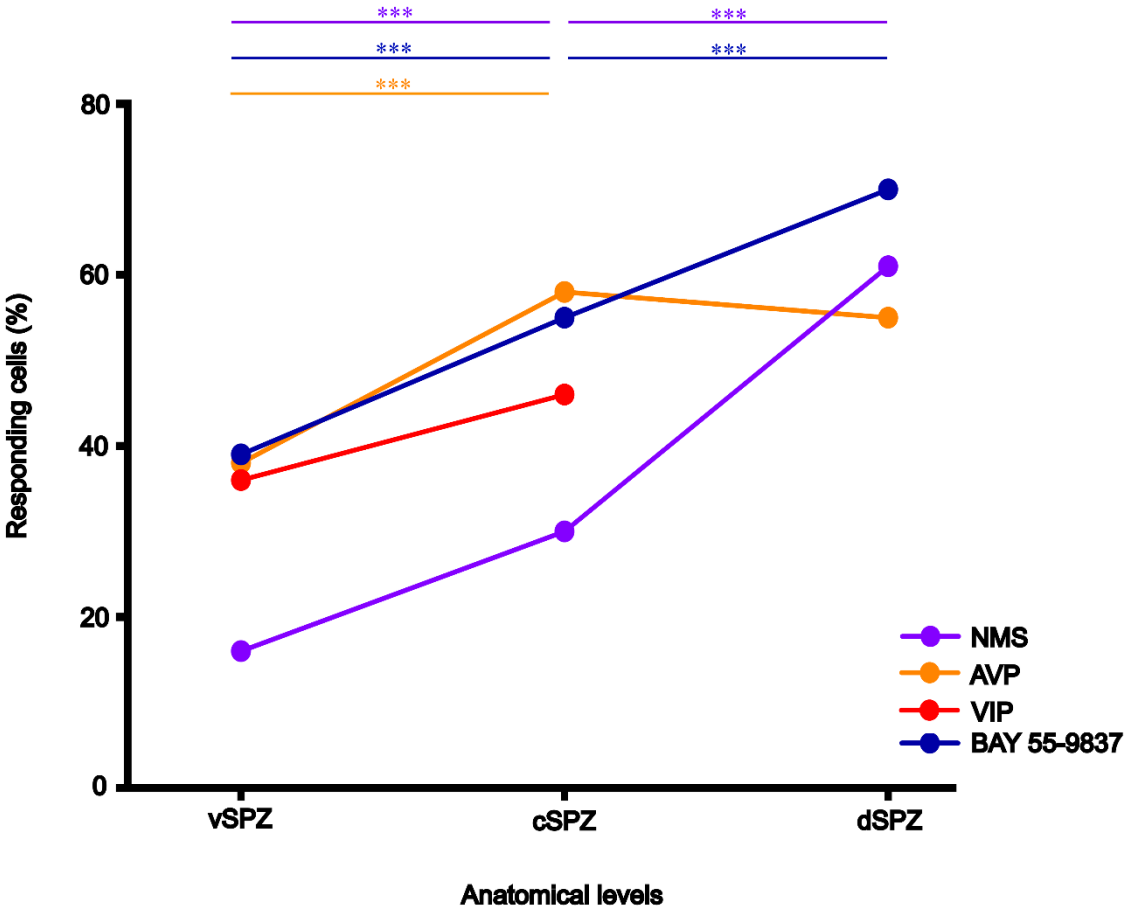

Figure 4.18: SPZ neuropeptidergic modulation. The SCN produces and releases many neuropeptides, such as NMS, AVP and VIP. Here we have shown that the SPZ neurons are able to respond to all these peptides with an anatomical organization where the majority of the responding cells reside in the central and in the dorsal SPZ.

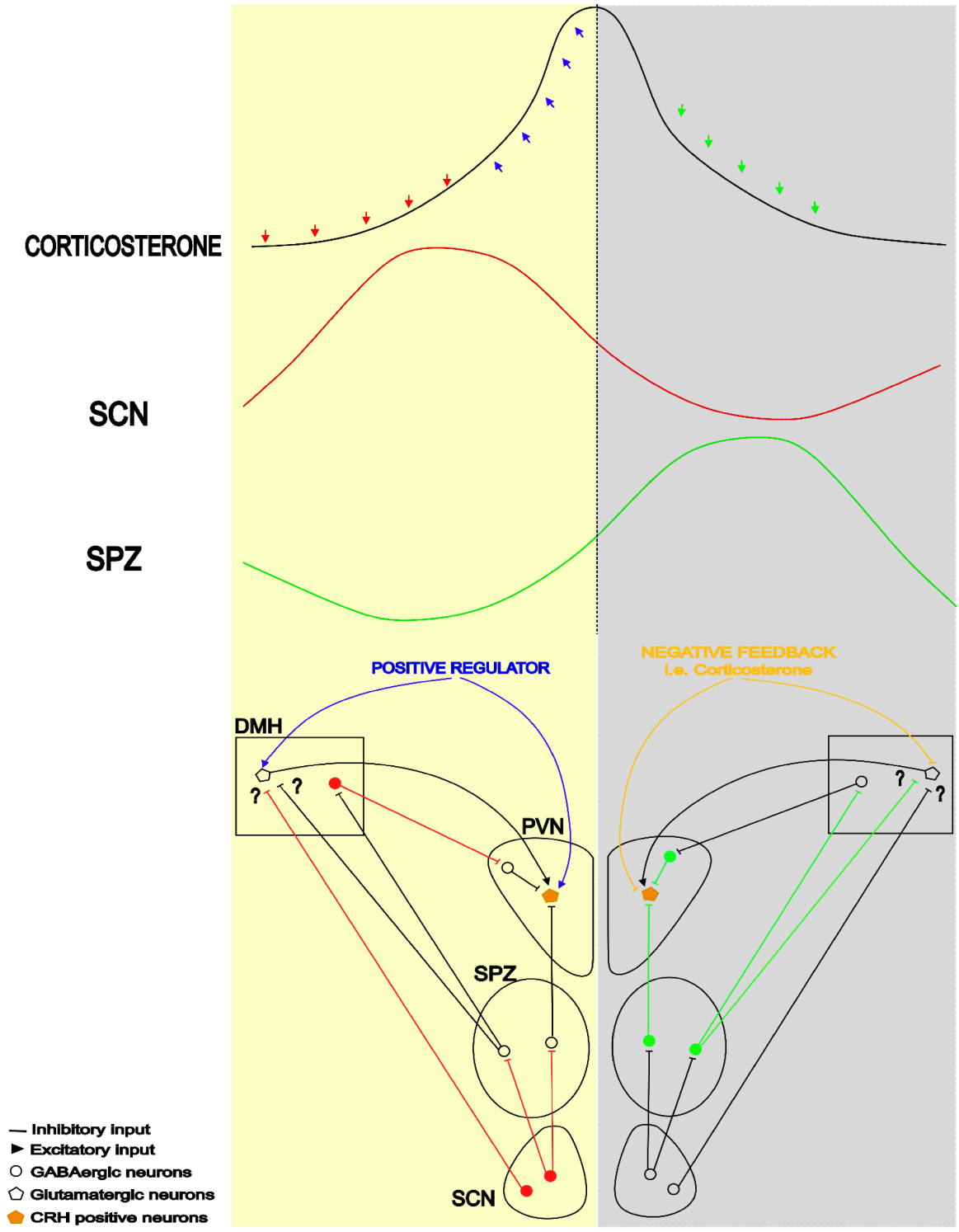

Figure 4.18: schematic representation of a hypothetic circuit for the corticosterone circadian release. The SCN neurons during the day inhibit the corticosterone release acting indirectly (or directly) onto the CRH neurons. As the SCN neurons become less active, the CRH neurons become more sensitive to positive regulators, leading to the rising phase of the corticosterone curve. During the night, the active SPZ neurons, together with other negative regulators (i.e. the corticosterone negative feedback), cause the descending phase of the corticosterone curve both indirectly, through the DMH, and presumably directly inhibiting the CRH neurons of the PVN. *Yellow rectangle*, light phase; *gray rectangle*, dark phase.

6. BIBLIOGRAPHY

Abrahamson EE, Moore RY. Suprachiasmatic nucleus in the mouse: retinal innervation, intrinsic organization and efferent projections. Brain Res. 2001 Oct 19;916(1-2):172-91. doi: 10.1016/s0006-8993(01)02890-6. PMID: 11597605.

Ahmed BY, Chakravarthy S, Eggers R, Hermens WT, Zhang JY, Niclou SP, Levelt C, Sablitzky F, Anderson PN, Lieberman AR, Verhaagen J. Efficient delivery of Crerecombinase to neurons in vivo and stable transduction of neurons using adeno-associated and lentiviral vectors. BMC Neurosci. 2004 Jan 30;5:4. doi: 10.1186/1471-2202-5-4. PMID: 15005815; PMCID: PMC343275.

Akerboom J, Rivera JD, Guilbe MM, Malavé EC, Hernandez HH, Tian L, Hires SA, Marvin JS, Looger LL, Schreiter ER. Crystal structures of the GCaMP calcium sensor reveal the mechanism of fluorescence signal change and aid rational design. J Biol Chem. 2009 Mar 6;284(10):6455-64. doi: 10.1074/jbc.M807657200. Epub 2008 Dec 18. PMID: 19098007; PMCID: PMC2649101

Agostinelli LJ, Geerling JC, Scammell TE. Basal forebrain subcortical projections. Brain Struct Funct. 2019 Apr;224(3):1097-1117. doi: 10.1007/s00429-018-01820-6. Epub 2019 Jan 5. PMID: 30612231; PMCID: PMC6500474.

Alamilla J, Perez-Burgos A, Quinto D, Aguilar-Roblero R. Circadian modulation of the Cl(-) equilibrium potential in the rat suprachiasmatic nuclei. Biomed Res Int. 2014;2014:424982. doi: 10.1155/2014/424982. Epub 2014 May 18. PMID: 24949446; PMCID: PMC4052495.

Albers HE, Stopa EG, Zoeller RT, Kauer JS, King JC, Fink JS, Mobtaker H, Wolfe H. Daynight variation in prepro vasoactive intestinal peptide/peptide histidine isoleucine mRNA within the rat suprachiasmatic nucleus. Brain Res Mol Brain Res. 1990 Jan;7(1):85-9. doi: 10.1016/0169-328x(90)90077-q. PMID: 2153898.

Albus H, Bonnefont X, Chaves I, Yasui A, Doczy J, van der Horst GT, Meijer JH. Cryptochrome-deficient mice lack circadian electrical activity in the suprachiasmatic nuclei. Curr Biol. 2002 Jul 9;12(13):1130-3. doi: 10.1016/s0960-9822(02)00923-5. PMID: 12121621.

Albus H, Vansteensel MJ, Michel S, Block GD, Meijer JH. A GABAergic mechanism is necessary for coupling dissociable ventral and dorsal regional oscillators within the circadian clock. Curr Biol. 2005 May 24;15(10):886-93. doi: 10.1016/j.cub.2005.03.051. PMID: 15916945

Allen Institute for Brain Science (2004). Allen Mouse Brain Atlas [dataset]. Available from mouse.brain-map.org.Allen Institute for Brain Science (2011). Allen Reference Atlas – Mouse Brain [brain atlas]. Available from atlas.brain-map.org.

Allen-Rowlands CF, Allen JP, Greer MA, Wilson M. Circadian rhythmicity of ACTH and corticosterone in the rat. J Endocrinol Invest. 1980 Oct-Dec;3(4):371-7. doi: 10.1007/BF03349373. PMID: 6259249.

An S, Tsai C, Ronecker J, Bayly A, Herzog ED. Spatiotemporal distribution of vasoactive intestinal polypeptide receptor 2 in mouse suprachiasmatic nucleus. J Comp Neurol. 2012 Aug 15;520(12):2730-41. doi: 10.1002/cne.23078. PMID: 22684939; PMCID: PMC3961765.

Anaclet C, De Luca R, Venner A, Malyshevskaya O, Lazarus M, Arrigoni E, Fuller PM. Genetic Activation, Inactivation, and Deletion Reveal a Limited And Nuanced Role for Somatostatin-Containing Basal Forebrain Neurons in Behavioral State Control. J Neurosci. 2018 May 30;38(22):5168-5181. doi: 10.1523/JNEUROSCI.2955-17.2018. Epub 2018 May 7. PMID: 29735555; PMCID: PMC5977448.

Ancellin N, Morel A. Homologous and heterologous acute desensitization of vasopressin V1a receptor in Xenopus oocytes. Cell Signal. 1998 Mar;10(3):217-23. doi: 10.1016/s0898-6568(97)00124-1. PMID: 9607146.

Ancellin N, Preisser L, Le Maout S, Barbado M, Créminon C, Corman B, Morel A. Homologous and heterologous phosphorylation of the vasopressin V1a receptor. Cell Signal. 1999 Oct;11(10):743-51. doi: 10.1016/s0898-6568(99)00035-2. PMID: 10574329.

Antoch MP, Song EJ, Chang AM, Vitaterna MH, Zhao Y, Wilsbacher LD, Sangoram AM, King DP, Pinto LH, Takahashi JS. Functional identification of the mouse circadian Clock gene by transgenic BAC rescue. Cell. 1997 May 16;89(4):655-67. doi: 10.1016/s0092- 8674(00)80246-9. PMID: 9160756; PMCID: PMC3764491.

Arrigoni E, Saper CB. What optogenetic stimulation is telling us (and failing to tell us) about fast neurotransmitters and neuromodulators in brain circuits for wake-sleep regulation. Curr Opin Neurobiol. 2014 Dec;29:165-71. doi: 10.1016/j.conb.2014.07.016. Epub 2014 Jul 26. PMID: 25064179; PMCID: PMC4268002.

Asrican B, Song J. Extracting meaningful circuit-based calcium dynamics in astrocytes and neurons from adult mouse brain slices using single-photon GCaMP imaging. STAR Protoc. 2021 Feb 1;2(1):100306. doi: 10.1016/j.xpro.2021.100306. PMID: 33554141; PMCID: PMC7856475.

Aton SJ, Herzog ED. Come together, right...now: synchronization of rhythms in a mammalian circadian clock. Neuron. 2005 Nov 23;48(4):531-4. doi: 10.1016/j.neuron.2005.11.001. PMID: 16301169; PMCID: PMC1780025.

Aton SJ, Colwell CS, Harmar AJ, Waschek J, Herzog ED. Vasoactive intestinal polypeptide mediates circadian rhythmicity and synchrony in mammalian clock neurons. Nat Neurosci. 2005 Apr;8(4):476-83. doi: 10.1038/nn1419. Epub 2005 Mar 6. PMID: 15750589; PMCID: PMC1628303.

Balsalobre A, Damiola F, Schibler U. A serum shock induces circadian gene expression in mammalian tissue culture cells. Cell. 1998 Jun 12;93(6):929-37. doi: 10.1016/s0092- 8674(00)81199-x. PMID: 9635423.

Ban Y, Shigeyoshi Y, Okamura H. Development of vasoactive intestinal peptide mRNA rhythm in the rat suprachiasmatic nucleus. J Neurosci. 1997 May 15;17(10):3920-31. doi: 10.1523/JNEUROSCI.17-10-03920.1997. PMID: 9133410; PMCID: PMC6573707.

Barca-Mayo O, Pons-Espinal M, Follert P, Armirotti A, Berdondini L, De Pietri Tonelli D. Astrocyte deletion of Bmal1 alters daily locomotor activity and cognitive functions via GABA signalling. Nat Commun. 2017 Feb 10;8:14336. doi: 10.1038/ncomms14336. PMID: 28186121; PMCID: PMC5309809.

Bartness TJ, Song CK, Demas GE. SCN efferents to peripheral tissues: implications for biological rhythms. J Biol Rhythms. 2001 Jun;16(3):196-204. doi: 10.1177/074873040101600302. PMID: 11407779.

Bedont JL, Blackshaw S. Constructing the suprachiasmatic nucleus: a watchmaker's perspective on the central clockworks. Front Syst Neurosci. 2015 May 8;9:74. doi: 10.3389/fnsys.2015.00074. PMID: 26005407; PMCID: PMC4424844.

Belle MD, Diekman CO, Forger DB, Piggins HD. Daily electrical silencing in the mammalian circadian clock. Science. 2009 Oct 9;326(5950):281-4. doi: 10.1126/science.1169657. PMID: 19815775.

Bellinger LL, Bernardis LL, Mendel VE. Effect of ventromedial and dorsomedial hypothalamic lesions on circadian corticosterone rhythms. Neuroendocrinology. 1976;22(3):216-25. doi: 10.1159/000122628. PMID: 1028952.

Berson DM, Dunn FA, Takao M. Phototransduction by retinal ganglion cells that set the circadian clock. Science. 2002 Feb 8;295(5557):1070-3. doi: 10.1126/science.1067262. PMID: 11834835.

Biel M, Michalakis S. Cyclic nucleotide-gated channels. Handb Exp Pharmacol. 2009;(191):111-36. doi: 10.1007/978-3-540-68964-5_7. PMID: 19089328.

Bittman EL, Doherty L, Huang L, Paroskie A. Period gene expression in mouse endocrine tissues. Am J Physiol Regul Integr Comp Physiol. 2003 Sep;285(3):R561-9. doi: 10.1152/ajpregu.00783.2002. Epub 2003 May 29. PMID: 12775559.

Boyden ES, Zhang F, Bamberg E, Nagel G, Deisseroth K. Millisecond-timescale, genetically targeted optical control of neural activity. Nat Neurosci. 2005 Sep;8(9):1263-8. doi: 10.1038/nn1525. Epub 2005 Aug 14. PMID: 16116447.

Bozek K, Relógio A, Kielbasa SM, Heine M, Dame C, Kramer A, Herzel H. Regulation of clock-controlled genes in mammals. PLoS One. 2009;4(3):e4882. doi: 10.1371/journal.pone.0004882. Epub 2009 Mar 16. PMID: 19287494; PMCID: PMC2654074.

Brancaccio M, Patton AP, Chesham JE, Maywood ES, Hastings MH. Astrocytes Control Circadian Timekeeping in the Suprachiasmatic Nucleus via Glutamatergic Signaling. Neuron. 2017 Mar 22;93(6):1420-1435.e5. doi: 10.1016/j.neuron.2017.02.030. Epub 2017 Mar 9. PMID: 28285822; PMCID: PMC5376383.

Brancaccio M, Edwards MD, Patton AP, Smyllie NJ, Chesham JE, Maywood ES, Hastings MH. Cell-autonomous clock of astrocytes drives circadian behavior in mammals. Science. 2019 Jan 11;363(6423):187-192. doi: 10.1126/science.aat4104. PMID: 30630934; PMCID: PMC6440650.

Brighton PJ, Szekeres PG, Wise A, Willars GB. Signaling and ligand binding by recombinant neuromedin U receptors: evidence for dual coupling to Galphaq/11 and Galphai and an irreversible ligand-receptor interaction. Mol Pharmacol. 2004 Dec;66(6):1544-56. doi: 10.1124/mol.104.002337. Epub 2004 Aug 26.

Brown TM, Piggins HD. Spatiotemporal heterogeneity in the electrical activity of suprachiasmatic nuclei neurons and their response to photoperiod. J Biol Rhythms. 2009 Feb;24(1):44-54. doi: 10.1177/0748730408327918. PMID: 19227579.

Brown AL, Johnson BE, Goodman MB. Making patch-pipettes and sharp electrodes with a programmable puller. J Vis Exp. 2008 Oct 8;(20):939. doi: 10.3791/939. PMID: 19078940; PMCID: PMC3233862.

Buijs RM, Wortel J, Van Heerikhuize JJ, Feenstra MG, Ter Horst GJ, Romijn HJ, Kalsbeek A. Anatomical and functional demonstration of a multisynaptic suprachiasmatic nucleus adrenal (cortex) pathway. Eur J Neurosci. 1999 May;11(5):1535-44. doi: 10.1046/j.1460-9568.1999.00575.x. PMID: 10215906.

Buijs RM, la Fleur SE, Wortel J, Van Heyningen C, Zuiddam L, Mettenleiter TC, Kalsbeek A, Nagai K, Niijima A. The suprachiasmatic nucleus balances sympathetic and parasympathetic output to peripheral organs through separate preautonomic neurons. J Comp Neurol. 2003 Sep 8;464(1):36-48. doi: 10.1002/cne.10765. PMID: 12866127.

Buijs FN, Guzmán-Ruiz M, León-Mercado L, Basualdo MC, Escobar C, Kalsbeek A, Buijs RM. Suprachiasmatic Nucleus Interaction with the Arcuate Nucleus; Essential for Organizing Physiological Rhythms. eNeuro. 2017 Mar 24;4(2):ENEURO.0028-17.2017. doi: 10.1523/ENEURO.0028-17.2017. PMID: 28374011; PMCID: PMC5364589.

Burgoon PW, Boulant JA. Temperature-sensitive properties of rat suprachiasmatic nucleus neurons. Am J Physiol Regul Integr Comp Physiol. 2001 Sep;281(3):R706-15. doi: 10.1152/ajpregu.2001.281.3.R706. PMID: 11506983.

Caldwell HK, Lee HJ, Macbeth AH, Young WS 3rd. Vasopressin: behavioral roles of an "original" neuropeptide. Prog Neurobiol. 2008 Jan;84(1):1-24. doi: 10.1016/j.pneurobio.2007.10.007. Epub 2007 Nov 4. PMID: 18053631; PMCID: PMC2292122.

Campos LM, Cruz-Rizzolo RJ, Watanabe IS, Pinato L, Nogueira MI. Efferent projections of the suprachiasmatic nucleus based on the distribution of vasoactive intestinal peptide (VIP) and arginine vasopressin (AVP) immunoreactive fibers in the hypothalamus of Sapajus apella. J Chem Neuroanat. 2014 May;57-58:42-53. doi: 10.1016/j.jchemneu.2014.03.004. Epub 2014 Apr 13. PMID: 24727411.

Canteras NS, Ribeiro-Barbosa ER, Goto M, Cipolla-Neto J, Swanson LW. The retinohypothalamic tract: comparison of axonal projection patterns from four major targets. 73 Brain Res Rev. 2011 Jan 1;65(2):150-83. doi: 10.1016/j.brainresrev.2010.09.006. Epub 2010 Sep 21. PMID: 20863850.

Carmeliet E. From Bernstein's rheotome to Neher-Sakmann's patch electrode. The action potential. Physiol Rep. 2019 Jan;7(1):e13861. doi: 10.14814/phy2.13861. PMID: 30604910; PMCID: PMC6316177.

Carmona-Alcocer V, Abel JH, Sun TC, Petzold LR, Doyle FJ 3rd, Simms CL, Herzog ED. Ontogeny of Circadian Rhythms and Synchrony in the Suprachiasmatic Nucleus. J Neurosci. 2018 Feb 7;38(6):1326-1334. doi: 10.1523/JNEUROSCI.2006-17.2017. Epub 2017 Oct 20. PMID: 29054877; PMCID: PMC5815340.

Carmona-Alcocer V, Brown LS, Anchan A, Rohr KE, Evans JA. Developmental patterning of peptide transcription in the central circadian clock in both sexes. Front Neurosci. 2023 May 19;17:1177458. doi: 10.3389/fnins.2023.1177458. PMID: 37274219; PMCID: PMC10235759.

Carrión M, Ramos-Leví AM, Seoane IV, Martínez-Hernández R, Serrano-Somavilla A, Castro D, Juarranz Y, González-Álvaro I, Gomariz RP, Marazuela M. Vasoactive intestinal peptide axis is dysfunctional in patients with Graves' disease. Sci Rep. 2020 Aug 3;10(1):13018. doi: 10.1038/s41598-020-70138-3. PMID: 32747757; PMCID: PMC7400547.

Carter M, Shieh J. (2015) Guide to Research Techniques in Neuroscience. Elsevier, second edition.

Cattaneo L. Neuroanatomia del sistema nervoso e periferico dell'uomo. Monduzzi 2ª ed. 1989.

Challet E, le Maho Y, Robin JP, Malan A, Cherel Y. Involvement of corticosterone in the fasting-induced rise in protein utilization and locomotor activity. Pharmacol Biochem Behav. 1995 Mar;50(3):405-12. doi: 10.1016/0091-3057(94)00287-s. PMID: 7617679.

Champigneulle A, Siga E, Vassent G, Imbert-Teboul M. V2-like vasopressin receptor mobilizes intracellular Ca2+ in rat medullary collecting tubules. Am J Physiol. 1993 Jul;265(1 Pt 2):F35-45. doi: 10.1152/ajprenal.1993.265.1.F35. PMID: 8342613.

Chen RX, Liu F, Li Y, Liu GA. Neuromedin S increases L-type Ca(2+) channel currents through G(i)α-protein and phospholipase C-dependent novel protein kinase C delta pathway in adult rat ventricular myocytes. Cell Physiol Biochem. 2012;30(3):618-30. doi: 10.1159/000341443. Epub 2012 Jul 27. PMID: 22832358.

Chen TW, Wardill TJ, Sun Y, Pulver SR, Renninger SL, Baohan A, Schreiter ER, Kerr RA, Orger MB, Jayaraman V, Looger LL, Svoboda K, Kim DS. Ultrasensitive fluorescent proteins for imaging neuronal activity. Nature. 2013 Jul 18;499(7458):295-300. doi: 10.1038/nature12354. PMID: 23868258; PMCID: PMC3777791.

Cho H, Zhao X, Hatori M, Yu RT, Barish GD, Lam MT, Chong LW, DiTacchio L, Atkins AR, Glass CK, Liddle C, Auwerx J, Downes M, Panda S, Evans RM. Regulation of circadian behaviour and metabolism by REV-ERB-α and REV-ERB-β. Nature. 2012 Mar 29;485(7396):123-7. doi: 10.1038/nature11048. PMID: 22460952; PMCID: PMC3367514.

Cho JH, Deisseroth K, Bolshakov VY. Synaptic encoding of fear extinction in mPFC-amygdala circuits. Neuron. 2013 Dec 18;80(6):1491-507. doi: 10.1016/j.neuron.2013.09.025. Epub 2013 Nov 27. PMID: 24290204; PMCID: PMC3872173.

Choi HJ, Lee CJ, Schroeder A, Kim YS, Jung SH, Kim JS, Kim DY, Son EJ, Han HC, Hong SK, Colwell CS, Kim YI. Excitatory actions of GABA in the suprachiasmatic nucleus. J Neurosci. 2008 May 21;28(21):5450-9. doi: 10.1523/JNEUROSCI.5750-07.2008. PMID: 18495878; PMCID: PMC2570697.

Chou TC, Scammell TE, Gooley JJ, Gaus SE, Saper CB, Lu J. Critical role of dorsomedial hypothalamic nucleus in a wide range of behavioral circadian rhythms. J Neurosci. 2003 Nov 19;23(33):10691-702. doi: 10.1523/JNEUROSCI.23-33-10691.2003. PMID: 14627654; PMCID: PMC6740926.

Chou CL, Yip KP, Michea L, Kador K, Ferraris JD, Wade JB, Knepper MA. Regulation of aquaporin-2 trafficking by vasopressin in the renal collecting duct. Roles of ryanodine-sensitive Ca2+ stores and calmodulin. J Biol Chem. 2000 Nov 24;275(47):36839-46. doi: 10.1074/jbc.M005552200. PMID: 10973964.

Chowdhury D, Wang C, Lu AP, Zhu HL. Understanding Quantitative Circadian Regulations Are Crucial Towards Advancing Chronotherapy. Cells. 2019 Aug 13;8(8):883. doi: 10.3390/cells8080883. PMID: 31412622; PMCID: PMC6721722.

Colwell CS. Linking neural activity and molecular oscillations in the SCN. Nat Rev Neurosci. 2011 Sep 2;12(10):553-69. doi: 10.1038/nrn3086. PMID: 21886186; PMCID: PMC4356239.

Crick FH. Thinking about the brain. Sci Am. 1979 Sep;241(3):219-32. doi: 10.1038/scientificamerican0979-219. PMID: 115087.

Crumbley C, Wang Y, Kojetin DJ, Burris TP. Characterization of the core mammalian clock component, NPAS2, as a REV-ERBalpha/RORalpha target gene. J Biol Chem. 2010 Nov 12;285(46):35386-92. doi: 10.1074/jbc.M110.129288. Epub 2010 Sep 3. PMID: 20817722; PMCID: PMC2975162.

Cui LN, Coderre E, Renaud LP. Glutamate and GABA mediate suprachiasmatic nucleus inputs to spinal-projecting paraventricular neurons. Am J Physiol Regul Integr Comp Physiol. 2001 Oct;281(4):R1283-9. doi: 10.1152/ajpregu.2001.281.4.R1283. PMID: 11557637.

Cunha-Reis D, Caulino-Rocha A. VIP Modulation of Hippocampal Synaptic Plasticity: A Role for VIP Receptors as Therapeutic Targets in Cognitive Decline and Mesial Temporal Lobe Epilepsy. Front Cell Neurosci. 2020 Jun 12;14:153. doi: 10.3389/fncel.2020.00153. Erratum in: Front Cell Neurosci. 2021 May 14;15:691978. PMID: 32595454; PMCID: PMC7303298.

Czeisler CA, Klerman EB. Circadian and sleep-dependent regulation of hormone release in humans. Recent Progress in Hormone Research. 1999 ;54:97-130; discussion 130-2.

De Jeu M, Pennartz C. Circadian modulation of GABA function in the rat suprachiasmatic nucleus: excitatory effects during the night phase. J Neurophysiol. 2002 Feb;87(2):834-44. doi: 10.1152/jn.00241.2001. PMID: 11826050.

Ding J, Luo AF, Hu L, Wang D, Shao F. Structural basis of the ultrasensitive calcium indicator GCaMP6. Sci China Life Sci. 2014 Mar;57(3):269-274. doi: 10.1007/s11427-013-4599-5. Epub 2014 Jan 4. PMID: 24390420.

Do MT, Yau KW. Intrinsically photosensitive retinal ganglion cells. Physiol Rev. 2010 Oct;90(4):1547-81. doi: 10.1152/physrev.00013.2010. PMID: 20959623; PMCID: PMC4374737.

Dobzhansky T. Nothing in Biology Makes Sense excepts in the Light of Evolution. Nat. Asso. Bio. Teach. . (1973) http://www.jstor.org/stable/4444260.

Dvornyk V, Vinogradova O, Nevo E. Origin and evolution of circadian clock genes in prokaryotes. Proc Natl Acad Sci U S A. 2003 Mar 4;100(5):2495-500. doi: 10.1073/pnas.0130099100. Epub 2003 Feb 25. PMID: 12604787; PMCID: PMC151369.

Folny V, Raufaste D, Lukovic L, Pouzet B, Rochard P, Pascal M, Serradeil-Le Gal C. Pancreatic vasopressin V1b receptors: characterization in In-R1-G9 cells and localization in human pancreas. Am J Physiol Endocrinol Metab. 2003 Sep;285(3):E566-76. doi: 10.1152/ajpendo.00148.2003. Epub 2003 May 7. PMID: 12736162.

Ecelbarger CA, Chou CL, Lolait SJ, Knepper MA, DiGiovanni SR. Evidence for dual signaling pathways for V2 vasopressin receptor in rat inner medullary collecting duct. Am J Physiol. 1996 Apr;270(4 Pt 2):F623-33. doi: 10.1152/ajprenal.1996.270.4.F623. PMID: 8967340.

Eide EJ, Vielhaber EL, Hinz WA, Virshup DM. The circadian regulatory proteins BMAL1 and cryptochromes are substrates of casein kinase Iepsilon. J Biol Chem. 2002 May 10;277(19):17248-54. doi: 10.1074/jbc.M111466200. Epub 2002 Mar 1. PMID: 11875063; PMCID: PMC1513548.

Eiden LE, Hernández VS, Jiang SZ, Zhang L. Neuropeptides and small-molecule amine transmitters: cooperative signaling in the nervous system. Cell Mol Life Sci. 2022 Aug 23;79(9):492. doi: 10.1007/s00018-022-04451-7. PMID: 35997826.

Engeland WC, Arnhold MM. Neural circuitry in the regulation of adrenal corticosterone rhythmicity. Endocrine. 2005 Dec;28(3):325-32. doi: 10.1385/ENDO:28:3:325. PMID: 16388123.

Enoki R, Kuroda S, Ono D, Hasan MT, Ueda T, Honma S, Honma K. Topological specificity and hierarchical network of the circadian calcium rhythm in the suprachiasmatic nucleus. Proc Natl Acad Sci U S A. 2012 Dec 26;109(52):21498-503. doi: 10.1073/pnas.1214415110. Epub 2012 Dec 4. PMID: 23213253; PMCID: PMC3535646.

Fain G, Sampath AP. Rod and cone interactions in the retina. F1000Res. 2018 May 23;7:F1000 Faculty Rev-657. doi: 10.12688/f1000research.14412.1. PMID: 29899971; PMCID: PMC5968360.

Felten D, O'Banion KM, Maida Summo M. Atlante di Neuroscienze di Netter. Edra 3ª ed. 2017.

Fernandes ACA, de Oliveira FP, Fernandez G, da Guia Vieira L, Rosa CG, do Nascimento T, de Castro França S, Donato J Jr, Vella KR, Antunes-Rodrigues J, Mecawi AS, Perello M, Elias LLK, Rorato R. Arcuate AgRP, but not POMC neurons, modulate paraventricular CRF synthesis and release in response to fasting. Cell Biosci. 2022 Jul 28;12(1):118. doi: 10.1186/s13578-022-00853-z. Erratum in: Cell Biosci. 2022 Sep 3;12(1):146. PMID: 35902915; PMCID: PMC9331576.

Ferrari LL, Park D, Zhu L, Palmer MR, Broadhurst RY, Arrigoni E. Regulation of Lateral Hypothalamic Orexin Activity by Local GABAergic Neurons. J Neurosci. 2018 Feb 7;38(6):1588-1599. doi: 10.1523/JNEUROSCI.1925-17.2017. Epub 2018 Jan 8. PMID: 29311142; PMCID: PMC5815356.

Fischman AJ, Kastin AJ, Graf MV, Moldow RL. Constant light and dark affect the circadian rhythm of the hypothalamic-pituitary-adrenal axis. Neuroendocrinology. 1988 Apr;47(4):309-16. doi: 10.1159/000124930. PMID: 2836747.

Foster RG, Kreitzman L. The rhythms of life: what your body clock means to you! Exp Physiol. 2014 Apr;99(4):599-606. doi: 10.1113/expphysiol.2012.071118. Epub 2013 Dec 20. PMID: 24363383.

Fujii R, Hosoya M, Fukusumi S, Kawamata Y, Habata Y, Hinuma S, Onda H, Nishimura O, Fujino M. Identification of neuromedin U as the cognate ligand of the orphan G protein-coupled receptor FM-3. J Biol Chem. 2000 Jul 14;275(28):21068-74. doi: 10.1074/jbc.M001546200. PMID: 10783389.

Füzesi T, Daviu N, Wamsteeker Cusulin JI, Bonin RP, Bains JS. Hypothalamic CRH neurons orchestrate complex behaviours after stress. Nat Commun. 2016 Jun 16;7:11937. doi: 10.1038/ncomms11937. PMID: 27306314; PMCID: PMC4912635.

Gall AJ, Todd WD, Blumberg MS. Development of SCN connectivity and the circadian control of arousal: a diminishing role for humoral factors? PLoS One. 2012;7(9):e45338. doi: 10.1371/journal.pone.0045338. Epub 2012 Sep 13. PMID: 23028945; PMCID: PMC3441626.

Gall AJ, Shuboni DD, Yan L, Nunez AA, Smale L. Suprachiasmatic Nucleus and Subparaventricular Zone Lesions Disrupt Circadian Rhythmicity but Not Light-Induced Masking Behavior in Nile Grass Rats. J Biol Rhythms. 2016 Apr;31(2):170-81. doi: 10.1177/0748730415626251. Epub 2016 Jan 22. PMID: 26801650.

Ganea D, Hooper KM, Kong W. The neuropeptide vasoactive intestinal peptide: direct effects on immune cells and involvement in inflammatory and autoimmune diseases. Acta Physiol (Oxf). 2015 Feb;213(2):442-52. doi: 10.1111/apha.12427. Epub 2014 Dec 11. PMID: 25422088; PMCID: PMC4484298.

Gandhi AV, Mosser EA, Oikonomou G, Prober DA. Melatonin is required for the circadian regulation of sleep. Neuron. 2015 Mar 18;85(6):1193-9. doi: 10.1016/j.neuron.2015.02.016. Epub 2015 Mar 5. PMID: 25754820; PMCID: PMC4851458.

Gillespie CF, Mintz EM, Marvel CL, Huhman KL, Albers HE. GABA(A) and GABA(B) agonists and antagonists alter the phase-shifting effects of light when microinjected into the suprachiasmatic region. Brain Res. 1997 Jun 13;759(2):181-9. doi: 10.1016/s0006- 8993(97)00235-7. PMID: 9221935.

Gomez F, Chapleur M, Fernette B, Burlet C, Nicolas JP, Burlet A. Arginine vasopressin (AVP) depletion in neurons of the suprachiasmatic nuclei affects the AVP content of the paraventricular neurons and stimulates adrenocorticotrophic hormone release. J Neurosci Res. 1997 Nov 15;50(4):565-74. doi: 10.1002/(SICI)1097-4547(19971115)50:4<565::AID-JNR7>3.0.CO;2-C. PMID: 9404718.

Goyer D, Roberts MT. Long-range Channelrhodopsin-assisted Circuit Mapping of Inferior Colliculus Neurons with Blue and Red-shifted Channelrhodopsins. J Vis Exp. 2020 Feb 7;(156):10.3791/60760. doi: 10.3791/60760. PMID: 32090997; PMCID: PMC7118657.

Graham DM, Wong KY. Melanopsin-expressing, Intrinsically Photosensitive Retinal Ganglion Cells (ipRGCs) 2008 Aug 1 [Updated 2016 Nov 2]. In: Kolb H, Fernandez E, Nelson R, editors. Webvision: The Organization of the Retina and Visual System [Internet]. Salt Lake City (UT): University of Utah Health Sciences Center; 1995-. Available from: https://www.ncbi.nlm.nih.gov/books/NBK27326/.

Graham ES, Turnbull Y, Fotheringham P, Nilaweera K, Mercer JG, Morgan PJ, Barrett P. Neuromedin U and Neuromedin U receptor-2 expression in the mouse and rat hypothalamus: effects of nutritional status. J Neurochem. 2003 Dec;87(5):1165-73. doi: 10.1046/j.1471-4159.2003.02079.x. PMID: 14622096.

Graham ES, Littlewood P, Turnbull Y, Mercer JG, Morgan PJ, Barrett P. Neuromedin-U is regulated by the circadian clock in the SCN of the mouse. Eur J Neurosci. 2005 Feb;21(3):814-9. doi: 10.1111/j.1460-9568.2005.03923.x. PMID: 15733101.

Green DJ, Gillette R. Circadian rhythm of firing rate recorded from single cells in the rat suprachiasmatic brain slice. Brain Res. 1982 Aug 5;245(1):198-200. doi: 10.1016/0006- 8993(82)90361-4. PMID: 6889453.

Guan XM, Yu H, Jiang Q, Van Der Ploeg LH, Liu Q. Distribution of neuromedin U receptor subtype 2 mRNA in the rat brain. Brain Res Gene Expr Patterns. 2001 Aug;1(1):1-4. doi: 10.1016/s1567-133x(00)00002-8. PMID: 15018811.

Güldner FH. Numbers of neurons and astroglial cells in the suprachiasmatic nucleus of male and female rats. Exp Brain Res. 1983;50(2-3):373-6. doi: 10.1007/BF00239203. PMID: 6641871.

Guo H, Brewer JM, Lehman MN, Bittman EL. Suprachiasmatic regulation of circadian rhythms of gene expression in hamster peripheral organs: effects of transplanting the 71 pacemaker. J Neurosci. 2006 Jun 14;26(24):6406-12. doi: 10.1523/JNEUROSCI.4676- 05.2006. Erratum in: J Neurosci. 2006 Jul 5;26(27):table of contents. Guo, Hongian [corrected to Guo, Hongnian]. PMID: 16775127; PMCID: PMC6674028.

Hamnett R, Crosby P, Chesham JE, Hastings MH. Vasoactive intestinal peptide controls the suprachiasmatic circadian clock network via ERK1/2 and DUSP4 signalling. Nat Commun. 2019 Feb 1;10(1):542. doi: 10.1038/s41467-019-08427-3. PMID: 30710088; PMCID: PMC6358603.

Hanada R, Nakazato M, Murakami N, Sakihara S, Yoshimatsu H, Toshinai K, Hanada T, Suda T, Kangawa K, Matsukura S, Sakata T. A role for neuromedin U in stress response. Biochem Biophys Res Commun. 2001 Nov 23;289(1):225-8. doi: 10.1006/bbrc.2001.5945. PMID: 11708803.

Hannibal J. Neurotransmitters of the retino-hypothalamic tract. Cell Tissue Res. 2002 Jul;309(1):73-88. doi: 10.1007/s00441-002-0574-3. Epub 2002 May 29. PMID: 12111538.

Hardin PE, Hall JC, Rosbash M. Feedback of the Drosophila period gene product on circadian cycling of its messenger RNA levels. Nature. 1990 Feb 8;343(6258):536-40. doi: 10.1038/343536a0. PMID: 2105471.

Harding C, Bechtold DA, Brown TM. Suprachiasmatic nucleus-dependent and independent outputs driving rhythmic activity in hypothalamic and thalamic neurons. BMC Biol. 2020 Sep 30;18(1):134. doi: 10.1186/s12915-020-00871-8. PMID: 32998726; PMCID: PMC7528611.

Harmar AJ, Marston HM, Shen S, Spratt C, West KM, Sheward WJ, Morrison CF, Dorin JR, Piggins HD, Reubi JC, Kelly JS, Maywood ES, Hastings MH. The VPAC(2) receptor is essential for circadian function in the mouse suprachiasmatic nuclei. Cell. 2002 May 17;109(4):497-508. doi: 10.1016/s0092-8674(02)00736-5. PMID: 12086606.

Harmar AJ, Fahrenkrug J, Gozes I, Laburthe M, May V, Pisegna JR, Vaudry D, Vaudry H, Waschek JA, Said SI. Pharmacology and functions of receptors for vasoactive intestinal peptide and pituitary adenylate cyclase-activating polypeptide: IUPHAR review 1. Br J Pharmacol. 2012 May;166(1):4-17. doi: 10.1111/j.1476-5381.2012.01871.x. PMID: 22289055; PMCID: PMC3415633.

Hastings MH, Duffield GE, Ebling FJ, Kidd A, Maywood ES, Schurov I. Non-photic signalling in the suprachiasmatic nucleus. Biol Cell. 1997 Nov;89(8):495-503. doi: 10.1016/s0248-4900(98)80005-1. PMID: 9618899.

Hastings MH, Herzog ED. Clock genes, oscillators, and cellular networks in the suprachiasmatic nuclei. J Biol Rhythms. 2004 Oct;19(5):400-13. doi: 10.1177/0748730404268786. PMID: 15534320.

Hattar S, Liao HW, Takao M, Berson DM, Yau KW. Melanopsin-containing retinal ganglion cells: architecture, projections, and intrinsic photosensitivity. Science. 2002 Feb 8;295(5557):1065-70. doi: 10.1126/science.1069609. PMID: 11834834; PMCID: PMC2885915.

Hattar S, Kumar M, Park A, Tong P, Tung J, Yau KW, Berson DM. Central projections of melanopsin-expressing retinal ganglion cells in the mouse. J Comp Neurol. 2006 Jul 20;497(3):326-49. doi: 10.1002/cne.20970. PMID: 16736474; PMCID: PMC2885916.

Herbert J. The Suprachiasmatic Nucleus. The Mind's Clock. J Anat. 1994 Apr;184(Pt 2):431. PMCID: PMC1260009.

Herman JP, McKlveen JM, Ghosal S, Kopp B, Wulsin A, Makinson R, Scheimann J, Myers B. Regulation of the Hypothalamic-Pituitary-Adrenocortical Stress Response. Compr Physiol. 2016 Mar 15;6(2):603-21. doi: 10.1002/cphy.c150015. PMID: 27065163; PMCID: PMC4867107.

Hermes ML, Coderre EM, Buijs RM, Renaud LP. GABA and glutamate mediate rapid neurotransmission from suprachiasmatic nucleus to hypothalamic paraventricular nucleus in rat. J Physiol. 1996 Nov 1;496 (Pt 3)(Pt 3):749-57. doi: 10.1113/jphysiol.1996.sp021724. PMID: 8930841; PMCID: PMC1160861.

Hermes ML, Kolaj M, Doroshenko P, Coderre E, Renaud LP. Effects of VPAC2 receptor activation on membrane excitability and GABAergic transmission in subparaventricular zone neurons targeted by suprachiasmatic nucleus. J Neurophysiol. 2009 Sep;102(3):1834-42. doi: 10.1152/jn.91261.2008. Epub 2009 Jul 1. PMID: 19571188.

Hirose S, Osada T, Ogawa A, Tanaka M, Wada H, Yoshizawa Y, Imai Y, Machida T, Akahane M, Shirouzu I, Konishi S. Lateral-Medial Dissociation in Orbitofrontal Cortex-Hypothalamus Connectivity. Front Hum Neurosci. 2016 May 26;10:244. doi: 10.3389/fnhum.2016.00244. PMID: 27303281; PMCID: PMC4880561.

Hoffert JD, Pisitkun T, Saeed F, Song JH, Chou CL, Knepper MA. Dynamics of the G protein-coupled vasopressin V2 receptor signaling network revealed by quantitative phosphoproteomics. Mol Cell Proteomics. 2012 Feb;11(2):M111.014613. doi: 10.1074/mcp.M111.014613. Epub 2011 Nov 21. PMID: 22108457; PMCID: PMC3277771.

Hogenesch JB, Panda S, Kay S, Takahashi JS. Circadian transcriptional output in the SCN and liver of the mouse. Novartis Found Symp. 2003;253:171-80; discussion 52-5, 102-9, 180-3 passim. PMID: 14712921.

Honma S, Shirakawa T, Katsuno Y, Namihira M, Honma K. Circadian periods of single suprachiasmatic neurons in rats. Neurosci Lett. 1998 Jul 10;250(3):157-60. doi: 10.1016/s0304-3940(98)00464-9. PMID: 9708856.

Hoorneman EM, Buijs RM. Vasopressin fiber pathways in the rat brain following suprachiasmatic nucleus lesioning. Brain Res. 1982 Jul 15;243(2):235-41. doi: 10.1016/0006-8993(82)90246-3. PMID: 7049323.

Hosoya M, Moriya T, Kawamata Y, Ohkubo S, Fujii R, Matsui H, Shintani Y, Fukusumi S, Habata Y, Hinuma S, Onda H, Nishimura O, Fujino M. Identification and functional characterization of a novel subtype of neuromedin U receptor. J Biol Chem. 2000 Sep 22;275(38):29528-32. doi: 10.1074/jbc.M004261200. PMID: 10887190.

Howard AD, Wang R, Pong SS, Mellin TN, Strack A, Guan XM, Zeng Z, Williams DL Jr, Feighner SD, Nunes CN, Murphy B, Stair JN, Yu H, Jiang Q, Clements MK, Tan CP, McKee KK, Hreniuk DL, McDonald TP, Lynch KR, Evans JF, Austin CP, Caskey CT, Van der Ploeg LH, Liu Q. Identification of receptors for neuromedin U and its role in feeding. Nature. 2000 Jul 6;406(6791):70-4. doi: 10.1038/35017610. PMID: 10894543.

Hsu SH, Luo CW. Molecular dissection of G protein preference using Gsalpha chimeras reveals novel ligand signaling of GPCRs. Am J Physiol Endocrinol Metab. 2007 Oct;293(4):E1021-9. doi: 10.1152/ajpendo.00003.2007. Epub 2007 Jul 24. PMID: 17652154.

Human Protein Atlas. Retrieved September 15, 2020. From The Human Protein Atlas: https://www.proteinatlas.org/ENSG00000146469-VIP/tissue.

Innamorati G, Le Gouill C, Balamotis M, Birnbaumer M. The long and the short cycle. Alternative intracellular routes for trafficking of G-protein-coupled receptors. J Biol Chem. 2001 Apr 20;276(16):13096-103. doi: 10.1074/jbc.M009780200. Epub 2001 Jan 9. PMID: 11150299.

Inouye ST, Kawamura H. Persistence of circadian rhythmicity in a mammalian hypothalamic "island" containing the suprachiasmatic nucleus. Proc Natl Acad Sci U S A. 1979 Nov;76(11):5962-6. doi: 10.1073/pnas.76.11.5962. PMID: 293695; PMCID: PMC411773.

Iremonger KJ, Bains JS. Retrograde opioid signaling regulates glutamatergic transmission in the hypothalamus. J Neurosci. 2009 Jun 3;29(22):7349-58. doi: 10.1523/JNEUROSCI.0381-09.2009. PMID: 19494156; PMCID: PMC6666467.

Irwin RP, Allen CN. GABAergic signaling induces divergent neuronal Ca2+ responses in the suprachiasmatic nucleus network. Eur J Neurosci. 2009 Oct;30(8):1462-75. doi: 10.1111/j.1460-9568.2009.06944.x. Epub 2009 Oct 12. PMID: 19821838; PMCID: PMC3700401.

Jászberényi M, Bujdosó E, Pataki I, Telegdy G. Effects of orexins on the hypothalamic-pituitary-adrenal system. J Neuroendocrinol. 2000 Dec;12(12):1174-8. doi: 10.1046/j.1365-2826.2000.00572.x. PMID: 11106974

Jászberényi M, Bagosi Z, Thurzó B, Földesi I, Telegdy G. Endocrine and behavioral effects of neuromedin S. Horm Behav. 2007 Dec;52(5):631-9. doi: 10.1016/j.yhbeh.2007.08.002. Epub 2007 Aug 14. PMID: 17900576.

Izumo M, Johnson CH, Yamazaki S. Circadian gene expression in mammalian fibroblasts revealed by real-time luminescence reporting: temperature compensation and damping. Proc Natl Acad Sci U S A. 2003 Dec 23;100(26):16089-94. doi: 10.1073/pnas.2536313100. Epub 2003 Dec 4. PMID: 14657355; PMCID: PMC307697.

Jin X, Shearman LP, Weaver DR, Zylka MJ, de Vries GJ, Reppert SM. A molecular mechanism regulating rhythmic output from the suprachiasmatic circadian clock. Cell. 1999 Jan 8;96(1):57-68. doi: 10.1016/s0092-8674(00)80959-9. PMID: 9989497.

Jindrich K, Roper KE, Lemon S, Degnan BM, Reitzel AM and Degnan SM (2017) Origin of the Animal Circadian Clock: Diurnal and Light-Entrained Gene Expression in the Sponge Amphimedon queenslandica. Front. Mar. Sci. 4:327. doi: 10.3389/fmars.2017.00327.

Jiang W, Zheng S. Structural insights into galanin receptor signaling. Proc Natl Acad Sci U S A. 2022 May 24;119(21):e2121465119. doi: 10.1073/pnas.2121465119. Epub 2022 May 20. PMID: 35594396; PMCID: PMC9173784.

Jolkkonen J, Tuomisto L, van Wimersma Greidanus TB, Riekkinen PJ. Vasopressin levels in the cerebrospinal fluid of rats with lesions of the paraventricular and suprachiasmatic nuclei. Neurosci Lett. 1988 Mar 31;86(2):184-8. doi: 10.1016/0304-3940(88)90568-x. PMID: 3368120.

Jones JR, Simon T, Lones L, Herzog ED. SCN VIP Neurons Are Essential for Normal LightMediated Resetting of the Circadian System. J Neurosci. 2018 Sep 12;38(37):7986-7995. doi: 10.1523/JNEUROSCI.1322-18.2018. Epub 2018 Aug 6. PMID: 30082421; PMCID: PMC6596148.

Jones JR, Chaturvedi S, Granados-Fuentes D, Herzog ED. Circadian neurons in the paraventricular nucleus entrain and sustain daily rhythms in glucocorticoids. Nat Commun. 2021 Oct 1;12(1):5763. doi: 10.1038/s41467-021-25959-9. PMID: 34599158; PMCID: PMC8486846.

Kabrita CS, Davis FC. Development of the mouse suprachiasmatic nucleus: determination of time of cell origin and spatial arrangements within the nucleus. Brain Res. 2008 Feb 21;1195:20-7. doi: 10.1016/j.brainres.2007.12.020. Epub 2007 Dec 23. PMID: 18201688; PMCID: PMC2716030.

Kaczmarek P, Malendowicz LK, Pruszynska-Oszmalek E, Wojciechowicz T, Szczepankiewicz D, Szkudelski T, Nowak KW. Neuromedin U receptor 1 expression in the rat endocrine pancreas and evidence suggesting neuromedin U suppressive effect on insulin secretion from isolated rat pancreatic islets. Int J Mol Med. 2006 Nov;18(5):951-5. PMID: 17016626.

Kakizawa K, Watanabe M, Mutoh H, Okawa Y, Yamashita M, Yanagawa Y, Itoi K, Suda T, Oki Y, Fukuda A. A novel GABA-mediated corticotropin-releasing hormone secretory mechanism in the median eminence. Sci Adv. 2016 Aug 17;2(8):e1501723. doi: 10.1126/sciadv.1501723. PMID: 27540587; PMCID: PMC4988769.

Kalamatianos T, Kalló I, Piggins HD, Coen CW. Expression of VIP and/or PACAP receptor mRNA in peptide synthesizing cells within the suprachiasmatic nucleus of the rat and in its 78 efferent target sites. J Comp Neurol. 2004 Jul 12;475(1):19-35. doi: 10.1002/cne.20168. PMID: 15176082.

Kalló I, Kalamatianos T, Wiltshire N, Shen S, Sheward WJ, Harmar AJ, Coen CW. Transgenic approach reveals expression of the VPAC2 receptor in phenotypically defined neurons in the mouse suprachiasmatic nucleus and in its efferent target sites. Eur J Neurosci. 2004 Apr;19(8):2201-11. doi: 10.1111/j.0953-816X.2004.03335.x. PMID: 15090046.

Kalsbeek A, Buijs RM, van Heerikhuize JJ, Arts M, van der Woude TP. Vasopressin-containing neurons of the suprachiasmatic nuclei inhibit corticosterone release. Brain Res. 1992 May 15;580(1-2):62-7. doi: 10.1016/0006-8993(92)90927-2. PMID: 1504818.

Kalsbeek A, Teclemariam-Mesbah R, Pévet P. Efferent projections of the suprachiasmatic nucleus in the golden hamster (Mesocricetus auratus). J Comp Neurol. 1993 Jun 15;332(3):293-314. doi: 10.1002/cne.903320304. PMID: 8331217.

Kalsbeek A, Buijs RM, Engelmann M, Wotjak CT, Landgraf R. In vivo measurement of a diurnal variation in vasopressin release in the rat suprachiasmatic nucleus. Brain Res. 1995 Jun 5;682(1-2):75-82. doi: 10.1016/0006-8993(95)00324-j. PMID: 7552330.

Kalsbeek A, van der Vliet J, Buijs RM. Decrease of endogenous vasopressin release necessary for expression of the circadian rise in plasma corticosterone: a reverse microdialysis study. J Neuroendocrinol. 1996 Apr;8(4):299-307. doi: 10.1046/j.1365-2826.1996.04597.x. PMID: 8861286.

Kalsbeek A, van Heerikhuize JJ, Wortel J, Buijs RM. A diurnal rhythm of stimulatory input to the hypothalamo-pituitary-adrenal system as revealed by timed intrahypothalamic administration of the vasopressin V1 antagonist. J Neurosci. 1996 Sep 1;16(17):5555-65. doi: 10.1523/JNEUROSCI.16-17-05555.1996. PMID: 8757267; PMCID: PMC6578885.

Kalsbeek A, Drijfhout WJ, Westerink BH, van Heerikhuize JJ, van der Woude TP, van der Vliet J, Buijs RM. GABA receptors in the region of the dorsomedial hypothalamus of rats are implicated in the control of melatonin and corticosterone release. Neuroendocrinology. 1996 Jan;63(1):69-78. doi: 10.1159/000126937. PMID: 8839357.

Kalsbeek A, Palm IF, La Fleur SE, Scheer FA, Perreau-Lenz S, Ruiter M, Kreier F, Cailotto C, Buijs RM. SCN outputs and the hypothalamic balance of life. J Biol Rhythms. 2006 Dec;21(6):458-69. doi: 10.1177/0748730406293854. PMID: 17107936.

Kassi EN, Chrousos GP. The central CLOCK system and the stress axis in health and disease. Hormones (Athens). 2013 Apr-Jun;12(2):172-91. doi: 10.14310/horm.2002.1402. PMID: 23933687.

Kaur S, Wang JL, Ferrari L, Thankachan S, Kroeger D, Venner A, Lazarus M, Wellman A, Arrigoni E, Fuller PM, Saper CB. A Genetically Defined Circuit for Arousal from Sleep during Hypercapnia. Neuron. 2017 Dec 6;96(5):1153-1167.e5. doi: 10.1016/j.neuron.2017.10.009. Epub 2017 Nov 2. PMID: 29103805; PMCID: PMC5720904.

Kendrick KM. Microdialysis measurement of in vivo neuropeptide release. J Neurosci Methods. 1990 Sep;34(1-3):35-46. doi: 10.1016/0165-0270(90)90040-m. PMID: 2259245.

Kent J, Meredith AL. BK channels regulate spontaneous action potential rhythmicity in the suprachiasmatic nucleus. PLoS One. 2008;3(12):e3884. doi: 10.1371/journal.pone.0003884. Epub 2008 Dec 8. PMID: 19060951; PMCID: PMC2586654.

Kim H, Kim M, Im SK, Fang S. Mouse Cre-LoxP system: general principles to determine tissue-specific roles of target genes. Lab Anim Res. 2018 Dec;34(4):147-159. doi: 10.5625/lar.2018.34.4.147. Epub 2018 Dec 31. PMID: 30671100; PMCID: PMC6333611.

Klapoetke NC, Murata Y, Kim SS, Pulver SR, Birdsey-Benson A, Cho YK, Morimoto TK, Chuong AS, Carpenter EJ, Tian Z, Wang J, Xie Y, Yan Z, Zhang Y, Chow BY, Surek B, Melkonian M, Jayaraman V, Constantine-Paton M, Wong GK, Boyden ES. Independent optical excitation of distinct neural populations. Nat Methods. 2014 Mar;11(3):338-46. doi: 10.1038/nmeth.2836. Epub 2014 Feb 9. Erratum in: Nat Methods. 2014 Sep;11(9):971. PMID: 24509633; PMCID: PMC3943671.

Klein DC, Smoot R, Weller JL, Higa S, Markey SP, Creed GJ, Jacobowitz DM. Lesions of the paraventricular nucleus of the hypothalamus disrupt the suprachiasmatic leads to spinal cord circuit in the melatonin rhythm generating system. Brain Res Bull. 1983 May;10(5):647- 52. doi: 10.1016/0361-9230(83)90033-3. PMID: 6307491.

Korenčič, A., Košir, R., Bordyugov, G. et al. Timing of circadian genes in mammalian tissues. Sci Rep 4, 5782 (2014). https://doi.org/10.1038/srep05782.

Krashes MJ, Shah BP, Madara JC, Olson DP, Strochlic DE, Garfield AS, Vong L, Pei H, Watabe-Uchida M, Uchida N, Liberles SD, Lowell BB. An excitatory paraventricular nucleus to AgRP neuron circuit that drives hunger. Nature. 2014 Mar 13;507(7491):238-42. doi: 10.1038/nature12956. Epub 2014 Feb 2. PMID: 24487620; PMCID: PMC3955843.

Krout KE, Kawano J, Mettenleiter TC, Loewy AD. CNS inputs to the suprachiasmatic nucleus of the rat. Neuroscience. 2002;110(1):73-92. doi: 10.1016/s0306-4522(01)00551-6. PMID: 11882374.

Kuhlman SJ, Quintero JE, McMahon DG. GFP fluorescence reports Period 1 circadian gene regulation in the mammalian biological clock. Neuroreport. 2000 May 15;11(7):1479-82. PMID: 10841361.

Kuhlman SJ, Craig LM, Duffy JF. Introduction to Chronobiology. Cold Spring Harb Perspect Biol. 2018 Sep 4;10(9):a033613. doi: 10.1101/cshperspect.a033613. PMID: 29038118; PMCID: PMC6120700.

Laburthe M, Couvineau A. Molecular pharmacology and structure of VPAC Receptors for VIP and PACAP. Regul Pept. 2002 Oct 15;108(2-3):165-73. doi: 10.1016/s0167- 0115(02)00099-x. PMID: 12220741.

Laburthe M, Couvineau A, Tan V. Class II G protein-coupled receptors for VIP and PACAP: structure, models of activation and pharmacology. Peptides. 2007 Sep;28(9):1631-9. doi: 10.1016/j.peptides.2007.04.026. Epub 2007 May 22. PMID: 17574305.

Langer I. Mechanisms involved in VPAC receptors activation and regulation: lessons from pharmacological and mutagenesis studies. Front Endocrinol (Lausanne). 2012 Oct 30;3:129. doi: 10.3389/fendo.2012.00129. PMID: 23115557; PMCID: PMC3483716.

Leak RK, Card JP, Moore RY. Suprachiasmatic pacemaker organization analyzed by viral transynaptic transport. Brain Res. 1999 Feb 20;819(1-2):23-32. doi: 10.1016/s0006- 8993(98)01317-1. PMID: 10082857.

Leak RK, Moore RY. Topographic organization of suprachiasmatic nucleus projection neurons. J Comp Neurol. 2001 May 7;433(3):312-34. doi: 10.1002/cne.1142. PMID: 11298358.

Lechan RM, Toni R. Functional Anatomy of the Hypothalamus and Pituitary. [Updated 2016 Nov 28]. In: Feingold KR, Anawalt B, Blackman MR, et al., editors. Endotext [Internet]. South Dartmouth (MA): MDText.com, Inc.; 2000-. Available from: https://www.ncbi.nlm.nih.gov/books/NBK279126/

Lee C, Etchegaray JP, Cagampang FR, Loudon AS, Reppert SM. Posttranslational mechanisms regulate the mammalian circadian clock. Cell. 2001 Dec 28;107(7):855-67. doi: 10.1016/s0092-8674(01)00610-9. PMID: 11779462.

Lee AK, Tse FW, Tse A. Arginine Vasopressin Potentiates the Stimulatory Action of CRH on Pituitary Corticotropes via a Protein Kinase C-Dependent Reduction of the Background TREK-1 Current. Endocrinology. 2015 Oct;156(10):3661-72. doi: 10.1210/en.2015-1293. Epub 2015 Aug 6. PMID: 26248219.

Lee IT, Chang AS, Manandhar M, Shan Y, Fan J, Izumo M, Ikeda Y, Motoike T, Dixon S, Seinfeld JE, Takahashi JS, Yanagisawa M. Neuromedin s-producing neurons act as essential pacemakers in the suprachiasmatic nucleus to couple clock neurons and dictate circadian rhythms. Neuron. 2015 Mar 4;85(5):1086-102. doi: 10.1016/j.neuron.2015.02.006. PMID: 25741729; PMCID: PMC5811223.

Lehman MN, Silver R, Gladstone WR, Kahn RM, Gibson M, Bittman EL. Circadian rhythmicity restored by neural transplant. Immunocytochemical characterization of the graft and its integration with the host brain. J Neurosci. 1987 Jun;7(6):1626-38. doi: 10.1523/JNEUROSCI.07-06-01626.1987. PMID: 3598638; PMCID: PMC6568867.

Lein ES, Hawrylycz MJ, Ao N, Ayres M, Bensinger A, Bernard A, Boe AF, Boguski MS, Brockway KS, Byrnes EJ, Chen L, Chen L, Chen TM, Chin MC, Chong J, Crook BE, Czaplinska A, Dang CN, Datta S, Dee NR, Desaki AL, Desta T, Diep E, Dolbeare TA, Donelan MJ, Dong HW, Dougherty JG, Duncan BJ, Ebbert AJ, Eichele G, Estin LK, Faber C, Facer BA, Fields R, Fischer SR, Fliss TP, Frensley C, Gates SN, Glattfelder KJ, Halverson KR, Hart MR, Hohmann JG, Howell MP, Jeung DP, Johnson RA, Karr PT, Kawal R, Kidney JM, Knapik RH, Kuan CL, Lake JH, Laramee AR, Larsen KD, Lau C, Lemon TA, Liang AJ, Liu Y, Luong LT, Michaels J, Morgan JJ, Morgan RJ, Mortrud MT, Mosqueda NF, Ng LL, Ng R, Orta GJ, Overly CC, Pak TH, Parry SE, Pathak SD, Pearson OC, Puchalski RB, Riley ZL, Rockett HR, Rowland SA, Royall JJ, Ruiz MJ, Sarno NR, Schaffnit K, Shapovalova NV, Sivisay T, Slaughterbeck CR, Smith SC, Smith KA, Smith BI, Sodt AJ, Stewart NN, Stumpf KR, Sunkin SM, Sutram M, Tam A, Teemer CD, Thaller C, Thompson CL, Varnam LR, Visel A, Whitlock RM, Wohnoutka PE, Wolkey CK, Wong VY, Wood M, Yaylaoglu MB, Young RC, Youngstrom BL, Yuan XF, Zhang B, Zwingman TA, Jones AR. Genome-wide atlas of gene expression in the adult mouse brain. Nature. 2007 Jan 11;445(7124):168-76. doi: 10.1038/nature05453. Epub 2006 Dec 6. PMID: 17151600.

Leng Y, Musiek ES, Hu K, Cappuccio FP, Yaffe K. Association between circadian rhythms and neurodegenerative diseases. Lancet Neurol. 2019;18(3):307-318. doi:10.1016/S1474- 4422(18)30461-7.

Li JD, Burton KJ, Zhang C, Hu SB, Zhou QY. Vasopressin receptor V1a regulates circadian rhythms of locomotor activity and expression of clock-controlled genes in the suprachiasmatic nuclei. Am J Physiol Regul Integr Comp Physiol. 2009 Mar;296(3):R824-30. doi: 10.1152/ajpregu.90463.2008. Epub 2008 Dec 3. PMID: 19052319; PMCID: PMC2665843.

Logan RW, McClung CA. Rhythms of life: circadian disruption and brain disorders across the lifespan. Nat Rev Neurosci. 2019 Jan;20(1):49-65. doi: 10.1038/s41583-018-0088-y. PMID: 30459365; PMCID: PMC6338075.

Lokshin M, LeSauter J, Silver R. Selective Distribution of Retinal Input to Mouse SCN Revealed in Analysis of Sagittal Sections. J Biol Rhythms. 2015 Jun;30(3):251-7. doi: 10.1177/0748730415584058. PMID: 25994103; PMCID: PMC4933594.

Logan RW, McClung CA. Rhythms of life: circadian disruption and brain disorders across the lifespan. Nat Rev Neurosci. 2019 Jan;20(1):49-65. doi: 10.1038/s41583-018-0088-y. PMID: 30459365; PMCID: PMC6338075.

Lu J, Zhang YH, Chou TC, Gaus SE, Elmquist JK, Shiromani P, Saper CB. Contrasting effects of ibotenate lesions of the paraventricular nucleus and subparaventricular zone on sleep-wake cycle and temperature regulation. J Neurosci. 2001 Jul 1;21(13):4864-74. doi: 10.1523/JNEUROSCI.21-13-04864.2001. Erratum in: J Neurosci. 2012 Oct 17;32(42):14849-50. PMID: 11425913; PMCID: PMC3508730.

Lucas RJ, Stirland JA, Darrow JM, Menaker M, Loudon AS. Free running circadian rhythms of melatonin, luteinizing hormone, and cortisol in Syrian hamsters bearing the circadian tau mutation. Endocrinology. 1999 Feb;140(2):758-64. doi: 10.1210/endo.140.2.6538. PMID: 9927303.

Luquet S, Perez FA, Hnasko TS, Palmiter RD. NPY/AgRP neurons are essential for feeding in adult mice but can be ablated in neonates. Science. 2005 Oct 28;310(5748):683-5. doi: 10.1126/science.1115524. PMID: 16254186

Madisen L, Mao T, Koch H, Zhuo JM, Berenyi A, Fujisawa S, Hsu YW, Garcia AJ 3rd, Gu X, Zanella S, Kidney J, Gu H, Mao Y, Hooks BM, Boyden ES, Buzsáki G, Ramirez JM, Jones AR, Svoboda K, Han X, Turner EE, Zeng H. A toolbox of Cre-dependent optogenetic transgenic mice for light-induced activation and silencing. Nat Neurosci. 2012 Mar 25;15(5):793-802. doi: 10.1038/nn.3078. PMID: 22446880; PMCID: PMC3337962.

Mahmoudi P, Veladi H, Pakdel FG. Optogenetics, Tools and Applications in Neurobiology. J Med Signals Sens. 2017 Apr-Jun;7(2):71-79. PMID: 28553579; PMCID: PMC5437765.

Malendowicz LK, Rucinski M. Neuromedins NMU and NMS: An Updated Overview of Their Functions. Front Endocrinol (Lausanne). 2021 Jul 1;12:713961. doi: 10.3389/fendo.2021.713961. PMID: 34276571; PMCID: PMC8283259.

Maywood ES, Reddy AB, Wong GK, O'Neill JS, O'Brien JA, McMahon DG, Harmar AJ, Okamura H, Hastings MH. Synchronization and maintenance of timekeeping in suprachiasmatic circadian clock cells by neuropeptidergic signaling. Curr Biol. 2006 Mar 21;16(6):599-605. doi: 10.1016/j.cub.2006.02.023. PMID: 16546085.

Mazuski C, Abel JH, Chen SP, Hermanstyne TO, Jones JR, Simon T, Doyle FJ 3rd, Herzog ED. Entrainment of Circadian Rhythms Depends on Firing Rates and Neuropeptide Release of VIP SCN Neurons. Neuron. 2018 Aug 8;99(3):555-563.e5. doi: 10.1016/j.neuron.2018.06.029. Epub 2018 Jul 12. PMID: 30017392; PMCID: PMC6085153.

Mazuski C, Chen SP, Herzog ED. Different Roles for VIP Neurons in the Neonatal and Adult Suprachiasmatic Nucleus. J Biol Rhythms. 2020 Oct;35(5):465-475. doi: 10.1177/0748730420932073. Epub 2020 Jun 15. PMID: 32536240; PMCID: PMC7541769.

McEwen BS, Gray JD, Nasca C. 60 YEARS OF NEUROENDOCRINOLOGY: Redefining neuroendocrinology: stress, sex and cognitive and emotional regulation. J Endocrinol. 2015 Aug;226(2):T67-83. doi: 10.1530/JOE-15-0121. Epub 2015 May 1. PMID: 25934706; PMCID: PMC4515381.

Mei L, Fan Y, Lv X, Welsh DK, Zhan C, Zhang EE. Long-term in vivo recording of circadian rhythms in brains of freely moving mice. Proc Natl Acad Sci U S A. 2018 Apr 17;115(16):4276-4281. doi: 10.1073/pnas.1717735115. Epub 2018 Apr 2. PMID: 29610316; PMCID: PMC5910830.

Meijer JH, Schwartz WJ. In search of the pathways for light-induced pacemaker resetting in the suprachiasmatic nucleus. J Biol Rhythms. 2003 Jun;18(3):235-49. doi: 10.1177/0748730403018003006. PMID: 12828281.

Meyer-Spasche A, Piggins HD. Vasoactive intestinal polypeptide phase-advances the rat suprachiasmatic nuclei circadian pacemaker in vitro via protein kinase A and mitogenactivated protein kinase. Neurosci Lett. 2004 Mar 25;358(2):91-4. doi: 10.1016/j.neulet.2003.12.114. PMID: 15026156.

Meyer-Bernstein EL, Jetton AE, Matsumoto SI, Markuns JF, Lehman MN, Bittman EL. Effects of suprachiasmatic transplants on circadian rhythms of neuroendocrine function in golden hamsters. Endocrinology. 1999 Jan;140(1):207-18. doi: 10.1210/endo.140.1.6428. PMID: 9886827

Minamino N, Kangawa K, Matsuo H. Neuromedin U-8 and U-25: novel uterus stimulating and hypertensive peptides identified in porcine spinal cord. Biochem Biophys Res Commun. 1985 Aug 15;130(3):1078-85. doi: 10.1016/0006-291x(85)91726-7. PMID: 3839674.

Mintz EM, Jasnow AM, Gillespie CF, Huhman KL, Albers HE. GABA interacts with photic signaling in the suprachiasmatic nucleus to regulate circadian phase shifts. Neuroscience. 2002;109(4):773-8. doi: 10.1016/s0306-4522(01)00519-x. PMID: 11927159.

Moga MM, Moore RY. Organization of neural inputs to the suprachiasmatic nucleus in the rat. J Comp Neurol. 1997 Dec 22;389(3):508-34. doi: 10.1002/(sici)1096- 9861(19971222)389:33.0.co;2-h. PMID: 9414010.

Molleman A (2003). Patch Clamping: An Introductory Guide To Patch Clamp Electrophysiology. Wiley, first edition.

Monfredi O, Lakatta EG. Complexities in cardiovascular rhythmicity: perspectives on circadian normality, ageing and disease. Cardiovasc Res. 2019 Sep 1;115(11):1576-1595. doi: 10.1093/cvr/cvz112. PMID: 31150049; PMCID: PMC6933509.

Moody TW, Ito T, Osefo N, Jensen RT. VIP and PACAP: recent insights into their functions/roles in physiology and disease from molecular and genetic studies. Curr Opin Endocrinol Diabetes Obes. 2011 Feb;18(1):61-7. doi: 10.1097/MED.0b013e328342568a. PMID: 21157320; PMCID: PMC3075877.

Moore RY, Eichler VB. Loss of a circadian adrenal corticosterone rhythm following suprachiasmatic lesions in the rat. Brain Res. 1972 Jul 13;42(1):201-6. doi: 10.1016/0006- 8993(72)90054-6. PMID: 5047187.

Moore RY, Speh JC, Leak RK. Suprachiasmatic nucleus organization. Cell Tissue Res. 2002 Jul;309(1):89-98. doi: 10.1007/s00441-002-0575-2. Epub 2002 Jun 8. PMID: 12111539.

Moore RY. The suprachiasmatic nucleus and the circadian timing system. Prog Mol Biol Transl Sci. 2013;119:1-28. doi: 10.1016/B978-0-12-396971-2.00001-4. PMID: 23899592.

Moore RY, Danchenko RL. Paraventricular-subparaventricular hypothalamic lesions selectively affect circadian function. Chronobiol Int. 2002 Mar;19(2):345-60. doi: 10.1081/cbi-120002876. PMID: 12025929.

Morell M, Souza-Moreira L, González-Rey E. VIP in neurological diseases: more than a neuropeptide. Endocr Metab Immune Disord Drug Targets. 2012 Dec;12(4):323-32. doi: 10.2174/187153012803832549. PMID: 23094829.

Morf J, Schibler U. Body temperature cycles: gatekeepers of circadian clocks. Cell Cycle. 2013 Feb 15;12(4):539-40. doi: 10.4161/cc.23670. Epub 2013 Jan 23. PMID: 23343768; PMCID: PMC3594249.

Mori K, Miyazato M, Ida T, Murakami N, Serino R, Ueta Y, Kojima M, Kangawa K. Identification of neuromedin S and its possible role in the mammalian circadian oscillator system. EMBO J. 2005 Jan 26;24(2):325-35. doi: 10.1038/sj.emboj.7600526. Epub 2005 Jan 6. PMID: 15635449; PMCID: PMC545815.

Morin LP, Shivers KY, Blanchard JH, Muscat L. Complex organization of mouse and rat suprachiasmatic nucleus. Neuroscience. 2006;137(4):1285-97. doi: 10.1016/j.neuroscience.2005.10.030. Epub 2005 Dec 7. PMID: 16338081.

Mukai Y, Nagayama A, Itoi K, Yamanaka A. Identification of substances which regulate activity of corticotropin-releasing factor-producing neurons in the paraventricular nucleus of the hypothalamus. Sci Rep. 2020 Aug 12;10(1):13639. doi: 10.1038/s41598-020-70481-5. PMID: 32788592; PMCID: PMC7424526.

Münch M, Bromundt V. Light and chronobiology: implications for health and disease. Dialogues Clin Neurosci. 2012 Dec;14(4):448-53. PMID: 23393421; PMCID: PMC3553574.

Murphy JR. Mechanism of diphtheria toxin catalytic domain delivery to the eukaryotic cell cytosol and the cellular factors that directly participate in the process. Toxins (Basel). 2011 Mar;3(3):294-308. doi: 10.3390/toxins3030294. Epub 2011 Mar 21. PMID: 22069710; PMCID: PMC3202816.

Muto A, Ohkura M, Kotani T, Higashijima S, Nakai J, Kawakami K. Genetic visualization with an improved GCaMP calcium indicator reveals spatiotemporal activation of the spinal motor neurons in zebrafish. Proc Natl Acad Sci U S A. 2011 Mar 29;108(13):5425-30. doi: 10.1073/pnas.1000887108. Epub 2011 Mar 7. PMID: 21383146; PMCID: PMC3069178.

Nagai T, Sawano A, Park ES, Miyawaki A. Circularly permuted green fluorescent proteins engineered to sense Ca2+. Proc Natl Acad Sci U S A. 2001 Mar 13;98(6):3197-202. doi: 10.1073/pnas.051636098. Epub 2001 Mar 6. PMID: 11248055; PMCID: PMC30630.

Nagel G, Ollig D, Fuhrmann M, Kateriya S, Musti AM, Bamberg E, Hegemann P. Channelrhodopsin-1: a light-gated proton channel in green algae. Science. 2002 Jun 28;296(5577):2395-8. doi: 10.1126/science.1072068. PMID: 12089443.

Nagel G, Szellas T, Huhn W, Kateriya S, Adeishvili N, Berthold P, Ollig D, Hegemann P, Bamberg E. Channelrhodopsin-2, a directly light-gated cation-selective membrane channel. 80 Proc Natl Acad Sci U S A. 2003 Nov 25;100(24):13940-5. doi: 10.1073/pnas.1936192100. Epub 2003 Nov 13. PMID: 14615590; PMCID: PMC283525.

Nagoshi E, Saini C, Bauer C, Laroche T, Naef F, Schibler U. Circadian gene expression in individual fibroblasts: cell-autonomous and self-sustained oscillators pass time to daughter cells. Cell. 2004 Nov 24;119(5):693-705. doi: 10.1016/j.cell.2004.11.015. PMID: 15550250.

Nakahara K, Hanada R, Murakami N, Teranishi H, Ohgusu H, Fukushima N, Moriyama M, Ida T, Kangawa K, Kojima M. The gut-brain peptide neuromedin U is involved in the mammalian circadian oscillator system. Biochem Biophys Res Commun. 2004 May 21;318(1):156-61. doi: 10.1016/j.bbrc.2004.04.014. PMID: 15110767.

Nakahara K, Katayama T, Maruyama K, Ida T, Mori K, Miyazato M, Kangawa K, Murakami N. Comparison of feeding suppression by the anorexigenic hormones neuromedin U and neuromedin S in rats. J Endocrinol. 2010 Nov;207(2):185-93. doi: 10.1677/JOE-10-0081. Epub 2010 Aug 23. PMID: 20732934.

Nakai J, Ohkura M, Imoto K. A high signal-to-noise Ca(2+) probe composed of a single green fluorescent protein. Nat Biotechnol. 2001 Feb;19(2):137-41. doi: 10.1038/84397. PMID: 11175727. 216.

Nakamura W, Yamazaki S, Nakamura TJ, Shirakawa T, Block GD, Takumi T. In vivo monitoring of circadian timing in freely moving mice. Curr Biol. 2008 Mar 11;18(5):381-5. doi: 10.1016/j.cub.2008.02.024. PMID: 18334203.

Naso MF, Tomkowicz B, Perry WL 3rd, Strohl WR. Adeno-Associated Virus (AAV) as a Vector for Gene Therapy. BioDrugs. 2017 Aug;31(4):317-334. doi: 10.1007/s40259-017- 0234-5. PMID: 28669112; PMCID: PMC5548848.

Neher E, Sakmann B. Single-channel currents recorded from membrane of denervated frog muscle fibres. Nature. 1976 Apr 29;260(5554):799-802. doi: 10.1038/260799a0. PMID: 1083489.

Neher E, Sakmann B. Noise analysis of drug induced voltage clamp currents in denervated frog muscle fibres. J Physiol. 1976 Jul;258(3):705-29. doi: 10.1113/jphysiol.1976.sp011442. PMID: 1086359; PMCID: PMC1309001.

Neumann JM, Couvineau A, Murail S, Lacapère JJ, Jamin N, Laburthe M. Class-B GPCR activation: is ligand helix-capping the key? Trends Biochem Sci. 2008 Jul;33(7):314-9. doi: 10.1016/j.tibs.2008.05.001. Epub 2008 Jun 12. PMID: 18555686.

Nielsen HS, Hannibal J, Fahrenkrug J. Vasoactive intestinal polypeptide induces per1 and per2 gene expression in the rat suprachiasmatic nucleus late at night. Eur J Neurosci. 2002 Feb;15(3):570-4. doi: 10.1046/j.0953-816x.2001.01882.x. PMID: 11876785.

Nussdorfer GG, Malendowicz LK. Role of VIP, PACAP, and related peptides in the regulation of the hypothalamo-pituitary-adrenal axis. Peptides. 1998;19(8):1443-67. doi: 10.1016/s0196-9781(98)00102-8. PMID: 9809661.

Oh J, Lee C, Kaang BK. Imaging and analysis of genetically encoded calcium indicators linking neural circuits and behaviors. Korean J Physiol Pharmacol. 2019 Jul;23(4):237-249. doi: 10.4196/kjpp.2019.23.4.237. Epub 2019 Jun 25. PMID: 31297008; PMCID: PMC6609268.

Oikonomou G, Altermatt M, Zhang RW, Coughlin GM, Montz C, Gradinaru V, Prober DA. The Serotonergic Raphe Promote Sleep in Zebrafish and Mice. Neuron. 2019 Aug 21;103(4):686-701.e8. doi: 10.1016/j.neuron.2019.05.038. Epub 2019 Jun 24. PMID: 31248729; PMCID: PMC6706304 187.

Olde Engberink AHO, Meijer JH, Michel S. Chloride cotransporter KCC2 is essential for GABAergic inhibition in the SCN. Neuropharmacology. 2018 Aug;138:80-86. doi: 10.1016/j.neuropharm.2018.05.023. Epub 2018 May 18. PMID: 29782876.

Ono D, Honma KI, Yanagawa Y, Yamanaka A, Honma S. Role of GABA in the regulation of the central circadian clock of the suprachiasmatic nucleus. J Physiol Sci. 2018 Jul;68(4):333-343. doi: 10.1007/s12576-018-0604-x. Epub 2018 Mar 20. PMID: 29560549; PMCID: PMC10717195.

Ono D, Mukai Y, Hung CJ, Chowdhury S, Sugiyama T, Yamanaka A. The mammalian circadian pacemaker regulates wakefulness via CRF neurons in the paraventricular nucleus of the hypothalamus. Sci Adv. 2020 Nov 6;6(45):eabd0384. doi: 10.1126/sciadv.abd0384. PMID: 33158870; PMCID: PMC7673716.

Ono D, Honma KI, Honma S. Roles of Neuropeptides, VIP and AVP, in the Mammalian Central Circadian Clock. Front Neurosci. 2021 Apr 15;15:650154. doi: 10.3389/fnins.2021.650154. Erratum in: Front Neurosci. 2021 Dec 07;15:810796. PMID: 33935635; PMCID: PMC8081951.

Oster H, Damerow S, Kiessling S, Jakubcakova V, Abraham D, Tian J, Hoffmann MW, Eichele G. The circadian rhythm of glucocorticoids is regulated by a gating mechanism residing in the adrenal cortical clock. Cell Metab. 2006 Aug;4(2):163-73. doi: 10.1016/j.cmet.2006.07.002. PMID: 16890544.

Packer AM, Roska B, Häusser M. Targeting neurons and photons for optogenetics. Nat Neurosci. 2013 Jul;16(7):805-15. doi: 10.1038/nn.3427. Epub 2013 Jun 25. PMID: 23799473; PMCID: PMC4928704.

Panda S, Sato TK, Castrucci AM, Rollag MD, DeGrip WJ, Hogenesch JB, Provencio I, Kay SA. Melanopsin (Opn4) requirement for normal light-induced circadian phase shifting. Science. 2002 Dec 13;298(5601):2213-6. doi: 10.1126/science.1076848. PMID: 12481141.

Pavithra S, Aich A, Chanda A, Zohra IF, Gawade P, Das RK. PER2 gene and its association with sleep-related disorders: A review. Physiol Behav. 2024 Jan 1;273:114411. doi: 10.1016/j.physbeh.2023.114411. Epub 2023 Nov 20. PMID: 37981094.

Petreanu L, Huber D, Sobczyk A, Svoboda K. Channelrhodopsin-2-assisted circuit mapping of long-range callosal projections. Nat Neurosci. 2007 May;10(5):663-8. doi: 10.1038/nn1891. Epub 2007 Apr 15. PMID: 17435752.

Petreanu L, Mao T, Sternson SM, Svoboda K. The subcellular organization of neocortical excitatory connections. Nature. 2009 Feb 26;457(7233):1142-5. doi: 10.1038/nature07709. PMID: 19151697; PMCID: PMC2745650.

Pachitariu, M., Stringer, C., Schröder, S., Dipoppa, M., Rossi, L. F., Carandini, M., & Harris, K. D. (2016). Suite2p: beyond 10,000 neurons with standard two-photon microscopy. BioRxiv, 061507.

Patton, A. P., & Hastings, M. H. (2023). The Mammalian Circadian Time-Keeping System. *Journal of Huntington's disease*, *12*(2), 91–104. https://doi.org/10.3233/JHD-230571.

Paul S, Hanna L, Harding C, Hayter EA, Walmsley L, Bechtold DA, Brown TM. Output from VIP cells of the mammalian central clock regulates daily physiological rhythms. Nat Commun. 2020 Mar 19;11(1):1453. doi: 10.1038/s41467-020-15277-x. PMID: 32193397; PMCID: PMC7081308.

Pavlova M. Circadian Rhythm Sleep-Wake Disorders. Continuum (Minneap Minn). 2017;23(4, Sleep Neurology):1051-1063. doi:10.1212/CON.0000000000000499

Paxinos G, Franklin KB (2001) The mouse brain in stereotaxic coordinates, Ed 2. Cambridge, MA: Academic.

Perreau-Lenz S, Kalsbeek A, Garidou ML, Wortel J, van der Vliet J, van Heijningen C, Simonneaux V, Pévet P, Buijs RM. Suprachiasmatic control of melatonin synthesis in rats: inhibitory and stimulatory mechanisms. Eur J Neurosci. 2003 Jan;17(2):221-8. doi: 10.1046/j.1460-9568.2003.02442.x. PMID: 12542658.

Petkov V, Mosgoeller W, Ziesche R, Raderer M, Stiebellehner L, Vonbank K, Funk GC, Hamilton G, Novotny C, Burian B, Block LH. Vasoactive intestinal peptide as a new drug for treatment of primary pulmonary hypertension. J Clin Invest. 2003 May;111(9):1339-46. doi: 10.1172/JCI17500. PMID: 12727925; PMCID: PMC154449.

Piggins HD, Antle MC, Rusak B. Neuropeptides phase shift the mammalian circadian pacemaker. J Neurosci. 1995 Aug;15(8):5612-22. doi: 10.1523/JNEUROSCI.15-08- 05612.1995. PMID: 7643205; PMCID: PMC6577626.

Pittendrigh CS. Circadian rhythms and the circadian organization of living systems. Cold Spring Harb Symp Quant Biol. 1960;25:159-84. doi: 10.1101/sqb.1960.025.01.015. PMID: 13736116.

Pittendrigh C.S. (1981) Circadian Systems: Entrainment. In: Aschoff J. (eds) Biological Rhythms. Springer, Boston, MA. https://doi.org/10.1007/978-1-4615-6552-9_7

Preitner N, Damiola F, Lopez-Molina L, Zakany J, Duboule D, Albrecht U, Schibler U. The orphan nuclear receptor REV-ERBalpha controls circadian transcription within the positive limb of the mammalian circadian oscillator. Cell. 2002 Jul 26;110(2):251-60. doi: 10.1016/s0092-8674(02)00825-5. PMID: 12150932.

Prolo LM, Takahashi JS, Herzog ED. Circadian rhythm generation and entrainment in astrocytes. J Neurosci. 2005 Jan 12;25(2):404-8. doi: 10.1523/JNEUROSCI.4133-04.2005. PMID: 15647483; PMCID: PMC3812245.

Provencio I, Rodriguez IR, Jiang G, Hayes WP, Moreira EF, Rollag MD. A novel human opsin in the inner retina. J Neurosci. 2000 Jan 15;20(2):600-5. doi: 10.1523/JNEUROSCI.20- 02-00600.2000. PMID: 10632589; PMCID: PMC6772411.

Qiu DL, Chu CP, Shirasaka T, Nabekura T, Kunitake T, Kato K, Nakazato M, Katoh T, Kannan H. Neuromedin U depolarizes rat hypothalamic paraventricular nucleus neurons in vitro by enhancing IH channel activity. J Neurophysiol. 2003 Aug;90(2):843-50. doi: 10.1152/jn.00225.2003. Epub 2003 Apr 23. PMID: 12711715.

Rae M, Lemos Duarte M, Gomes I, Camarini R, Devi LA. Oxytocin and vasopressin: Signalling, behavioural modulation and potential therapeutic effects. Br J Pharmacol. 2022 Apr;179(8):1544-1564. doi: 10.1111/bph.15481. Epub 2021 May 21. PMID: 33817785; PMCID: PMC8488062.

Raff H. CORT, Cort, B, Corticosterone, and now Cortistatin: Enough Already! Endocrinology. 2016 Sep;157(9):3307-8. doi: 10.1210/en.2016-1500. Epub 2016 Jul 28. PMID: 27466840.

Ralph MR, Foster RG, Davis FC, Menaker M. Transplanted suprachiasmatic nucleus determines circadian period. Science. 1990 Feb 23;247(4945):975-8. doi: 10.1126/science.2305266. PMID: 2305266.

Ramkisoensing A, Meijer JH. Synchronization of Biological Clock Neurons by Light and Peripheral Feedback Systems Promotes Circadian Rhythms and Health. Front Neurol. 2015 Jun 5;6:128. doi: 10.3389/fneur.2015.00128. PMID: 26097465; PMCID: PMC4456861.

Reed HE, Cutler DJ, Brown TM, Brown J, Coen CW, Piggins HD. Effects of vasoactive intestinal polypeptide on neurones of the rat suprachiasmatic nuclei in vitro. J Neuroendocrinol. 2002 Aug;14(8):639-46. doi: 10.1046/j.1365-2826.2002.00826.x. PMID: 12153466.

Reppert SM, Weaver DR. Coordination of circadian timing in mammals. Nature. 2002 Aug 29;418(6901):935-41. doi: 10.1038/nature00965. PMID: 12198538

Richter CP. Sleep and activity: their relation to the 24-hour clock. Res Publ Assoc Res Nerv Ment Dis. 1967;45:8-29. PMID: 6083201.

Rogilmore. psu-psychology/psy-511-scan-fdns-2019. Github, 2019. https://github.com/psu-psychology/psy-511-scan-fdns-2’19/blob/master/lectures/511-anatomy.md

Ross WN. Understanding calcium waves and sparks in central neurons. Nat Rev Neurosci. 2012 Feb 8;13(3):157-68. doi: 10.1038/nrn3168. PMID: 22314443; PMCID: PMC4501263.

Ruby NF, Brennan TJ, Xie X, Cao V, Franken P, Heller HC, O'Hara BF. Role of melanopsin in circadian responses to light. Science. 2002 Dec 13;298(5601):2211-3. doi: 10.1126/science.1076701. PMID: 12481140.

Said SI, Mutt V. Polypeptide with broad biological activity: isolation from small intestine. Science. 1970 Sep 18;169(3951):1217-8. doi: 10.1126/science.169.3951.1217. PMID: 5450698.

Saper CB, Lu J, Chou TC, Gooley J. The hypothalamic integrator for circadian rhythms. Trends Neurosci. 2005;28(3):152-157. doi:10.1016/j.tins.2004.12.009.

Saper CB. The central circadian timing system. Curr Opin Neurobiol. 2013 Oct;23(5):747-51. doi: 10.1016/j.conb.2013.04.004. Epub 2013 May 22. PMID: 23706187; PMCID: PMC3758384.

Sato T, Kawamura H. Circadian rhythms in multiple unit activity inside and outside the suprachiasmatic nucleus in the diurnal chipmunk (Eutamias sibiricus). Neurosci Res. 1984 Feb;1(1):45-52. doi: 10.1016/0168-0102(84)90029-4. PMID: 6543592.

Sato TK, Panda S, Miraglia LJ, Reyes TM, Rudic RD, McNamara P, Naik KA, FitzGerald GA, Kay SA, Hogenesch JB. A functional genomics strategy reveals Rora as a component of the mammalian circadian clock. Neuron. 2004 Aug 19;43(4):527-37. doi: 10.1016/j.neuron.2004.07.018. PMID: 15312651.

Shen S, Spratt C, Sheward WJ, Kallo I, West K, Morrison CF, Coen CW, Marston HM, Harmar AJ. Overexpression of the human VPAC2 receptor in the suprachiasmatic nucleus alters the circadian phenotype of mice. Proc Natl Acad Sci U S A. 2000 Oct 10;97(21):11575- 80. doi: 10.1073/pnas.97.21.11575. PMID: 11027354; PMCID: PMC17242.

Sheward WJ, Maywood ES, French KL, Horn JM, Hastings MH, Seckl JR, Holmes MC, Harmar AJ. Entrainment to feeding but not to light: circadian phenotype of VPAC2 receptor-null mice. J Neurosci. 2007 Apr 18;27(16):4351-8. doi: 10.1523/JNEUROSCI.4843-06.2007. PMID: 17442819; PMCID: PMC6672325.

Schindelin J, Arganda-Carreras I, Frise E, Kaynig V, Longair M, Pietzsch T, Preibisch S, Rueden C, Saalfeld S, Schmid B, Tinevez JY, White DJ, Hartenstein V, Eliceiri K, Tomancak P, Cardona A. Fiji: an open-source platform for biological-image analysis. Nat Methods. 2012 Jun 28;9(7):676-82. doi: 10.1038/nmeth.2019. PMID: 22743772; PMCID: PMC3855844.

Shinohara K, Tominaga K, Isobe Y, Inouye ST. Photic regulation of peptides located in the ventrolateral subdivision of the suprachiasmatic nucleus of the rat: daily variations of vasoactive intestinal polypeptide, gastrin-releasing peptide, and

neuropeptide Y. J Neurosci. 1993 Feb;13(2):793-800. doi: 10.1523/JNEUROSCI.13-02-00793.1993. PMID: 8426236; PMCID: PMC6576648.

Shinohara K, Inouye ST. Photic information coded by vasoactive intestinal polypeptide and neuropeptide Y. Neurosci Biobehav Rev. 1995 Fall;19(3):349-52. doi: 10.1016/0149- 7634(94)00048-6. PMID: 7566737.

Shinohara K, Funabashi T, Kimura F. Temporal profiles of vasoactive intestinal polypeptide precursor mRNA and its receptor mRNA in the rat suprachiasmatic nucleus. Brain Res Mol Brain Res. 1999 Jan 8;63(2):262-7. doi: 10.1016/s0169-328x(98)00289-7. PMID: 9878775.

Schmutz I, Chavan R, Ripperger JA, Maywood ES, Langwieser N, Jurik A, Stauffer A, Delorme JE, Moosmang S, Hastings MH, Hofmann F, Albrecht U. A specific role for the REV-ERBα-controlled L-Type Voltage-Gated Calcium Channel CaV1.2 in resetting the circadian clock in the late night. J Biol Rhythms. 2014 Aug;29(4):288-98. doi: 10.1177/0748730414540453. PMID: 25238857; PMCID: PMC4608047.

Schwartz WJ, Davidsen LC, Smith CB. In vivo metabolic activity of a putative circadian oscillator, the rat suprachiasmatic nucleus. J Comp Neurol. 1980 Jan 1;189(1):157-67. doi: 10.1002/cne.901890109. PMID: 7351445.

Schwartz WJ, Reppert SM. Neural regulation of the circadian vasopressin rhythm in cerebrospinal fluid: a pre-eminent role for the suprachiasmatic nuclei. J Neurosci. 1985 Oct;5(10):2771-8. doi: 10.1523/JNEUROSCI.05-10-02771.1985. PMID: 4045552; PMCID: PMC6565152.

Schwartz MD, Nunez AA, Smale L. Differences in the suprachiasmatic nucleus and lower subparaventricular zone of diurnal and nocturnal rodents. Neuroscience. 2004;127(1):13-23. doi: 10.1016/j.neuroscience.2004.04.049. PMID: 15219664.

Schwartz MD, Nuñez AA, Smale L. Rhythmic cFos expression in the ventral subparaventricular zone influences general activity rhythms in the Nile grass rat, Arvicanthis niloticus. Chronobiol Int. 2009 Oct;26(7):1290-306. doi: 10.3109/07420520903415742. PMID: 19916832.

Shearman LP, Sriram S, Weaver DR, Maywood ES, Chaves I, Zheng B, Kume K, Lee CC, van der Horst GT, Hastings MH, Reppert SM. Interacting molecular loops in the mammalian circadian clock. Science. 2000 May 12;288(5468):1013-9. doi: 10.1126/science.288.5468.1013. PMID: 10807566.

Silver R, LeSauter J, Tresco PA, Lehman MN. A diffusible coupling signal from the transplanted suprachiasmatic nucleus controlling circadian locomotor rhythms. Nature. 1996 Aug 29;382(6594):810-3. doi: 10.1038/382810a0. PMID: 8752274.

Skofitsch G, Jacobowitz DM. Immunohistochemical mapping of galanin-like neurons in the rat central nervous system. Peptides. 1985 May-Jun;6(3):509-46. doi: 10.1016/0196-9781(85)90118-4. PMID: 2415952.

Sjöstedt E, Zhong W, Fagerberg L, Karlsson M, Mitsios N, Adori C, Oksvold P, Edfors F, Limiszewska A, Hikmet F, Huang J, Du Y, Lin L, Dong Z, Yang L, Liu X, Jiang H, Xu X, Wang J, Yang H, Bolund L, Mardinoglu A, Zhang C, von Feilitzen K, Lindskog C, Pontén F, Luo Y, Hökfelt T, Uhlén M, Mulder J. An atlas of the protein-coding genes in the human, pig, and mouse brain. Science. 2020 Mar 6;367(6482):eaay5947. doi: 10.1126/science.aay5947. PMID: 32139519.

Solt LA, Kojetin DJ, Burris TP. The REV-ERBs and RORs: molecular links between circadian rhythms and lipid homeostasis. Future Med Chem. 2011 Apr;3(5):623-38. doi: 10.4155/fmc.11.9. PMID: 21526899; PMCID: PMC3134326.

Sofroniew M.V. Vasopressin and oxytocin in the mammalian brain and spinal cord. *Front. Neuroendocrinol.* 1983;40:1–23. doi: 10.1016/0166-2236(83)90221-7

Starnes AN, Jones JR. Inputs and Outputs of the Mammalian Circadian Clock. Biology (Basel). 2023 Mar 28;12(4):508. doi: 10.3390/biology12040508. PMID: 37106709; PMCID: PMC10136320.

Stamper CE, Hennessey PA, Hale MW, Lukkes JL, Donner NC, Lowe KR, Paul ED, Spencer RL, Renner KJ, Orchinik M, Lowry CA. Role of the dorsomedial hypothalamus in glucocorticoid-mediated feedback inhibition of the hypothalamic-pituitary-adrenal axis. Stress. 2015 Jan;18(1):76-87. doi: 10.3109/10253890.2015.1004537. Epub 2015 Feb 17. PMID: 25556980; PMCID: PMC4367871.

Stephan FK, Zucker I. Circadian rhythms in drinking behavior and locomotor activity of rats are eliminated by hypothalamic lesions. Proc Natl Acad Sci U S A. 1972 Jun;69(6):1583-6. doi: 10.1073/pnas.69.6.1583. PMID: 4556464; PMCID: PMC426753.

Storch KF, Lipan O, Leykin I, Viswanathan N, Davis FC, Wong WH, Weitz CJ. Extensive and divergent circadian gene expression in liver and heart. Nature. 2002 May 2;417(6884):78- 83. doi: 10.1038/nature744. Epub 2002 Apr 21. Erratum in: Nature 2002 Aug 8;418(6898):665. PMID: 11967526.

Tahara Y, Kuroda H, Saito K, Nakajima Y, Kubo Y, Ohnishi N, Seo Y, Otsuka M, Fuse Y, Ohura Y, Komatsu T, Moriya Y, Okada S, Furutani N, Hirao A, Horikawa K, Kudo T, Shibata S. In vivo monitoring of peripheral circadian clocks in the mouse. Curr Biol. 2012 Jun 5;22(11):1029-34. doi: 10.1016/j.cub.2012.04.009. Epub 2012 May 10. PMID: 22578421.

Takahashi JS. Transcriptional architecture of the mammalian circadian clock. Nat Rev Genet. 2017 Mar;18(3):164-179. doi: 10.1038/nrg.2016.150. Epub 2016 Dec 19. PMID: 27990019; PMCID: PMC5501165.

Tan YV, Couvineau A, Murail S, Ceraudo E, Neumann JM, Lacapère JJ, Laburthe M. Peptide agonist docking in the N-terminal ectodomain of a class II G protein-coupled receptor, the VPAC1 receptor. Photoaffinity, NMR, and molecular modeling. J Biol Chem. 2006 May 5;281(18):12792-8. doi: 10.1074/jbc.M513305200. Epub 2006 Mar 6. PMID: 16520374.

Taub A, Carbajal Y, Rimu K, Holt R, Yao Y, Hernandez AL, LeSauter J, Silver R. Arginine Vasopressin-Containing Neurons of the Suprachiasmatic Nucleus Project to CSF. eNeuro. 2021 Apr 16;8(2):ENEURO.0363-20.2021. doi: 10.1523/ENEURO.0363-20.2021. PMID: 33472866; PMCID: PMC8174031.

Thibonnier M, Berti-Mattera LN, Dulin N, Conarty DM, Mattera R. Signal transduction pathways of the human V1-vascular, V2-renal, V3-pituitary vasopressin and oxytocin receptors. Prog Brain Res. 1998;119:147-61. doi: 10.1016/s0079-6123(08)61568-x. PMID: 1007478.

Tian L, Hires SA, Mao T, Huber D, Chiappe ME, Chalasani SH, Petreanu L, Akerboom J, McKinney SA, Schreiter ER, Bargmann CI, Jayaraman V, Svoboda K, Looger LL. Imaging neural activity in worms, flies and mice with improved GCaMP calcium indicators. Nat Methods. 2009 Dec;6(12):875-81. doi: 10.1038/nmeth.1398. Epub 2009 Nov 8. PMID: 19898485; PMCID: PMC2858873.

Ting JT, Daigle TL, Chen Q, Feng G. Acute brain slice methods for adult and aging animals: application of targeted patch clamp analysis and optogenetics. Methods Mol Biol. 2014;1183:221-42. doi: 10.1007/978-1-4939-1096-0_14. PMID: 25023312; PMCID: PMC4219416.

Todd WD, Gall AJ, Weiner JA, Blumberg MS. Distinct retinohypothalamic innervation patterns predict the developmental emergence of species-typical circadian phase preference in nocturnal Norway rats and diurnal nile grass rats. J Comp Neurol. 2012 Oct 1;520(14):3277-92. doi: 10.1002/cne.23098. PMID: 22431036; PMCID: PMC3676184.

Todd WD, Fenselau H, Wang JL, Zhang R, Machado NL, Venner A, Broadhurst RY, Kaur S, Lynagh T, Olson DP, Lowell BB, Fuller PM, Saper CB. A hypothalamic circuit for the circadian control of aggression. Nat Neurosci. 2018 May;21(5):717-724. doi: 10.1038/s41593-018-0126-0. Epub 2018 Apr 9. PMID: 29632359; PMCID: PMC5920747.

Todd WD, Venner A, Anaclet C, Broadhurst RY, De Luca R, Bandaru SS, Issokson L, Hablitz LM, Cravetchi O, Arrigoni E, Campbell JN, Allen CN, Olson DP, Fuller PM. Suprachiasmatic VIP neurons are required for normal circadian rhythmicity and comprised of molecularly distinct subpopulations. Nat Commun. 2020 Sep 2;11(1):4410. doi: 10.1038/s41467-020-17197-2. PMID: 32879310; PMCID: PMC7468160.

Torres-Farfan C, Serón-Ferré M, Dinet V, Korf HW. Immunocytochemical demonstration of day/night changes of clock gene protein levels in the murine adrenal gland: differences between melatonin-proficient (C3H) and melatonin-deficient (C57BL) mice. J Pineal Res. 2006 Jan;40(1):64-70. doi: 10.1111/j.1600-079X.2005.00279.x. PMID: 16313500.

Touitou Y, Auzeby A, Bogdan A. Cortisol and cortisone production in rat and mouse adrenal incubations. J Steroid Biochem Mol Biol. 1990 Oct;37(2):279-84. doi: 10.1016/0960-0760(90)90339-m. PMID: 2268561.

Tousson E, Meissl H. Suprachiasmatic nuclei grafts restore the circadian rhythm in the paraventricular nucleus of the hypothalamus. J Neurosci. 2004 Mar 24;24(12):2983-8. doi: 10.1523/JNEUROSCI.5044-03.2004. PMID: 15044537; PMCID: PMC6729855.

Tso CF, Simon T, Greenlaw AC, Puri T, Mieda M, Herzog ED. Astrocytes Regulate Daily Rhythms in the Suprachiasmatic Nucleus and Behavior. Curr Biol. 2017 Apr 3;27(7):1055- 1061. doi: 10.1016/j.cub.2017.02.037. Epub 2017 Mar 23. PMID: 28343966; PMCID: PMC5380592.

Tsuji T, Allchorne AJ, Zhang M, Tsuji C, Tobin VA, Pineda R, Raftogianni A, Stern JE, Grinevich V, Leng G, Ludwig M. Vasopressin casts light on the suprachiasmatic nucleus. J Physiol. 2017 Jun 1;595(11):3497-3514. doi: 10.1113/JP274025. Epub 2017 May 14. PMID: 28402052; PMCID: PMC5451709.

Ueda HR, Chen W, Adachi A, Wakamatsu H, Hayashi S, Takasugi T, Nagano M, Nakahama K, Suzuki Y, Sugano S, Iino M, Shigeyoshi Y, Hashimoto S. A transcription factor response element for gene expression during circadian night. Nature. 2002 Aug 1;418(6897):534-9. doi: 10.1038/nature00906. PMID: 12152080.

Ueyama T, Krout KE, Nguyen XV, Karpitskiy V, Kollert A, Mettenleiter TC, Loewy AD. Suprachiasmatic nucleus: a central autonomic clock. Nat Neurosci. 1999 Dec;2(12):1051-3. doi: 10.1038/15973. PMID: 10570479.

Uht RM, McKelvy JF, Harrison RW, Bohn MC. Demonstration of glucocorticoid receptor-like immunoreactivity in glucocorticoid-sensitive vasopressin and corticotropin-releasing factor neurons in the hypothalamic paraventricular nucleus. J Neurosci Res. 1988 Apr;19(4):405-11, 468-9. doi: 10.1002/jnr.490190404. PMID: 3260289.

Ungar F, Halberg F. Circadian Rhythm In The In Vitro Response Of Mouse Adrenal To Adrenocorticotropic Hormone. Science. 1962 Sep 28;137(3535):1058-60. Doi: 10.1126/Science.137.3535.1058. Pmid: 13923797.

Ungar F. In Vitro Studies Of Adrenal-Pituitary Circadian Rhythms In The Mouse. Ann N Y Acad Sci. 1964 Sep 10;117:374-85. Doi: 10.1111/J.1749-6632.1964.Tb48194.X. Pmid: 14196655.

Usdin TB, Bonner TI, Mezey E. Two receptors for vasoactive intestinal polypeptide with similar specificity and complementary distributions. Endocrinology. 1994 Dec;135(6):2662- 80. doi: 10.1210/endo.135.6.7988457. PMID: 7988457.

Vallotton MB. The multiple faces of the vasopressin receptors. Mol Cell Endocrinol. 1991 Jun;78(1-2):C73-6. doi: 10.1016/0303-7207(91)90173-p. PMID: 1657657.

van Weerden WM, Bierings HG, van Steenbrugge GJ, de Jong FH, Schröder FH. Adrenal glands of mouse and rat do not synthesize androgens. Life Sci. 1992;50(12):857-61. doi: 10.1016/0024-3205(92)90204-3. PMID: 1312193.

van der Westhuizen ET, Choy KHC, Valant C, McKenzie-Nickson S, Bradley SJ, Tobin AB, Sexton PM, Christopoulos A. Fine Tuning Muscarinic Acetylcholine Receptor Signaling Through Allostery and Bias. Front Pharmacol. 2021 Jan 29;11:606656. doi: 10.3389/fphar.2020.606656. PMID: 33584282; PMCID: PMC7878563.

Vogt JH, Schippers JH. Setting the PAS, the role of circadian PAS domain proteins during environmental adaptation in plants. Front Plant Sci. 2015 Jul 9;6:513. doi: 10.3389/fpls.2015.00513. PMID: 26217364; PMCID: PMC4496561.

Voigt RM, Forsyth CB, Keshavarzian A. Circadian disruption: potential implications in inflammatory and metabolic diseases associated with alcohol. Alcohol Res. 2013;35(1):87- 96.

Vong L, Ye C, Yang Z, Choi B, Chua S, Lowell BB (2011) Leptin action on GABAergic neurons prevents obesity and reduces inhibitory tone to POMC neurons. Neuron 71:142–154.

Vrang N, Larsen PJ, Mikkelsen JD. Direct projection from the suprachiasmatic nucleus to hypophysiotrophic corticotropin-releasing factor immunoreactive cells in the paraventricular nucleus of the hypothalamus demonstrated by means of Phaseolus vulgaris-leucoagglutinin tract tracing. Brain Res. 1995 Jun 26;684(1):61-9. doi: 10.1016/0006-8993(95)00425-p. PMID: 7583205.

Vujovic, Nina. 2014. Functional organization of the circadian timing system. Doctoral dissertation, Harvard University.

Vujovic N, Gooley JJ, Jhou TC, Saper CB. Projections from the subparaventricular zone define four channels of output from the circadian timing system. J Comp Neurol. 2015 Dec 15;523(18):2714-37. doi: 10.1002/cne.23812. Epub 2015 Aug 18. PMID: 26010698; PMCID: PMC4607558.

Wagner S, Sagiv N, Yarom Y. GABA-induced current and circadian regulation of chloride in neurones of the rat suprachiasmatic nucleus. J Physiol. 2001 Dec 15;537(Pt 3):853-69. doi: 10.1111/j.1469-7793.2001.00853.x. PMID: 11744760; PMCID: PMC2279012.

Welsh DK, Logothetis DE, Meister M, Reppert SM. Individual neurons dissociated from rat suprachiasmatic nucleus express independently phased circadian firing rhythms. Neuron. 1995 Apr;14(4):697-706. doi: 10.1016/0896-6273(95)90214-7. PMID: 7718233.

Wen S, Ma D, Zhao M, Xie L, Wu Q, Gou L, Zhu C, Fan Y, Wang H, Yan J. Spatiotemporal single-cell analysis of gene expression in the mouse suprachiasmatic nucleus. Nat Neurosci. 2020 Mar;23(3):456-467. doi: 10.1038/s41593-020-0586-x. Epub 2020 Feb 17. PMID: 32066983.

Wenzel EV, Bosnak M, Tierney R, Schubert M, Brown J, Dübel S, Efstratiou A, Sesardic D, Stickings P, Hust M. Human antibodies neutralizing diphtheria toxin in vitro and in vivo. Sci Rep. 2020 Jan 17;10(1):571. doi: 10.1038/s41598-019-57103-5. PMID: 31953428; PMCID: PMC6969050.

Wickersham IR, Finke S, Conzelmann KK, Callaway EM. Retrograde neuronal tracing with a deletion-mutant rabies virus. Nat Methods. 2007 Jan;4(1):47-9. doi: 10.1038/nmeth999. Epub 2006 Dec 10. PMID: 17179932; PMCID: PMC2755236.

Wickersham IR, Lyon DC, Barnard RJ, Mori T, Finke S, Conzelmann KK, Young JA, Callaway EM. Monosynaptic restriction of transsynaptic tracing from single, genetically targeted neurons. Neuron. 2007 Mar 1;53(5):639-47. doi: 10.1016/j.neuron.2007.01.033. PMID: 17329205; PMCID: PMC2629495.

Winsky-Sommerer R, Yamanaka A, Diano S, Borok E, Roberts AJ, Sakurai T, Kilduff TS, Horvath TL, de Lecea L. Interaction between the corticotropin-releasing factor system and hypocretins (orexins): a novel circuit mediating stress response. J Neurosci. 2004 Dec 15;24(50):11439-48. doi: 10.1523/JNEUROSCI.3459-04.2004. PMID: 15601950; PMCID: PMC6730356.

Winzell MS, Ahrén B. Role of VIP and PACAP in islet function. Peptides. 2007 Sep;28(9):1805-13. doi: 10.1016/j.peptides.2007.04.024. Epub 2007 May 6. PMID: 17559974.

Wren AM, Small CJ, Abbott CR, Jethwa PH, Kennedy AR, Murphy KG, Stanley SA, Zollner AN, Ghatei MA, Bloom SR. Hypothalamic actions of neuromedin U. Endocrinology. 2002 Nov;143(11):4227-34. doi: 10.1210/en.2002-220308. PMID: 12399416.

Wu D, Lee D, Sung YK. Prospect of vasoactive intestinal peptide therapy for COPD/PAH and asthma: a review. Respir Res. 2011 Apr 11;12(1):45. doi: 10.1186/1465-9921-12-45. PMID: 21477377; PMCID: PMC3090995.

Xu Y, Padiath QS, Shapiro RE, Jones CR, Wu SC, Saigoh N, Saigoh K, Ptácek LJ, Fu YH. Functional consequences of a CKIdelta mutation causing familial advanced sleep phase syndrome. Nature. 2005 Mar 31;434(7033):640-4. doi: 10.1038/nature03453. PMID: 15800623.

Yizhar O, Fenno LE, Davidson TJ, Mogri M, Deisseroth K. Optogenetics in neural systems. Neuron. 2011 Jul 14;71(1):9-34. doi: 10.1016/j.neuron.2011.06.004. PMID: 21745635.

Yamaguchi S, Isejima H, Matsuo T, Okura R, Yagita K, Kobayashi M, Okamura H. Synchronization of cellular clocks in the suprachiasmatic nucleus. Science. 2003 Nov 21;302(5649):1408-12. doi: 10.1126/science.1089287. PMID: 14631044.

Yamaguchi Y, Suzuki T, Mizoro Y, Kori H, Okada K, Chen Y, Fustin JM, Yamazaki F, Mizuguchi N, Zhang J, Dong X, Tsujimoto G, Okuno Y, Doi M, Okamura H. Mice genetically deficient in vasopressin V1a and V1b receptors are resistant to jet lag. Science. 2013 Oct 4;342(6154):85-90. doi: 10.1126/science.1238599. PMID:24092737.

Yamamoto T, Nakahata Y, Soma H, Akashi M, Mamine T, Takumi T. Transcriptional oscillation of canonical clock genes in mouse peripheral tissues. BMC Mol Biol. 2004 Oct 9;5:18. doi: 10.1186/1471-2199-5-18. PMID: 15473909; PMCID: PMC535906.

Yan L, Karatsoreos I, Lesauter J, Welsh DK, Kay S, Foley D, Silver R. Exploring spatiotemporal organization of SCN circuits. Cold Spring Harb Symp Quant Biol. 2007;72:527-41. doi: 10.1101/sqb.2007.72.037. PMID: 18419312; PMCID: PMC3281753.

Yesmin R, Watanabe M, Sinha AS, Ishibashi M, Wang T, Fukuda A. A subpopulation of agouti-related peptide neurons exciting corticotropin-releasing hormone axon terminals in median eminence led to hypothalamic-pituitary-adrenal axis activation in response to food restriction. Front Mol Neurosci. 2022 Sep 29;15:990803. doi: 10.3389/fnmol.2022.990803. PMID: 36245920; PMCID: PMC9557964.

Yoo SH, Yamazaki S, Lowrey PL, Shimomura K, Ko CH, Buhr ED, Siepka SM, Hong HK, Oh WJ, Yoo OJ, Menaker M, Takahashi JS. PERIOD2::LUCIFERASE real-time reporting of circadian dynamics reveals persistent circadian oscillations in mouse peripheral tissues. Proc Natl Acad Sci U S A. 2004 Apr 13;101(15):5339-46. doi: 10.1073/pnas.0308709101. Epub 2004 Feb 12. PMID: 14963227; PMCID: PMC397382.

Yoshikawa T, Pauls S, Foley N, Taub A, LeSauter J, Foley D, Honma KI, Honma S, Silver R. Phase Gradients and Anisotropy of the Suprachiasmatic Network: Discovery of Phaseoids. eNeuro. 2021 Sep 9;8(5):ENEURO.0078-21.2021. doi: 10.1523/ENEURO.0078-21.2021. PMID: 34385151; PMCID: PMC8431825.

You C, Zhang Y, Xu P, Huang S, Yin W, Eric Xu H, Jiang Y. Structural insights into the peptide selectivity and activation of human neuromedin U receptors. Nat Commun. 2022 Apr 19;13(1):2045. doi: 10.1038/s41467-022-29683-w. PMID: 35440625; PMCID: PMC9019041.

Zemkova H, Tomić M, Kucka M, Aguilera G, Stojilkovic SS. Spontaneous and CRH-Induced Excitability and Calcium Signaling in Mice Corticotrophs Involves Sodium, Calcium, and Cation-Conducting Channels. Endocrinology. 2016 Apr;157(4):1576-89. doi: 10.1210/en.2015-1899. Epub 2016 Feb 22. PMID: 26901094; PMCID: PMC4816721.

Zhang C, Truong KK, Zhou QY. Efferent projections of prokineticin 2 expressing neurons in the mouse suprachiasmatic nucleus. PLoS One. 2009 Sep 28;4(9):e7151. doi: 10.1371/journal.pone.0007151. PMID: 19784373; PMCID: PMC2747004.

Zincarelli C, Soltys S, Rengo G, Rabinowitz JE. Analysis of AAV serotypes 1-9 mediated gene expression and tropism in mice after systemic injection. Mol Ther. 2008 Jun;16(6):1073- 80. doi: 10.1038/mt.2008.76. Epub 2008 Apr 15. PMID: 18414476.

iii. ACKNOWLEDGEMENTS

There are no words to express how grateful I am for the opportunity to have participated in the Ph.D. course in Biomedical Science at University of Pavia.

I would like to express my deepest gratitude to Professor Gerardo Rosario Biella (University of Pavia, Pavia, Italy) and Professor Elda Arrigoni (Beth Israel Lahey Health-Harvard Medical School, Boston, USA) for welcoming me into their laboratories since my master's degree training and for guiding me during these 3-years of Ph.D. formation. Very special thanks to Elda, her scientific approach has been fundamental for the development of this research in her laboratory.

A special thanks to Ph.D. Roberto De Luca and Ph.D. Oscar Ramirez Plascencia for introducing me to their *in vitro* and *in vivo* work in the field of circadian rhythms, which has represented a chance for a collaboration and experimental challenges.

The chance to work in a stimulating environment is essential for professional growth. Therefore, I would like to express my gratitude to Professor Thomas Scammel, Professor Clifford Saper (Beth Israel Lahey Health-Harvard Medical School, Boston, USA) and Professor Patrick M. Fuller (University of California, Davis, CA, USA) to being guiding lights along this path with their scientific papers and contributions during meetings.

In this journey I've had the amazing opportunity to work alongside different Postdocs who have been equally essential for my professional growth. Special thanks to Ph.D. Yaniv Sela, Ph.D. Natalia Machado (Beth Israel Lahey Health-Harvard Medical School, Boston, USA) and Ph.D. Francesca Talpo (University of Pavia, Pavia, Italy) for entrusting me to be part of their research projects. Working in their projects has been extremely rewarding.

Finally, I want to thank all the members of Biella's laboratory for being precious colleagues during this journey. Special thanks to Doctors Paolo Spaiardi, Niccolò Mattiello, Arianna Trucco, Antonio N. Castagno, Jessica Cazzola.

I'd like to emphasize my gratefulness to all of them because having had the opportunity to work with them and because they entrusted me with this project and many others, represent an opportunity without precedence in my scientific career.